

ABSTRACT

MILHEM, FADIA JAMAL THEEB. Mechanisms Underlying the Resistance to Diet-Induced Obesity (Under the direction of Dr. Slavko Komarnytsky).

Obesity is a worldwide epidemic that has been increasing affecting most age categories and affecting health negatively giving rise to metabolic disorders, such as insulin resistance, and proinflammatory state. Obesity is multifactorial, caused mainly by increased energy intake, and sedentary lifestyle, however, other factors such as social, environmental, genetic, and, epigenetic, all seem to have an influence. While most of the world is living in an obesogenic environment, some individuals are resistant to obesity or remain lean. Similarly, some animal models have shown different responses to overfeeding, where animals can be classified as obese prone (super-responders, SR) or obesity-resistant (non-responders, NR). This makes it possible to use such animal models to have a better understanding of the underlying causes of resistance to obesity.

Chapter 1 outlines the different attributes related to super-responders and non-responders, including different metabolic and biochemical processes, including fatty acid oxidation and citrate levels. Additionally, this discussion delves into other factors influencing these phenotypes, including considerations of fat depots and variations in gut immunity. This exploration aims to enhance comprehension regarding weight maintenance.

Chapter 2 evaluates how metabolic fluctuations shape obesity susceptibility, resulting in super-responders and non-responders in C57BL/6J mice model on low-fat diet (LFD) or high-fat diet (HFD) for a total of 14 weeks. Despite having a similar respiratory exchange ratio (RER) to NR mice, SR mice gained greater weight and body mass, as well as higher water content and feed efficiency. NR showed high food intake and physical activity yet showed decreased feed efficiency. Upon fecal lipid analysis, they had lower fat content and reduction

in *Actinobacteria* counts, underscoring the need for a comprehensive investigation into the mechanisms associated with obesity resistance. Developing customized approaches to managing a healthy weight is significantly dependent on improving our understanding of the molecular pathways behind the diverse obesity phenotypes.

Chapter 3 studied obesity-resistant (NR) phenotype that is less susceptible to obesity on a high-fat diet, which exhibited favorable fat/lean body mass ratios through upregulated gene networks promoting specific muscle tissues. This metabolic adaptation, however, impaired glucose tolerance. NR resistance correlates with increased mitoferrin 1 (*Slc25a37*), a crucial mitochondrial iron importer. Obesity-prone (SR) mice show altered fecal volatile metabolites, which reverse in NR mice. Studying obesity-resistant phenotypes provides insights into obesity mechanisms, offering potential for personalized weight management strategies.

© Copyright 2024 by Fadia Jamal Theeb Milhem

All Rights Reserved

Mechanisms Underlying the Resistance to Diet-Induced Obesity

by
Fadia Jamal Theeb Milhem

A dissertation submitted to the Graduate Faculty of
North Carolina State University
in partial fulfillment of the
requirements for the Degree of
Doctor of Philosophy

Nutrition

Raleigh, North Carolina
2024

APPROVED BY:

Dr. Slavko Komarnytsky
Committee Chair

Dr. Lora Goodell

Dr. Mary Ann Lila

Dr. Marvin Moncada Reyes

DEDICATION

I dedicate this work with deep gratitude to my beloved family, loving husband, and precious child to be.

BIOGRAPHY

Inspired by personal nutritional challenges in her adolescence, Fadia Milhem developed a profound interest in nutrition, seeking a deeper understanding of health. Her parents fully supported her decision to enroll in Jordan University of Science and Technology's Bachelor of Science program in Nutrition and Food Technology (JUST).

She recognized that her curiosity was growing and that she was becoming very curious in this area. She put up a lot of effort, which paid off as she was recognized for several semesters and eventually graduated first in her class. She was able to pursue a MSc in nutrition at JUST, thanks to a fully supported scholarship. Her thesis was titled “Effect of Amurca (Olive Oil Lees) on Gut Microbiota in the Rat”. Balancing roles as a Teaching Assistant (TA) and Research Assistant (RA) in the department, she gained valuable experience. Eventually, she decided to expand her expertise in teaching and academia, spending three years as a biology science teacher in high school in Jordan.

She subsequently was awarded a scholarship from the University of Petra, which allowed her to pursue a Ph.D. in Nutrition at NCSU under the supervision of Dr. Komarnytsky at PHHI. As her understanding of nutrition grew, she focused on the different pathways that lead to obesity, including the impact of gut bacteria. Fadia's goals include making significant contributions to the academic realm of nutrition and gaining a better understanding of obesity through research.

ACKNOWLEDGMENTS

“He who does not thank people does not thank Allah”, Prophet (PBUH). I am grateful to the University of Petra for giving me the chance to pursue my education and funding my education. I am thankful to all the effort, guidance, patience, and opportunities offered by my advisor, Dr. Slavko Komarnytsky. It would not have been possible without your constant support, history, and culture talks. Every day, there is something new to learn from you. I thank my committee members (Dr. Goodell, Dr. Lila, and Dr. Moncada) for their guidance and for being a valuable part of my journey. Also, I thank Dr. Eroglu for giving me the opportunity to further extend my research expertise.

I am very appreciative of my husband’s support, Dr. Malik for believing in me when my faith was fading. You got my back all the time and endured the long distance and moved continents for the sake of my success and happiness. May we continue doing great things for our family.

To my Mama and Baba, I grew up being called “our doctor”, and you helped me all the way until I was able to fulfill your wishes. My dearest siblings, Khalid, Sara, Mohammad, and beloved Yousef, you were always my guardian angels and gave me unconditional support and laughter. Thank you.

I am very happy and thankful to meet great people here at NCSU and PHHI who contributed in their own way to make this journey happier: Shehla, Catie, Sawsan, Reham, Janelle, Kathya, Connor, Emilize, Wen, Zeren, Dr. Basheer and Dr. Rasha, Fabio, Emilio, Diego, Majd, Dr. Thiru, Pam, Sanaz, Mickey, and Manveen.

TABLE OF CONTENTS

LIST OF TABLES	vii
LIST OF FIGURES	viii
Chapter 1: Progression to Obesity: Variations in Patterns of Metabolic Fluxes, Fat Accumulation, and Gastrointestinal Responses	1
Abstract	1
Introduction	2
Progression to Obesity	4
Calorie Intake	5
Energy Expenditure	6
Obesity as Body Weight Set Point	7
Utilization of Nutrients	9
Macronutrient Selection and Weight Control	11
Pathophysiology of Body Fat Distribution	13
Patterns of Fat Accumulation	13
Ectopic Fat	15
Contribution of Gastrointestinal Microbiota and Inflammation to Obesity	18
Microbiome in Obesity	18
Inflammation in Obesity	21
Conclusions	23
References	25
Chapter 2: Obesity-Resistant Mice on High Fat Diet Display a Distinct Phenotype Linked to Enhanced Lipid Metabolism	41
Abstract	41
Introduction	43
Materials and methods	45
Animals and diets	45
Body composition	46
Energy expenditure	46
Exercise capacity	47
Fecal parameters	48
Fecal microbiome profile	48
Statistical analysis	49
Results	49
Changes in body weight and body weight gain	49
Changes in body composition	52
Metabolic responses to dietary fat	54
Irreversible changes in exercise capacity	58
Food intake and feed efficiency	59
Fecal lipids and microbiome profiles	60
Discussion	62
Conclusions	65
References	67

Chapter 3: Molecular insights into obesity resistance in C57BL/6J mice include biomarkers of muscle fiber dynamics and mitochondrial adaptation to high dietary fat

.....	73
Abstract.....	73
Introduction.....	75
Materials and methods	77
Animals and diets.....	77
Body composition and fat/lean body mass ratios	77
Fasting glucose and oral glucose tolerance (OGTT)	78
Insulin glucose tolerance (ITT).....	78
RNA extraction and cDNA synthesis	79
RT2 Profiler qPCR Array	79
Volatile fecal metabolites	80
Cell culture.....	80
Nitric oxide production and gene expression.....	81
Statistical analysis	82
Results.....	82
Body weight gain and metabolic phenotypes	82
Relative changes in lean and fat body mass.....	83
Nutrigenomic profiling of skeletal muscles	84
Changes in glucose metabolism and insulin resistance	86
Nutrigenomic profiling of skeletal muscle mitochondria	91
Fecal microbiome metabolites	95
Inflammatory responses	97
Discussion.....	100
Conclusions.....	105
References.....	107
Chapter 4: Conclusions and Future Directions.....	115
References.....	118
APPENDICES.....	119
APPENDIX 1- Supplementary data.....	120

LIST OF TABLES

Table 1.1. Energy reserves available to a 70 kg male (kcal)	12
Table 1.2. Turnover fluxes for selected circulating carbon metabolites	18
Table 3.1. Fecal volatile metabolites signatures exhibiting significant differences	97

LIST OF FIGURES

Figure 1.1. Schematic representation of major pathways of energy metabolism	17
Figure 1.2. Microbiota-mediated metabolism of complex carbohydrates.	20
Figure 1.3. Complexity of contributions of the gastrointestinal system to development of multiple obesity phenotypes.	23
Figure 2.1. Flowchart of the study	24
Figure 2.2. Body weight of lean controls (LFD), obese controls (HFD), obesity-resistant non-responders (NR), obesity-prone super-responders (SR), and super-responders fed LFD diet during the study weeks -14 (SR-LFD).....	51
Figure 2.3. Body weight gain of lean controls (LFD), obese controls (HFD), obesity-resistant non-responders (NR), obesity-prone super-responders (SR), and super-responders fed LFD diet during the study weeks -14 (SR-LFD).....	52
Figure 2.4. Body composition of lean controls (LFD), obese controls (HFD), obesity-resistant non-responders (NR), obesity-prone super-responders (SR), and super-responders fed LFD diet, including (a) lean body mass, (b) free water, (c) fat body mass, (d) total water.	53
Figure 2.5. Changes in whole-body energy balance in response to dietary fats as compared among lean controls (LFD), obese controls (HFD), obesity-resistant non-responders (NR), obesity-prone super-responders (SR), and super-responders fed LFD diet	55
Figure 2.6. Exercise capacity of lean controls (LFD), obese controls (HFD), obesity-resistant non-responders (NR), obesity-prone super-responders (SR), and super-responders fed LFD diet at the end of the study.	59
Figure 2.7. Changes in (a) food intake, (b) energy intake, and (c) feed efficiency among lean controls (LFD), obese controls (HFD), obesity-resistant non-responders (NR), obesity-prone super-responders (SR), and super-responders fed LFD diet.	60
Figure 2.8. Fecal outputs and microbiome profiles determined at the end of the study among lean controls (LFD), obese controls (HFD), obesity-resistant non-responders (NR), obesity-prone super-responders (SR), and super-responders fed LFD diet, including (a) fecal pellet weight, (b) fecal fat content, (c) microbiome composition at the phylum level	61
Figure 3.1. Ratios of (a) lean/total body mass, (b) fat/total body mass, and (c) fat/lean body mass as determined by EchoMRI body composition analysis after 14 weeks of high dietary fats challenge in lean controls (LFD), obese controls (HFD), obesity-resistant non-responders (NR), obesity-prone super-responders (SR), and super-responders fed LFD diet (SR-LFD) .	81

Figure 3.2. Nutrigenomic responses to high dietary fats of the obesity-resistant non-responders (NR) versus the normal obese controls (HFD).85

Figure 3.3. Changes in fasting blood glucose as observed after 14 weeks of high dietary fats challenge in lean controls (LFD), obese controls (HFD), obesity-resistant non-responders (NR), obesity-prone super-responders (SR), and super-responders fed LFD diet (SR-LFD).87

Figure 3.4. Parameters of carbohydrate metabolism affected by high dietary fats in lean controls (LFD), obese controls (HFD), obesity-resistant non-responders (NR), obesity-prone super-responders (SR), and super-responders fed LFD diet at the end of the study89

Figure 3.5. Nutrigenomic responses to high dietary fats of (a) lean controls (LFD), (b) obesity-resistant non-responders (NR), (c) obesity-prone super-responders (SR), (d) super-responders fed LFD diet during the second phase of the study (SR-LFD) as compared to the obese controls (HFD), and (e) obesity-resistant non-responders (NR) as compared to the obesity-prone super-responders (SR).....92

Figure 3.6. Shifts in the phylum-level microbiome profiles determined at the end of the study among lean controls (LFD), obese controls (HFD), obesity-resistant non-responders (NR), obesity-prone super-responders (SR), and super-responders fed LFD diet96

Figure 3.7. Effects of selected metabolites on nitric oxide production in activated macrophages, including (a) acetic acid, (b) ammonium acetate, (c) butanoic acid, (d) 2-methylbutanoic acid, (e) trans-2-dodecenol, and (f) citric acid98

Figure 3.8. Heatmap of anti-inflammatory effects of trans-2-dodecenol based on the qPCR gene expression profiles of key biomarkers of acute and chronic inflammation, including inducible nitric oxide synthase (iNOS), cyclooxygenase-2 (Cox-2), tumor necrosis factor alpha (TNF- α), interleukins IL-1 β , IL-6, IL-17 and IL-1899

CHAPTER 1- Progression to Obesity: Variations in Patterns of Metabolic Fluxes, Fat Accumulation, and Gastrointestinal Responses

Abstract

Obesity is a multifactorial disorder that is remarkably heterogeneous. It presents itself in a variety of phenotypes that can be metabolically unhealthy or healthy, associate with no or multiple metabolic risk factors, gain extreme body weight (super-responders), as well as resist obesity despite the obesogenic environment (non-responders). Progression to obesity is ultimately linked to the overall net energy balance and activity of different metabolic fluxes. This is particularly evident from variations in fatty acids oxidation, metabolic fluxes through the pyruvate-phosphoenolpyruvate- oxaloacetate node, and extracellular accumulation of Krebs cycle metabolites, such as citrate. Patterns of fat accumulation with a focus on visceral and ectopic adipose tissue, microbiome composition, and the immune status of the gastrointestinal tract have emerged as the most promising targets that allow personalization of obesity and warrant further investigations into the critical issue of a wider and long-term weight control. Advances in understanding the biochemistry mechanisms underlying the heterogenous obesity phenotypes are critical to the development of targeted strategies to maintain healthy weight.

Published as:

Milhem F, Komarnytsky S. Progression to Obesity: Variations in Patterns of Metabolic Fluxes, Fat Accumulation, and Gastrointestinal Responses. *Metabolites*. 2023;13(9):1016. doi:[10.3390/metabo13091016](https://doi.org/10.3390/metabo13091016)

1. Introduction

The prevalence of obesity worldwide has increased in the last several decades indicating a global obesity trend [1]. Between 1980 and 2015, the prevalence of obesity doubled in 73 countries, largely in direct correlation with the sociodemographic development statuses of the countries studied (Global Burden of Disease study) [2]. Unexpected rapid increases in obesity prevalence were observed even in previously considered “safer” younger populations of 25-to-29-year old men residing in low-middle degree developmental countries, where the obesity rates tripled from 1.1% in 1980 to 3.8% in 2015 (NCD-RisC study) [3]. In the U.S., the National Health and Nutrition Examination Survey (NHANES) tracks similar obesity trends over a long period of time through repeated cross-sectional surveys of the population [4]. The prevalence of obesity in the U.S. was estimated to be 33.5% in men and 35.7% in women in 2005–2006 [5], and it increased to 36.5% in men and 40.8% in women in 2013–2016 [6]. In the most recently released NHANES data (2020), 42.4% of adults and 20.9% of youth are obese [6]. In some countries, obesity rates plateaued at alarming levels. One of the highest, obesity prevalence in Jordan reached 60.4% among men and 75.6% among women [7]. Another evaluation of Jordanian women age 18 and older showed that 70.6% were overweight or obese as defined by body mass index (BMI) [8]. This increase is related to modern obesogenic environments, which are influenced by the decrease in physical activity and conversions in food systems [9].

BMI, however, is a simple and convenient index to monitor the obesity that overlooks the remarkable heterogeneity of obesity when people with similar body weights or BMI can present with different sets of metabolic risk factors and comorbidities despite similar stratifications [10]. This heterogeneity presents itself as the wide spectrum response to positive

energy balance [11] that includes additional metabolically unhealthy individuals (normal weight phenotypes), obese individuals with no associated metabolic risk factors (metabolically healthy phenotypes), extreme obesity (super-responder phenotypes), and healthy individuals that resist obesity despite the obesogenic environment (obesity resistant or non-responder phenotypes) [12]. The diversity of the obesity phenotypes could be explained in part by differences in visceral (central, abdominal) adipose tissue distribution and ectopic fat accumulation that are not captured by BMI [13]. While a general measure of visceral obesity can be estimated by taking the waist circumference (a single threshold of 102 cm in men and 88 cm in women in the U.S. or 94 cm for men and 80 cm for women in Europe), more advanced analyses, such as MRI and CT scan, are often necessary [14]. Visceral obesity follows the general obesity trends; in U.S. adults it increased from 29.1% for men and 46.0% in women in 1988–1994 to 42.0% for men and 61.5% for women in 2009–2010 [15]. However, visceral obesity is an independent marker of morbidity and mortality [16] and is associated with metabolic risk factors, such as hyperlipidemia, cardiovascular diseases, and systemic inflammation [17]. These effects may be mediated by a variety of pathophysiological abnormalities, including changes in fat deposition, adipocyte function, inflammatory and adipokine responses, and insulin resistance [13]. It is presently not clear how visceral obesity and associated metabolic dysregulation contribute to the development of the vast spectrum of obesity phenotypes; however, it is generally accepted that it adds to the unexpected observations that obesity may differently affect mortality risks in chronic disease states and fit obese individuals, with overweight status being somewhat protective in normal populations, and metabolically healthy obese states being advantageous over the spectrum of other obesity-related outcomes [18].

The variety of individual responses to obesogenic environment and the onset of obesity and their relationship to various health outcomes are not fully understood. Apart from the compounding genetic and lifestyle variables, two parameters are considered as the main contributors to an individual's response to obesity: metabolic perturbations in visceral fat alongside ectopic accumulation of fat in the liver and enhanced inflammatory responses associated with visceral fat activation. Our understanding of the altered cellular metabolism, often driven by mitochondrial dysfunction to produce metabolic disparity, which in turn influences inflammation and energy balance in the metabolically active tissues, is critically lacking. These areas are the focus of the present review.

2. Progression to Obesity

Adipose weight gain may appear at any age with certain trends in different age groups, including children, adolescents, and adults, with differences between genders [19]. It is modulated through dietary intake, physical activity, and metabolism, all which are affected by genetic traits [20]. Socioeconomic influences and social vulnerability further affect obesity rates in communities [21]. Adolescence obesity commonly occurs before the age of 5 and continues into adulthood, specifically if one of the parents is obese [22]. The risk of developing obesity in early life can also be influenced by the mother's excessive weight, high BMI, and type 2 diabetes mellitus during pregnancy [23]. The weight trajectory varies between women and men, with women experiencing more fluctuations throughout their lives [24]. There are at least three developmental stages at which women are at greater risk to gain adipose tissue, after puberty starts [25], after their first pregnancy [26], and when they reach menopause [27].

Research studying male obesity is not widespread due to a variety of social and cultural stigmas [28].

Progression to obesity is ultimately linked to the overall energy balance of the body when energy intake (EI) exceeds energy expenditure (EE) [29]. The excess energy is deposited in body tissues, including conventional adipose depots as well as ectopic accumulation in the non-target organs, such as liver and muscle [30], based on the individual hypothetical body weight set points and patterns of fat accumulation.

2.1. Calorie Intake

An important factor in the control of body weight is dietary energy density (DED) as it correlates with increase in body weight [31]. Energy density levels range from 0 kcal/g to 9 kcal/g and are determined by the macronutrient composition and moisture content of meals and drinks, with pure carbohydrate or protein (4 kcal/g each), ethanol (7 kcal/g), and fat (9 kcal/g) being the major sources of caloric intake [32]. However, energy intake does not essentially represent total energy absorption [33]. For this reason, the previously reported Wishnofsky guideline that recommends achieving a daily 500–750 kcal deficit to support adult weight loss [34] may no longer hold true as it does not account for either catabolism-induced differences in energy expenditure among macronutrients [35] or the modern shift towards energy-dense foods depleted of essential nutrients known to act against metabolic disorders [36]. At the same time, a constant error of 175 kcal energy intake per day may translate to 3 kg body weight gain or loss per year, suggesting that such a small margin of error cannot be fully controlled at the individual level [37].

Even though twin studies suggested significant heritability for the amounts of foods and fluids ingested, short-term energy intake appears to be unregulated and varies spontaneously within a relatively wide range [38]. However, long-term trends in body weight changes lead to alterations in physiology and the nature of the food consumed to replace loss or avoid gain, and this phenomenon shows high individual variability in the range of 40% to 100% energy compensation [39]. This compensation is not immediate as it is not observed after 1–2 days following the deviation from the average energy intake but reaches significance after 3–4 days of observations [40].

2.2. Energy Expenditure

The second major variable in the relationship of obesity with energy imbalances is energy expenditure [41]. Daily energy expenditure varies based on basic metabolic rate, type, and duration of physical activity, sleep patterns, and variations in body temperature. The compounding nature of energy expenditure mechanisms includes resting metabolic rate (RMR, cellular metabolism, and digestion processes), non-exercise activity (NEAT, including habitual sitting, standing, walking, and social interaction activities), low-intensity and high-intensity work or exercise-related activity, and environment-related adaptive thermogenesis [42]. While generally believed that changing levels of physical activity could equilibrate the energy intake and promote a negative energy balance, the scale of the compensatory mechanisms is often overlooked. For example, an adult consuming 290 kcal meal is expected to walk for around 90 min or 5 km to regain the hypothetical net energy balance [43]. For this reason, the direct relationship between obesity and physical activity in long-term longitudinal studies is not as

prominent [44,45]. Significant associations between physical activity with incident obesity were reported in three subsequent longitudinal studies published after 2012 [46].

Energy expenditure was found in the reciprocal compensatory adaptation loop with dietary intake [47]. First, habitual NEAT may decrease in response to increased exercise, especially if it is associated with fatigue or discomfort [48]. Second, exercise may be associated with at least a partial compensatory increase in energy intake [49], although high-intensity exercise may have the opposite effect due to reduced appetite and delayed gastric emptying [50]. These effects may also correlate to individual differences in carbohydrate and fat metabolism as at least one study showed lower energy intake in subjects with higher fat oxidation rates [51]. Third, reduced energy intake in the form of caloric restriction is generally associated with lower physical activity [52]. However, the overall mismatch in net energy balance does not continue indefinitely and at some point, increased energy expenditure always results in an increase in energy intake as a protective adaptation for long-term body weight preservation [53].

2.3. Obesity as Body Weight Set Point

Typical variance in individual body weights is very small over both short-term (0.5% over 6–10 weeks) and long-term, even when associated with chronic metabolic disorders (3–4% over 5 years) [54]. The observed weight stability is suggestive of homeostatic control, colloquially defined as a body weight “set point” (or settling point). Resting metabolic rate consisting of energy expended from skeletal muscles and the digestive tract comprises near 70% of total energy expenditure and has a major impact on the dynamic equilibrium of weight maintenance [55]. Thermic effect of physical activity of the skeletal muscles (10–20%) and

the adaptive thermogenesis in skeletal muscles and brown adipose tissue (5–10%) form secondary streams of the total energy expenditure. In the resting state, 70% of energy is generated via mitochondrial ATP production, 20% as compensation for proton leakage and 10% is non-mitochondrial [56]. However, obese states have higher basal metabolism than lean states, suggesting that adipose tissue also contributes to energy expenditure [57]. When food intake was restricted, a reduction in metabolic rate and heat production occur to facilitate a return to the set weight [58]. The set weight also seems to increase annually at the small average rate of 0.2–0.3 kg per year, and considering the large amount of calories consumed at the same time, other physiological factors must be considered at least partially responsible for this increase [39]. Additionally, nearly 20% of subjects showed little body weight change over the observed period, suggesting high individual differences and the existence of non-responders that manage to maintain their body weight [59].

Such a nearly precise control of body weight over long periods of time then questions the notion that the onset and progression to obesity are major disturbances of metabolic homeostasis. The emerging evidence suggests that the primary inability to maintain weight is linked to the rate of replacement of energy lost due to caloric restriction (dieting) or increased physical activity (expenditure). In obese states, the reduction of caloric intake was not compensated only when low-energy dense foods were consumed [60]. In other words, high-energy dense foods delayed satiety and allowed for overcompensation, even if similar amounts of foods were consumed [61].

As such, a variety of fasting forms and food restriction practices will be effective for promoting initial weight loss [62] but will fail to prevent the long-term compensatory mechanisms from defending the overweight set point and returning to it within 1–3 years [63].

Modulation of individual socioeconomic choices to consume certain types of food and at a certain frequency are often routed in the activity of several neurophysiological factors that arise from dopamine, opioid, endocannabinoid, and melanocortin regulatory networks [64], which add an additional level of complexity in the attempt to understand individual variability under *ad libitum* food intake.

2.4. Utilization of Nutrients

Human subjects spending several days in the metabolic chambers typically show low variations in energy expenditure (2%) and high variations in food intake (20%) [65], thus pointing at dietary intake as a more critical individual determinant of energy homeostasis. From these numbers, it is also reasonable to conclude that (i) variations in the resting metabolic rate alone are not sufficient to justify the onset and progression to obesity, and (ii) failure to adjust food intake to the current energy expenditure must be the major culprit.

Three macronutrients found in all foods in different proportions have different efficiencies of nutrient utilization, with different fats (2–3%), carbohydrates (6–8%), and proteins (25–30%) associated with energy losses due to differences in their metabolism and storage [66]. Digestion of a carbohydrate meal and extra glucose appearance in the bloodstream stimulates glucose uptake and oxidation in the insulin-sensitive tissues coupled with a simultaneous suppression of lipolysis and lipid oxidation [67]. All dietary glucose is typically oxidized within 24 h of intake (glycolysis to acetyl-CoA that enters Krebs cycle) due to the limited capacity of body carbohydrate storage in the form of glycogen [68] and a very limited ability of human tissues to metabolize glucose into fatty acids via *de novo* lipogenesis (2–4%) [69]. Thus, dietary carbohydrate will favor suppression of fat metabolism and fat deposition

into the adipose tissue via insulin signaling [70]. Early insulin response (30 min after food ingestion) rather than maximum insulin response seems to better predict changes in fat mass and body weight gain [71].

The macronutrient capacity to promote satiety follows a similar pattern (protein > carbohydrate > fat), with fats typically more likely to promote overconsumption of energy and the subsequent weight gain. However, subjects with increased capacity to oxidize fat appear to gain little weight under these conditions and therefore, present with a non-responder phenotype [72]. A hidden variable in this progressive transformation towards increased fat production and storage is the fact that it requires higher energy demands to support the additional adipose tissue as well as larger lean body mass to sustain a similar level of physical activity. Together, these compensatory body weight gains may result in a new setpoint that is defended as a part of the revised homeostatic control.

One of the key substrates that connects utilization of macronutrients is oxaloacetate, a Krebs cycle intermediate. Oxaloacetate is typically regenerated within the Krebs cycle; however, this molecule forms a core metabolism node that connects to gluconeogenesis and the regeneration of glucose in the liver from non-carbohydrate substrates, such as amino acids and glycerol, during prolonged fasting or diabetes [73]. When dietary intake is balanced, oxaloacetate is replenished in the liver through glycolysis glucose > pyruvate > oxaloacetate to support normal fatty acid oxidation within the Krebs cycle. In the adipose tissue, oxaloacetate can also exit mitochondria via interconversion to citrate, and the cytosolic oxaloacetate is then used for fatty acid synthesis. Oxaloacetate also participates in the reduction of elevated levels of free fatty acids by conversion to phosphoenolpyruvate and glycerol that is used for their re-esterification to triglycerides [74]. Therefore, when oxaloacetate is

excessively used in other metabolic pathways, its concentration in the Krebs cycle decreases to the point that acetyl-CoA can be no longer used for energy production. In this instance, acetyl-CoA is diverted to the ketogenic formation of acetoacetate, hydroxybutyrate, and acetone [75]. A similar metabolic shift is also observed during the intermittent fasting [76], although an 18 h fast is often not sufficient to fully deplete the glycogen stores [77]. Finally, depleted oxaloacetate levels can be replenished via consumption of amino acids derived from proteins and catabolism of lean body mass.

Several Krebs cycle metabolites can exit mitochondria, including citrate and malate. Plasma citrate levels are typically elevated in obesity, and inhibition of the mitochondrial citrate carrier, Slc25a1, reverts steatosis, glucose intolerance, and inflammation in metabolic disorders [78]. Citrate also plays an important role in the reprogramming of metabolic pathways upon activation of immune cells and onset of inflammation [79], although exact molecular mechanisms and effector functions of Krebs cycle metabolites in the pathophysiology of obesity remain unknown.

2.5. Macronutrient Selection and Weight Control

To better understand how macronutrients interact to maintain a stable body weight, we need to evaluate the typical energy stores available to the body and how newly ingested energy is partitioned into these stores (Table 1). In healthy states, only 5 g of free glucose are present in the bloodstream and 15–25 g in the whole body, which are negligible amounts when compared to 200–350 g of daily carbohydrate intake. Since glucose is oxidized at the maximum rate of 10 g/h, most of the ingested carbohydrate must be imported into the metabolically active tissues and stored as glycogen [80]. The body glycogen reserve is therefore similar to a daily

carbohydrate intake and is tightly regulated; thus, carbohydrates are immediately and preferentially metabolized when available.

In contrast, dietary fat is primarily targeted for deposition. This is achieved via a series of hydrolysis and re-esterification steps during which triglycerides are broken down to free fatty acids and glucose in the intestine, reassembled in the intestinal cells, secreted into the mesenteric lymphatic system, hydrolyzed on the surface of the epithelial cells of the adipose tissue capillaries, and re-esterified once again when they enter adipocytes for storage [81]. Insulin secreted in response to the carbohydrate load of the mixed meal further facilitates fat storage and decreases fat oxidation. Since the insulin-signaling network is primarily responsible for the precise regulation of carbohydrate metabolism, its indirect effects on lipid metabolism are not expected to be exact or follow predictable compensation patterns. For this reason, errors of fat metabolism are believed to be the primary determinants of long-term energy balance and should be thoroughly investigated for their relationships to individual variability and progression to obesity.

Table 1.1. Energy reserves available to a 70 kg male (kcal, after [77]).

Tissues	Carbohydrates (Glucose, Glycogen)	Proteins (Mobilizable)	Fats (Triacylglycerols)
Liver	400	400	450
Muscle	1200	24,000	450
Adipose	80	40	135,000
Blood	60	0	45
Brain	8	0	0

When compared with fat energy reserves typically available to the body (Table 1), short-term effects of high-fat meals are expected to be negligible. Long term, however, the body responds to excessive fat intake by expanding its capacity to store fat by increasing the number of adipocytes in the various adipose tissue depots. This gradual expansion is expected

to continue until a sufficient amount of adipose tissue is developed to successfully match the current fat intake to the appropriate fat oxidation rates that ensure a new equilibrium. The long-term nature of this process holds the potential to amplify even minor individual differences in lipid metabolism and adipocyte differentiation to achieve substantial variability and the emergence of both super-responder and non-responder phenotypes. Substantial physical activity may counteract these effects by increasing substrate oxidation in muscle and post-activity depletion of glycogen reserves both in muscle and liver, with the liver shift from a glucose-removing to a glucose-producing state being an important checkpoint for changes in the overall energy balance.

3. Pathophysiology of Body Fat Distribution

Adipose weight gain may appear at any age with certain trends in different age groups, including major developmental shifts, such as puberty, adolescence, pregnancy, menopause, and normal physiological aging. Adipose tissue tends to increase in middle age and decrease in the elderly, and this change is often accompanied by fat redistribution from subcutaneous tissue to abdominal and ectopic locations [82]. The wide range of individual obesity phenotypes presented by these populations as well as the increased risk of developing insulin resistance that is associated with both excessive and insufficient fat mass [83] suggests that intrinsic differences between adipose tissue depots may be in part responsible for this variation.

3.1. Patterns of Fat Accumulation

Unequal distribution of the adipose tissue among individuals paired together with different levels of ectopic fat deposition and inflammatory dysregulation add another level of complexity to homeostatic control of the body weight [13]. Different locations and/or rates of

the adipose tissue expansion suggests the maximum capacity of adipose tissue expansion as another individualized trait, possibly under genetic control [84]. Regional fat distribution is strongly influenced by genetic factors as shown in young and elderly twins [85]. Additionally, in GWAS studies, several developmental genes have been suggested to correlate with adiposity and fat distribution, including white fat adipogenesis and browning of the adipose tissue [86].

The major striking difference between individual fat depots is observed in the subcutaneous versus visceral (intraabdominal) adipose tissue, where transplantation of the subcutaneous fat into the visceral cavity improves body weight, adiposity, and carbohydrate metabolism but not vice versa [87]. Increased visceral fat is also associated with a greater risk of type 2 diabetes in obese but otherwise healthy subjects [88]. Individual variations in visceral fat accumulation may depend on gender and ethnicity [89]. The molecular mechanisms responsible for these genetic effects are largely not determined at the present time. Overall, around 80–90% of adipose tissue is accumulated in subcutaneous depots, including the abdominal, subscapular, gluteal, and femoral areas [90]. Females have significantly greater mean anterior and posterior subcutaneous fat than in males. However, males possess more posterior fat than anterior fat in their body, whereas women have no difference between posterior and anterior fat distribution [91]. Comparing individuals of similar weight and age, females have an additional 22 mm of subcutaneous fat mainly accumulated in the breasts and posterolateral sites [92]. Although women have higher subcutaneous fat accumulation and men accumulate more visceral fat, estrogen decrease post menopause causes an increase in visceral fat [93]. On the contrary, lower body subcutaneous fat is associated with a lower risk of metabolic and cardiovascular complications, possibly due to increased capacity to support the

triglyceride clearance, a healthier lipid profile, and a healthier energy reserve that protects the body from lipotoxicity [94].

Both dietary change and aerobic exercise (walking, running, swimming) were correlated with weight loss and preferential loss of visceral fat; however, the correlation for diet was strong ($R^2 = 0.737$, $p < 0.001$) and the one for exercise was modest ($R^2 = 0.451$, $p < 0.001$) [95]. This effect may be partially responsible for the success of surgical therapies, such as gastric bypass or gastric sleeve to preferentially reduce visceral fat by 40% as they typically lead to substantial dietary changes [96]. Prolonged sedentary patterns associated with watching TV/video are more likely to promote visceral adiposity and increase metabolic risk across all sex and gender groups, with a clear dose-response relationship evident after 2 h per day [97].

3.2. Ectopic Fat

The subsequent failures of subcutaneous and visceral fat to increase lipid storage capacity under the conditions of excessive energy reserves culminates in ectopic partitioning of fat to other organs and tissues, such as muscle and liver. Excess fat can be deposited intracellularly in the form of triglycerides as observed in liver hepatocytes under the condition of the nonalcoholic fatty liver disease (NAFLD) or alternatively deposited into newly developed adipocytes that infiltrate the parenchyma of other organs, such as pancreas [98]. Subsequent ballooning of the cells and infiltration of the organ tissues with inflammatory cells leads to a more aggressive presentation, including steatosis and/or fibrosis. Perilipin 2 (Plin2), a major protein found on the surface of the oil bodies, was shown to be one of the major players in this process [99]. Dysregulated ectopic fat tissue is believed to be the factor that promotes

and sustains insulin resistance, thus being a dominant regulator of glucose and lipid metabolism [100].

Local paracrine affects the visceral cavity as expected for mesenteric, pararenal, and epicardial fat depots and could be partially responsible for detrimental metabolic effects associated with the expansion of visceral fat; however, they remain virtually not explored. Direct and potentially continuous delivery of gluconeogenic substrates (Figure 1), such as fatty acids and glycerol [101], from the mesenteric fat into the portal circulation and therefore, to the liver, hold potential to sustain liver tissues in the glucose-producing state, despite the actual fed status of the body. In these metabolic states, individual diversity of obese phenotypes is driven by their ability to sustain higher subcutaneous adipogenesis (a larger number of smaller adipocytes in the adipose tissues), with less visceral adiposity and ectopic lipid accumulation [102]. Overfeeding young subjects by 40% of their energy requirement for only 8 weeks caused a 7.6 kg weight gain, induced visceral and hepatic lipid deposition and mild hepatic and skeletal muscle insulin resistance, and triggered systemic and skeletal muscle inflammation [100].

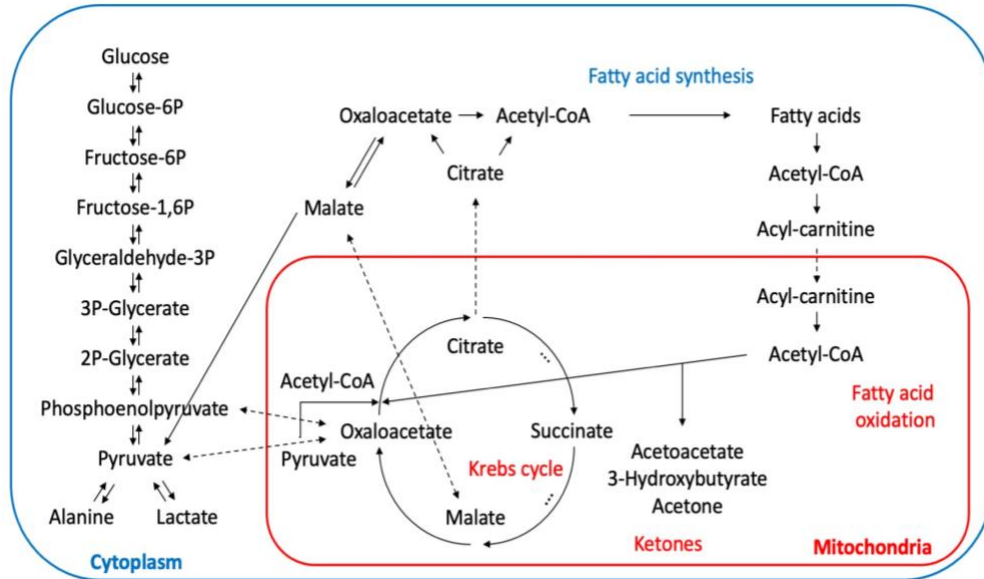


Figure 1.1. Schematic representation of major pathways of energy metabolism. Pyruvate (rapidly interconverted to lactate and back) forms a primary energy metabolism node with phosphoenolpyruvate and oxaloacetate that connects carbohydrate, lipid, and protein metabolism. Pyruvate, citrate, and malate can be shuffled between cytosol and mitochondria to change the direction of metabolic fluxes.

The reduced capacity to oxidize fatty acids in the muscle due to disturbances in mitochondrial metabolism (metabolic inflexibility) [103] is one of the reasons of ectopic fat accumulation in skeletal muscle tissues. In healthy states, the insulin-driven uptake of lipids triggers their acylation with CoA and transfers into mitochondria for beta-oxidation (Figure 1). In insulin-resistant states, it triggers the inhibition of lipolysis, the accumulation of diacylglycerides, and the slower esterification of free fatty acids [104]. While skeletal muscle gene expression profiles remained similar for triacylglyceride synthesis (DGAT1/2, GPAT1) and ceramide synthesis (SPTLC1/2, ASAH2, CERK), oxidative metabolism was clearly reduced (mCPT1, PGC1 α , PPAR α/δ , SDHB, NDFU5B) [104]. Acetyl-CoA, derived from

beta-oxidation or pyruvate oxidation (Figure 1), is the only fuel that enters the Krebs cycle and cannot be transported outside of mitochondria. For this reason, the Krebs cycle can be broken at certain points as citrate can be transferred to cytosol to increase fatty acid and cholesterol synthesis, while malate can be transferred to cytosol and promote gluconeogenesis via conversion to oxaloacetate.

Somewhat surprising, lactate derived from anaerobic glycolysis showed the major contribution to metabolic fluxes through the Krebs cycle in all tissues except the brain [105] (Table 2). Low metabolic fluxes of citrate, succinate, and malate may suggest that circulating levels of these metabolites represent the long-term trends of energy metabolism and the net energy balance in the body. The quantitative relevance of these circulating metabolic intermediates as fuels remains unclear and warrants further investigation.

Table 1.2. Turnover fluxes for selected circulating carbon metabolites (adapted from [105]).

Metabolite	Flux Rate (nmol g⁻¹ min⁻¹)
Lactate	374.4 ± 112.4
Glucose	150.9 ± 46.7
Acetate	72.7 ± 17.5
Alanine	70.2 ± 5.4
Pyruvate	57.3 ± 14.2
Glycerol	53.3 ± 2.1
Glutamine	45.6 ± 4.7
3-Hydroxybutyrate	43.3 ± 17.1
Palmitic acid	24.6 ± 4.2
Citrate	16.2 ± 6.6
Succinate	3.1 ± 1.1
Malate	2.0 ± 0.4

4. Contribution of Gastrointestinal Microbiota and Inflammation to Obesity

Dietary factors, the intestinal microbiota that partially digests them [106], and their metabolites [107] shape visceral fat accumulation (mesenteric fat), intestinal permeability and

activation, the transient migration of immune cells [108], and intestinal hormone responses. Understanding these pathways may provide additional clues towards high diversity and individual variability of obese phenotypes.

4.1. Microbiome in Obesity

The human body hosts a complex community of microorganisms, such as bacteria, fungi, protozoa, and viruses, that make up the microbiome. The gastrointestinal micro-biome is dominated by bacteria, the majority of which inhabit the colon at a concentration range of 10⁹–10¹² CFU/mL [109]. The model minimal microbiome includes seven major phyla and one hundred seventy-one microbial genomes: *Firmicutes* (104), *Bacteroidetes* (29), *Proteobacteria* (22), *Actinobacteria* (12), *Fusobacteria* (2), *Verrucomicrobia* (1), and *Euryarchaeota* (1) [110]. Trace phyla may further include *Lentisphaerae*, *Spirochaetes*, *Thermotogae*, *Synergistetes*, *Tenericutes*, *Elusimicrobia*, and *Cyanobacteria* [111]. As gut microbiota affects nutrient acquisition and energy harvest and feeds metabolites into a wide variety of host metabolic pathways, the effective matching of metagenomic and metabolite profiles of the intestinal microbiome is critically required to understand these contributions [112].

Age, race, geographical location, and ethnicity often present with variations in gut microbiota, which are larger than interpersonal differences and may be attributed to dietary patterns, food composition, and its availability [113]. The major source of energy harvested and used by the gut microbiome are simple and complex carbohydrates that were not digested by the host organs (Figure 2). In addition to the short-chain fatty acids (propionate, acetate, butyrate) that can be absorbed and metabolized by enterocytes, these carbon fluxes can be

further fermented into methane, carbon dioxide, and hydrogen [114]. Once again, pyruvate remains as a central node that connects different energy pathways, and the contributions of bacterial lactate and metabolites of Krebs cycle to the host metabolism are poorly understood.

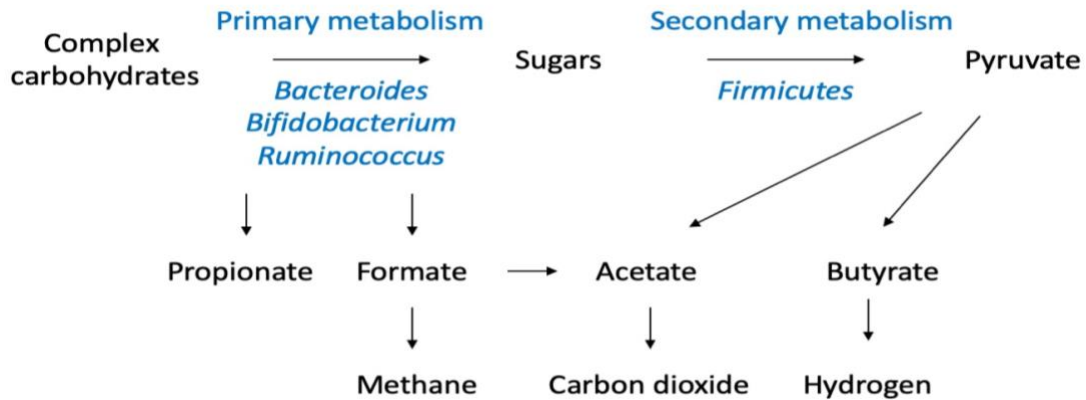


Figure 1.2. Microbiota-mediated metabolism of complex carbohydrates. Different groups of bacteria preferentially utilize polymeric, oligomeric, monomeric carbohydrates and short-chain fatty acids to complete the fermentation process in the gastrointestinal lumen (adapted from [106]). Variations in microbiome composition, substrate availability, luminal oxygen, and inflammatory status of the gastrointestinal tissues are expected to contribute to the diversity of the metabolic outcomes.

Bacterial fermentation of complex carbohydrates as a part of plant-based dietary patterns that are especially evident in vegetarian or vegan diets contributes to lower pH levels of the intestinal lumen and feces [115]. Healthy fermentation also rapidly depletes luminal oxygen to promote a proper anaerobic environment in the gut that can be altered through increased inflammation and blood flow in the intestine [116] as well as high-fat diets [117]. Dietary fats also stimulate the production of bile acids that promote the emulsification and absorption of lipids, cholesterol turnover, and the harvest of the fat-soluble vitamins. Bile acids, however, also present with selective antimicrobial properties and typically enrich gut

microbiota with bile-acid-tolerant *Bacteroides*, *Alistipes*, and *Bilophila*. Both obese *ob/ob* mice as well as obese human subjects had marked reductions in Bacteroidetes and compensatory increases in Firmicutes, thus showing abnormal *Bacteroidetes/Firmicutes* ratios [118]. In the absence of the gut microbiota, however, germ-free mice do not develop obesity despite consuming high-carbohydrate or high-lipid diets, suggesting that the microbiome is critical for excessive energy harvest and retention [119].

Metabolic fates of different short-chain fatty acid metabolites are different, suggesting that certain microbiome profiles and host–microbiome interactions may be more beneficial than others. While bacteria-derived butyrate has a rapid turnover flux similar to 3-hydroxybutyrate and are mostly consumed in situ to support colonic epithelium, propionate is targeted by the liver into the gluconeogenesis pathway, and acetate feeds into lipid metabolism [120]. Likewise, the metabolism of unassimilated amino acids and dietary phenolic acids yields glycine conjugates of phenylpropionic and glutamine conjugates of phenylacetic acids as a part of the xenobiotic detoxification response and de-toxification of waste nitrogen [107]. The intestinal epithelial tissues also express a wide variety of the extraoral bitter taste receptors family (T2R, TAS2R) that do not support the bitter sensing in the gut but act as chemosensors to detect many dietary and micro-biota-derived metabolites, such as N-acyl-homoserine lactones [121], that modulate host–microbiome interactions, immune responses, and nutrient absorption [122].

4.2. Inflammation in Obesity

Inflammatory cells that infiltrate the hypertrophic adipose tissue find themselves in the ischemic environment that promotes their polarization towards pro-inflammatory states. Both

lipid-overloaded adipocytes and associated inflammatory cells provoke insulin resistance [123] in an effort to gain access to more rapid but less efficient, energy fluxes that are generated by glycolytic pathways and not oxidative phosphorylation (Figure 1). Metabolic dysfunction therefore expresses itself as a low-grade inflammation, insulin resistance, and metabolic homeostasis disruption [124]. These signals can be further modified by the adipose tissue adipokines. Expanding adipose tissue releases different levels of leptin and adiponectin, with leptin levels generally associated with total fat mass, and adiponectin levels loosely associated with increased subcutaneous depots [125].

Inflammation of the adipose tissues promotes *de novo* lipogenesis, reduces fat oxidation in mitochondria, and accumulates ceramides and diacylglycerides in the metabolically active cells that inhibit insulin signaling [126]. Similar to metabolic mediators, inflammatory cytokines, such as TNF- α , IL-6, and IL-1 β , also impair the insulin-signaling pathway, leading to insulin-resistant metabolic conditions [127]. These pro-inflammatory signals circulate to the periphery, where they affect the liver to increase infiltration with resident Kupffer cells and skeletal muscle to promote M1 macrophage infiltration [128]. The gastrointestinal tract that represents a major component of the immune system responds similarly by increasing intestinal perfusion, reducing the integrity of the epithelial barrier, and enhancing recognition of the food and microbial antigens that diffuse from the intestinal lumen [129]. Together, this leads to a highly variable gastrointestinal inflammatory response that depends on the part of the gastro-intestinal tract involved (Figure 3). As mesenteric fat is closely associated with the gastrointestinal tissues and feeds its metabolites directly into the portal circulation, the process is likely to sustain liver tissues in the glucose-producing state, thus contributing to hyperglycemia and oxidative stress. Activated immune cells achieve faster

energy fluxes by lowering their metabolic efficiency and relying nearly exclusively on the faster glycolytic reactions in the cytosol [130].

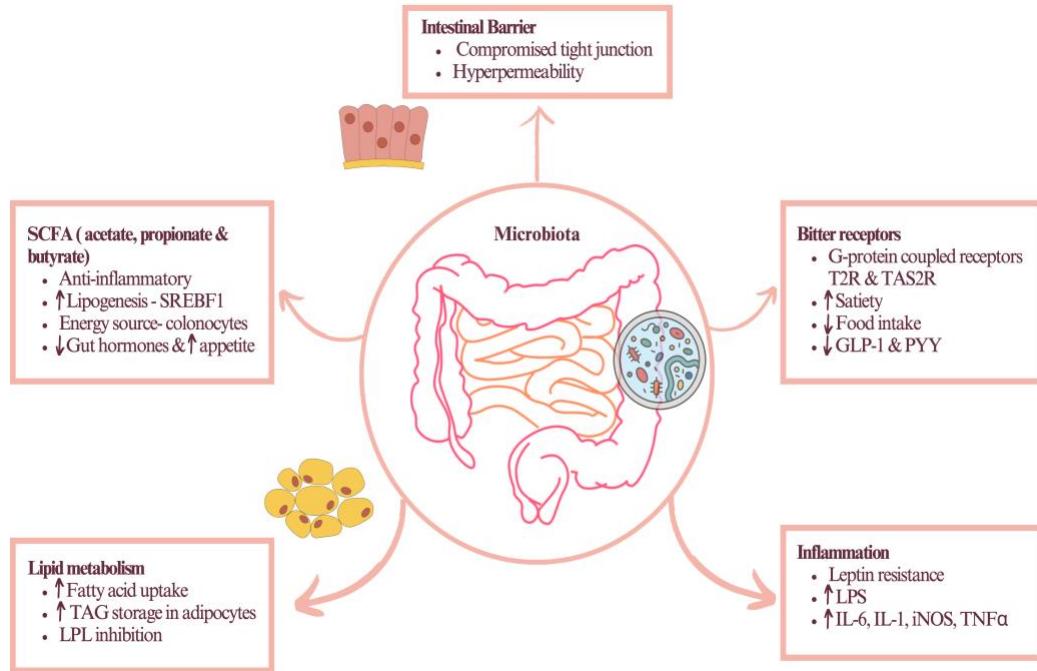


Figure 1.3. Complexity of contributions of the gastrointestinal system to development of multiple obesity phenotypes. Variations in microbiome-derived short-chain fatty acids, intestinal permeability, dietary metabolites, inflammatory signals, and chemoreceptors responsible for sensing nutrient and immune status of host-microbiome interactions all contribute to complexity of gastrointestinal signaling in obesity. Up (↑) and down (↓) arrows indicate increases or decreases in the levels of the indicated metabolites, respectively.

5. Conclusions

The etiology of obesity is very complex, with individual genetic, metabolic, microbiome, and lifestyle factors defining multiple pathophysiological states of this disorder.

To achieve and sustain meaningful weight loss as well as support individuals with different obesity types, we need to understand the molecular mechanism behind this classification. Variations in fatty acids oxidation, metabolic fluxes of different energy substrates with a particular focus on pyruvate-phosphoenolpyruvate-oxaloacetate node, high turnover rates of lactate, and extracellular accumulation of Krebs cycle metabolites, such as citrate, emerged as the most promising metabolic targets that allow personalization of obesity and warrant further investigations.

The additional modulation of gut microbiota [119] and brain axis [131] through dietary interventions, pharmacological treatments, and surgery provides a unique set of tools to individually address multiple obesity phenotypes. For example, phenotype-guided pharmacotherapy with phentermine-topiramate (hungry brain), bupropion-naltrexone (emotional hunger), liraglutide (hungry gut), and low-dose phentermine plus resistance training (slow burn) shows a very interesting recent example of such an approach [132]. Given that the existing body weight is actively maintained and protected, we need to understand how to overcome the multiplicity of the obesity mechanisms and metabolic fluxes that sustain them.

REFERENCES

1. Inoue, Y.; Qin, B.; Poti, J.; Sokol, R.; Gordon-Larsen, P. Epidemiology of Obesity in Adults: Latest Trends. *Curr Obes Rep* **2018**, *7*, 276–288, doi:10.1007/s13679-018-0317-8.
2. GBD Collaborators Health Effects of Overweight and Obesity in 195 Countries over 25 Years. *New England Journal of Medicine* **2017**, *377*, 13–27, doi:10.1056/NEJMoa1614362.
3. Abarca-Gómez, L.; Abdeen, Z.A.; Hamid, Z.A.; Abu-Rmeileh, N.M.; Acosta-Cazares, B.; Acuin, C.; Adams, R.J.; Aekplakorn, W.; Afsana, K.; Aguilar-Salinas, C.A.; et al. Worldwide Trends in Body-Mass Index, Underweight, Overweight, and Obesity from 1975 to 2016: A Pooled Analysis of 2416 Population-Based Measurement Studies in 128·9 Million Children, Adolescents, and Adults. *The Lancet* **2017**, *390*, 2627–2642, doi:10.1016/S0140-6736(17)32129-3.
4. Cameron, N.A.; Petito, L.C.; McCabe, M.; Allen, N.B.; O'Brien, M.J.; Carnethon, M.R.; Khan, S.S. Quantifying the Sex-Race/Ethnicity-Specific Burden of Obesity on Incident Diabetes Mellitus in the United States, 2001 to 2016: MESA and NHANES. *Journal of the American Heart Association* **2021**, *10*, e018799, doi:10.1161/JAHA.120.018799.
5. Flegal, K.M.; Kruszon-Moran, D.; Carroll, M.D.; Fryar, C.D.; Ogden, C.L. Trends in Obesity Among Adults in the United States, 2005 to 2014. *JAMA* **2016**, *315*, 2284–2291, doi:10.1001/jama.2016.6458.
6. Hales, C.M.; Carroll, M.D.; Fryar, C.D.; Ogden, C.L. Prevalence of Obesity and Severe Obesity Among Adults: United States, 2017-2018. *NCHS Data Brief* **2020**, *1*, 1–8.
7. Ajlouni, K.; Khader, Y.; Batiha, A.; Jaddou, H.; El-Khateeb, M. An Alarming High and Increasing Prevalence of Obesity in Jordan. *Epidemiol Health* **2020**, *42*, e2020040, doi:10.4178/epih.e2020040.

8. Bustami, M.; Matalaka, K.Z.; Mallah, E.; Abu-Qatouseh, L.; Dayyih, W.A.; Hussein, N.; Safieh, N.A.; Elyyan, Y.; Hussein, N.; Arafat, T. <p>The Prevalence of Overweight and Obesity Among Women in Jordan: A Risk Factor for Developing Chronic Diseases</P>. *JMDH* **2021**, *14*, 1533–1541, doi:10.2147/JMDH.S313172.
9. Di Cesare, M.; Sorić, M.; Bovet, P.; Miranda, J.J.; Bhutta, Z.; Stevens, G.A.; Laxmaiah, A.; Kengne, A.-P.; Bentham, J. The Epidemiological Burden of Obesity in Childhood: A Worldwide Epidemic Requiring Urgent Action. *BMC Medicine* **2019**, *17*, 212, doi:10.1186/s12916-019-1449-8.
10. González-Muniesa, P.; Martínez-González, M.-A.; Hu, F.B.; Després, J.-P.; Matsuzawa, Y.; Loos, R.J.F.; Moreno, L.A.; Bray, G.A.; Martínez, J.A. Obesity. *Nat Rev Dis Primers* **2017**, *3*, 17034, doi:10.1038/nrdp.2017.34.
11. Preda, A.; Carbone, F.; Tirandi, A.; Montecucco, F.; Liberale, L. Obesity Phenotypes and Cardiovascular Risk: From Pathophysiology to Clinical Management. *Rev Endocr Metab Disord* **2023**, *24*, 906-919, doi:10.1007/s11154-023-09813-5.
12. Goossens, G.H. The Metabolic Phenotype in Obesity: Fat Mass, Body Fat Distribution, and Adipose Tissue Function. *Obes Facts* **2017**, *10*, 207–215, doi:10.1159/000471488.
13. Neeland, I.J.; Poirier, P.; Després, J.-P. Cardiovascular and Metabolic Heterogeneity of Obesity: Clinical Challenges and Implications for Management. *Circulation* **2018**, *137*, 1391–1406, doi:10.1161/CIRCULATIONAHA.117.029617.
14. Fang, H.; Berg, E.; Cheng, X.; Shen, W. How to Best Assess Abdominal Obesity. *Current Opinion in Clinical Nutrition & Metabolic Care* **2018**, *21*, 360, doi:10.1097/MCO.0000000000000485.
15. Ladabaum, U.; Mannalithara, A.; Myer, P.A.; Singh, G. Obesity, Abdominal Obesity, Physical Activity, and Caloric Intake in US Adults: 1988 to 2010. *The American Journal of Medicine* **2014**, *127*, 717-727.e12, doi:10.1016/j.amjmed.2014.02.026.
16. Hiuge-Shimizu, A.; Kishida, K.; Funahashi, T.; Ishizaka, Y.; Oka, R.; Okada, M.; Suzuki, S.; Takaya, N.; Nakagawa, T.; Fukui, T.; et al. Absolute Value of Visceral Fat Area Measured

on Computed Tomography Scans and Obesity-Related Cardiovascular Risk Factors in Large-Scale Japanese General Population (the VACATION-J Study). *Ann Med* **2012**, *44*, 82–92, doi:10.3109/07853890.2010.526138.

17. Pedersen, B.K.; Saltin, B. Exercise as Medicine – Evidence for Prescribing Exercise as Therapy in 26 Different Chronic Diseases. *Scandinavian Journal of Medicine & Science in Sports* **2015**, *25*, 1–72, doi:10.1111/sms.12581.

18. Phillips, C.M. Metabolically Healthy Obesity: Definitions, Determinants and Clinical Implications. *Rev Endocr Metab Disord* **2013**, *14*, 219–227, doi:10.1007/s11154-013-9252-x.

19. Ozanne, S.E. Epigenetic Signatures of Obesity. *N Engl J Med* **2015**, *372*, 973–974, doi:10.1056/NEJMcibr1414707.

20. Weinsier, R.L.; Hunter, G.R.; Heini, A.F.; Goran, M.I.; Sell, S.M. The Etiology of Obesity: Relative Contribution of Metabolic Factors, Diet, and Physical Activity. *The American Journal of Medicine* **1998**, *105*, 145–150, doi:10.1016/S0002-9343(98)00190-9.

21. Gay, J.L.; Robb, S.W.; Benson, K.M.; White, A. Can the Social Vulnerability Index Be Used for More Than Emergency Preparedness? An Examination Using Youth Physical Fitness Data. *Journal of Physical Activity and Health* **2016**, *13*, 121–130, doi:10.1123/jpah.2015-0042.

22. Mehrzad, R. Chapter 4 - Etiology of Obesity. In *Obesity*; Mehrzad, R., Ed.; Elsevier: Amsterdam, The Netherlands, 2020; pp. 43–54 ISBN 978-0-12-818839-2.

23. Bray, G.A. *A Guide to Obesity and the Metabolic Syndrome: Origins and Treatment*; CRC Press: Boca Raton, FL, USA, 2011; ISBN 978-0-429-13092-2.

24. Welch, N.; Hunter, W.; Butera, K.; Willis, K.; Cleland, V.; Crawford, D.; Ball, K. Women's Work. Maintaining a Healthy Body Weight. *Appetite* **2009**, *53*, 9–15, doi:10.1016/j.appet.2009.04.221.

25. Deshmukh-Taskar, P.; Nicklas, T.A.; Morales, M.; Yang, S.-J.; Zakeri, I.; Berenson, G.S. Tracking of Overweight Status from Childhood to Young Adulthood: The Bogalusa Heart Study. *Eur J Clin Nutr* **2006**, *60*, 48–57, doi:10.1038/sj.ejcn.1602266.
26. Smith, D.E.; Lewis, C.E.; Caveny, J.L.; Perkins, L.L.; Burke, G.L.; Bild, D.E. Longitudinal Changes in Adiposity Associated With Pregnancy: The CARDIA Study. *JAMA* **1994**, *271*, 1747–1751, doi:10.1001/jama.1994.03510460039030.
27. Sowers, M.; Zheng, H.; Tomey, K.; Karvonen-Gutierrez, C.; Jannausch, M.; Li, X.; Yosef, M.; Symons, J. Changes in Body Composition in Women over Six Years at Midlife: Ovarian and Chronological Aging. *The Journal of Clinical Endocrinology & Metabolism* **2007**, *92*, 895–901, doi:10.1210/jc.2006-1393.
28. Kim, K.-B.; Shin, Y.-A. Males with Obesity and Overweight. *Journal of Obesity & Metabolic Syndrome* **2020**, *29*, 18–25, doi:10.7570/jomes20008.
29. Romieu, I.; Dossus, L.; Barquera, S.; Blotière, H.M.; Franks, P.W.; Gunter, M.; Hwalla, N.; Hursting, S.D.; Leitzmann, M.; Margetts, B.; et al. Energy Balance and Obesity: What Are the Main Drivers? *Cancer Causes Control* **2017**, *28*, 247–258, doi:10.1007/s10552-017-0869-z.
30. Anderson, A.S.; Key, T.J.; Norat, T.; Scoccianti, C.; Cecchini, M.; Berrino, F.; Boutron-Ruault, M.-C.; Espina, C.; Leitzmann, M.; Powers, H.; et al. European Code against Cancer 4th Edition: Obesity, Body Fatness and Cancer. *Cancer Epidemiology* **2015**, *39*, S34–S45, doi:10.1016/j.canep.2015.01.017.
31. Arango-Angarita, A.; Rodríguez-Ramírez, S.; Serra-Majem, L.; Shamah-Levy, T. Dietary Energy Density and Its Association with Overweight or Obesity in Adolescents: A Systematic Review of Observational Studies. *Nutrients* **2018**, *10*, 1612, doi:10.3390/nu10111612.
32. Drewnowski, A. Energy Density, Palatability, and Satiety: Implications for Weight Control. *Nutrition Reviews* **1998**, *56*, 347–353, doi:10.1111/j.1753-4887.1998.tb01677.x.

33. Riera-Crichton, D.; Tefft, N. Macronutrients and Obesity: Revisiting the Calories in, Calories out Framework. *Economics & Human Biology* **2014**, *14*, 33–49, doi:10.1016/j.ehb.2014.04.002.
34. Wishnofsky, M. Caloric Equivalents of Gained or Lost Weight. *American Journal of Clinical Nutrition* **1958**, *6*, 542–546.
35. Jéquier, E. Pathways to Obesity. *Int J Obes* **2002**, *26*, S12–S17, doi:10.1038/sj.ijo.0802123.
36. Komarnytsky, S.; Retchin, S.; Vong, C.I.; Lila, M.A. Gains and Losses of Agricultural Food Production: Implications for the Twenty-First Century. *Annu Rev Food Sci Technol* **2022**, *13*, 239–261, doi:10.1146/annurev-food-082421-114831.
37. Hall, K.D.; Sacks, G.; Chandramohan, D.; Chow, C.C.; Wang, Y.C.; Gortmaker, S.L.; Swinburn, B.A. Quantification of the Effect of Energy Imbalance on Bodyweight. *Lancet* **2011**, *378*, 826–837, doi:10.1016/S0140-6736(11)60812-X.
38. De Castro, J.M. How Can Eating Behavior Be Regulated in the Complex Environments of Free-Living Humans? *Neurosci Biobehav Rev* **1996**, *20*, 119–131, doi:10.1016/0149-7634(95)00047-i.
39. Benton, D.; Young, H.A. Reducing Calorie Intake May Not Help You Lose Body Weight. *Perspect Psychol Sci* **2017**, *12*, 703–714, doi:10.1177/1745691617690878.
40. Bray, G.A.; Flatt, J.-P.; Volaufova, J.; Delany, J.P.; Champagne, C.M. Corrective Responses in Human Food Intake Identified from an Analysis of 7-d Food-Intake Records. *Am J Clin Nutr* **2008**, *88*, 1504–1510, doi:10.3945/ajcn.2008.26289.
41. Blüher, M. Obesity: Global Epidemiology and Pathogenesis. *Nat Rev Endocrinol* **2019**, *15*, 288–298, doi:10.1038/s41574-019-0176-8.
42. Bosy-Westphal, A.; Hägele, F.A.; Müller, M.J. What Is the Impact of Energy Expenditure on Energy Intake? *Nutrients* **2021**, *13*, 3508, doi:10.3390/nu13103508.

43. Swartz, J.J.; Dowray, S.; Braxton, D.; Mihas, P.; Viera, A.J. Simplifying Healthful Choices: A Qualitative Study of a Physical Activity Based Nutrition Label Format. *Nutr J* **2013**, *12*, 72, doi:10.1186/1475-2891-12-72.
44. Katzmarzyk, P.T.; Craig, C.L.; Gauvin, L. Adiposity, Physical Fitness and Incident Diabetes: The Physical Activity Longitudinal Study. *Diabetologia* **2007**, *50*, 538–544, doi:10.1007/s00125-006-0554-3.
45. Petersen, L.; Schnohr, P.; Sørensen, T.I.A. Longitudinal Study of the Long-Term Relation between Physical Activity and Obesity in Adults. *Int J Obes* **2004**, *28*, 105–112, doi:10.1038/sj.ijo.0802548.
46. Cleven, L.; Krell-Roesch, J.; Nigg, C.R.; Woll, A. The Association between Physical Activity with Incident Obesity, Coronary Heart Disease, Diabetes and Hypertension in Adults: A Systematic Review of Longitudinal Studies Published after 2012. *BMC Public Health* **2020**, *20*, 1-15, doi:10.1186/s12889-020-08715-4.
47. Drenowatz, C. Reciprocal Compensation to Changes in Dietary Intake and Energy Expenditure within the Concept of Energy Balance. *Adv Nutr* **2015**, *6*, 592–599, doi:10.3945/an.115.008615.
48. King, N.A.; Caudwell, P.; Hopkins, M.; Byrne, N.M.; Colley, R.; Hills, A.P.; Stubbs, J.R.; Blundell, J.E. Metabolic and Behavioral Compensatory Responses to Exercise Interventions: Barriers to Weight Loss. *Obesity (Silver Spring)* **2007**, *15*, 1373–1383, doi:10.1038/oby.2007.164.
49. Donnelly, J.E.; Herrmann, S.D.; Lambourne, K.; Szabo, A.N.; Honas, J.J.; Washburn, R.A. Does Increased Exercise or Physical Activity Alter Ad-Libitum Daily Energy Intake or Macronutrient Composition in Healthy Adults? A Systematic Review. *PLoS One* **2014**, *9*, e83498, doi:10.1371/journal.pone.0083498.
50. Sim, A.Y.; Wallman, K.E.; Fairchild, T.J.; Guelfi, K.J. High-Intensity Intermittent Exercise Attenuates Ad-Libitum Energy Intake. *Int J Obes (Lond)* **2014**, *38*, 417–422, doi:10.1038/ijo.2013.102.

51. Alméras, N.; Lavallée, N.; Després, J.P.; Bouchard, C.; Tremblay, A. Exercise and Energy Intake: Effect of Substrate Oxidation. *Physiol Behav* **1995**, *57*, 995–1000, doi:10.1016/0031-9384(94)00360-h.
52. Camps, S.G.; Verhoef, S.P.; Westerterp, K.R. Weight Loss-Induced Reduction in Physical Activity Recovers during Weight Maintenance. *Am J Clin Nutr* **2013**, *98*, 917–923, doi:10.3945/ajcn.113.062935.
53. Melzer, K.; Kayser, B.; Saris, W.H.M.; Pichard, C. Effects of Physical Activity on Food Intake. *Clin Nutr* **2005**, *24*, 885–895, doi:10.1016/j.clnu.2005.06.003.
54. Keeseey, R.E.; Hirvonen, M.D. Body Weight Set-Points: Determination and Adjustment¹. *The Journal of Nutrition* **1997**, *127*, 1875S–1883S, doi:10.1093/jn/127.9.1875S.
55. Tran, L.T.; Park, S.; Kim, S.K.; Lee, J.S.; Kim, K.W.; Kwon, O. Hypothalamic Control of Energy Expenditure and Thermogenesis. *Exp Mol Med* **2022**, *54*, 358–369, doi:10.1038/s12276-022-00741-z.
56. Rolfe, D.F.; Brown, G.C. Cellular Energy Utilization and Molecular Origin of Standard Metabolic Rate in Mammals. *Physiol Rev* **1997**, *77*, 731–758, doi:10.1152/physrev.1997.77.3.731.
57. Kaiyala, K.J.; Morton, G.J.; Leroux, B.G.; Ogimoto, K.; Wisse, B.; Schwartz, M.W. Identification of Body Fat Mass as a Major Determinant of Metabolic Rate in Mice. *Diabetes* **2010**, *59*, 1657–1666, doi:10.2337/db09-1582.
58. Dulloo, A.G.; Jacquet, J. Adaptive Reduction in Basal Metabolic Rate in Response to Food Deprivation in Humans: A Role for Feedback Signals from Fat Stores. *Am J Clin Nutr* **1998**, *68*, 599–606, doi:10.1093/ajcn/68.3.599.
59. Ebrahimi-Mameghani, M.; Scott, J.A.; Der, G.; Lean, M.E.J.; Burns, C.M. Changes in Weight and Waist Circumference over 9 Years in a Scottish Population. *Eur J Clin Nutr* **2008**, *62*, 1208–1214, doi:10.1038/sj.ejcn.1602839.

60. Poppitt, S.D.; Prentice, A.M. Energy Density and Its Role in the Control of Food Intake: Evidence from Metabolic and Community Studies. *Appetite* **1996**, *26*, 153–174, doi:10.1006/appe.1996.0013.
61. Buckland, N.J.; James Stubbs, R.; Finlayson, G. Towards a Satiety Map of Common Foods: Associations between Perceived Satiety Value of 100 Foods and Their Objective and Subjective Attributes. *Physiol Behav* **2015**, *152*, 340–346, doi:10.1016/j.physbeh.2015.07.001.
62. Patterson, R.E.; Laughlin, G.A.; LaCroix, A.Z.; Hartman, S.J.; Natarajan, L.; Senger, C.M.; Martínez, M.E.; Villaseñor, A.; Sears, D.D.; Marinac, C.R.; et al. Intermittent Fasting and Human Metabolic Health. *Journal of the Academy of Nutrition and Dietetics* **2015**, *115*, 1203–1212, doi:10.1016/j.jand.2015.02.018.
63. Kelly, S.; Martin, S.; Kuhn, I.; Cowan, A.; Brayne, C.; Lafortune, L. Barriers and Facilitators to the Uptake and Maintenance of Healthy Behaviours by People at Mid-Life: A Rapid Systematic Review. *PLOS ONE* **2016**, *11*, e0145074, doi:10.1371/journal.pone.0145074.
64. Richard, D. Cognitive and Autonomic Determinants of Energy Homeostasis in Obesity. *Nat Rev Endocrinol* **2015**, *11*, 489–501, doi:10.1038/nrendo.2015.103.
65. Bingham, S.A.; Gill, C.; Welch, A.; Day, K.; Cassidy, A.; Khaw, K.T.; Sneyd, M.J.; Key, T.J.; Roe, L.; Day, N.E. Comparison of Dietary Assessment Methods in Nutritional Epidemiology: Weighed Records v. 24 h Recalls, Food-Frequency Questionnaires and Estimated-Diet Records. *Br J Nutr* **1994**, *72*, 619–643, doi:10.1079/bjn19940064.
66. Jéquier, E. Nutrient Effects: Post-Absorptive Interactions. *Proc Nutr Soc* **1995**, *54*, 253–265, doi:10.1079/pns19950052.
67. Mengeste, A.M.; Rustan, A.C.; Lund, J. Skeletal Muscle Energy Metabolism in Obesity. *Obesity (Silver Spring)* **2021**, *29*, 1582–1595, doi:10.1002/oby.23227.
68. Andriessen, C.; Fealy, C.E.; Veelen, A.; van Beek, S.M.M.; Roumans, K.H.M.; Connell, N.J.; Mevenkamp, J.; Moonen-Kornips, E.; Havekes, B.; Schrauwen-Hinderling, V.B.; et al. Three Weeks of Time-Restricted Eating Improves Glucose Homeostasis in Adults with Type

2 Diabetes but Does Not Improve Insulin Sensitivity: A Randomised Crossover Trial. *Diabetologia* **2022**, *65*, 1710–1720, doi:10.1007/s00125-022-05752-z.

69. Cohen, C.C.; Li, K.W.; Alazraki, A.L.; Beysen, C.; Carrier, C.A.; Cleeton, R.L.; Dandan, M.; Figueroa, J.; Knight-Scott, J.; Knott, C.J.; et al. Dietary Sugar Restriction Reduces Hepatic de Novo Lipogenesis in Adolescent Boys with Fatty Liver Disease. *J Clin Invest* **2021**, *131*, e150996, doi:10.1172/JCI150996.

70. Zamanillo-Campos, R.; Chaplin, A.; Romaguera, D.; Abete, I.; Salas-Salvadó, J.; Martín, V.; Estruch, R.; Vidal, J.; Ruiz-Canela, M.; Babio, N.; et al. Longitudinal Association of Dietary Carbohydrate Quality with Visceral Fat Deposition and Other Adiposity Indicators. *Clin Nutr* **2022**, *41*, 2264–2274, doi:10.1016/j.clnu.2022.08.008.

71. Hron, B.M.; Ebbeling, C.B.; Feldman, H.A.; Ludwig, D.S. Relationship of Insulin Dynamics to Body Composition and Resting Energy Expenditure Following Weight Loss. *Obesity* **2015**, *23*, 2216–2222, doi:10.1002/oby.21213.

72. Ravussin, E.; Swinburn, B.A. Metabolic Predictors of Obesity: Cross-Sectional versus Longitudinal Data. *Int J Obes Relat Metab Disord* **1993**, *17 Suppl 3*, S28-31; discussion S41-42.

73. Jitrapakdee, S.; Maurice, M.St.; Rayment, I.; Cleland, W.W.; Wallace, J.C.; Attwood, P.V. Structure, Mechanism and Regulation of Pyruvate Carboxylase. *Biochem J* **2008**, *413*, 369–387, doi:10.1042/BJ20080709.

74. Reshef, L.; Olswang, Y.; Cassuto, H.; Blum, B.; Croniger, C.M.; Kalhan, S.C.; Tilghman, S.M.; Hanson, R.W. Glyceroneogenesis and the Triglyceride/Fatty Acid Cycle. *J Biol Chem* **2003**, *278*, 30413–30416, doi:10.1074/jbc.R300017200.

75. Merra, G.; Gratteri, S.; De Lorenzo, A.; Barrucco, S.; Perrone, M.A.; Avolio, E.; Bernardini, S.; Marchetti, M.; Di Renzo, L. Effects of Very-Low-Calorie Diet on Body Composition, Metabolic State, and Genes Expression: A Randomized Double-Blind Placebo-Controlled Trial. *Eur Rev Med Pharmacol Sci* **2017**, *21*, 329–345.

76. Malinowski, B.; Zalewska, K.; Węsierska, A.; Sokołowska, M.M.; Socha, M.; Liczner, G.; Pawlak-Osińska, K.; Wiciński, M. Intermittent Fasting in Cardiovascular Disorders—An Overview. *Nutrients* **2019**, *11*, 673, doi:10.3390/nu11030673.
77. Cahill, G.F. Starvation in Man. *Clin Endocrinol Metab* **1976**, *5*, 397–415, doi:10.1016/s0300-595x(76)80028-x.
78. Tan, M.; Mosaoa, R.; Graham, G.T.; Kasprzyk-Pawelec, A.; Gadre, S.; Parasido, E.; Catalina-Rodriguez, O.; Foley, P.; Giaccone, G.; Cheema, A.; et al. Inhibition of the Mitochondrial Citrate Carrier, Slc25a1, Reverts Steatosis, Glucose Intolerance, and Inflammation in Preclinical Models of NAFLD/NASH. *Cell Death Differ* **2020**, *27*, 2143–2157, doi:10.1038/s41418-020-0491-6.
79. Williams, N.C.; O’Neill, L.A.J. A Role for the Krebs Cycle Intermediate Citrate in Metabolic Reprogramming in Innate Immunity and Inflammation. *Frontiers in Immunology* **2018**, *9*, 141.
80. Flatt, J. Use and Storage of Carbohydrate and Fat. *The American Journal of Clinical Nutrition* **1995**, *61*, 952S–959S, doi:10.1093/ajcn/61.4.952S.
81. Nagarajan, S.R.; Cross, E.; Sanna, F.; Hodson, L. Dysregulation of Hepatic Metabolism with Obesity: Factors Influencing Glucose and Lipid Metabolism. *Proc Nutr Soc* **2022**, *81*, 1–11, doi:10.1017/S0029665121003761.
82. Kuk, J.L.; Saunders, T.J.; Davidson, L.E.; Ross, R. Age-Related Changes in Total and Regional Fat Distribution. *Ageing Res Rev* **2009**, *8*, 339–348, doi:10.1016/j.arr.2009.06.001.
83. Jura, M.; Kozak, Leslie.P. Obesity and Related Consequences to Ageing. *Age (Dordr)* **2016**, *38*, 23, doi:10.1007/s11357-016-9884-3.
84. Virtue, S.; Vidal-Puig, A. Adipose Tissue Expandability, Lipotoxicity and the Metabolic Syndrome--an Allostatic Perspective. *Biochim Biophys Acta* **2010**, *1801*, 338–349, doi:10.1016/j.bbailip.2009.12.006.

85. Malis, C.; Rasmussen, E.L.; Poulsen, P.; Petersen, I.; Christensen, K.; Beck-Nielsen, H.; Astrup, A.; Vaag, A.A. Total and Regional Fat Distribution Is Strongly Influenced by Genetic Factors in Young and Elderly Twins. *Obes Res* **2005**, *13*, 2139–2145, doi:10.1038/oby.2005.265.
86. Hilton, C.; Karpe, F.; Pinnick, K.E. Role of Developmental Transcription Factors in White, Brown and Beige Adipose Tissues. *Biochim Biophys Acta* **2015**, *1851*, 686–696, doi:10.1016/j.bbaliip.2015.02.003.
87. Tran, T.T.; Yamamoto, Y.; Gesta, S.; Kahn, C.R. Beneficial Effects of Subcutaneous Fat Transplantation on Metabolism. *Cell Metab* **2008**, *7*, 410–420, doi:10.1016/j.cmet.2008.04.004.
88. Neeland, I.J.; Turer, A.T.; Ayers, C.R.; Powell-Wiley, T.M.; Vega, G.L.; Farzaneh-Far, R.; Grundy, S.M.; Khera, A.; McGuire, D.K.; de Lemos, J.A. Dysfunctional Adiposity and the Risk of Prediabetes and Type 2 Diabetes in Obese Adults. *JAMA* **2012**, *308*, 1150–1159, doi:10.1001/2012.jama.11132.
89. Shah, A.D.; Kandula, N.R.; Lin, F.; Allison, M.A.; Carr, J.; Herrington, D.; Liu, K.; Kanaya, A.M. Less Favorable Body Composition and Adipokines in South Asians Compared with Other US Ethnic Groups: Results from the MASALA and MESA Studies. *Int J Obes (Lond)* **2016**, *40*, 639–645, doi:10.1038/ijo.2015.219.
90. Karastergiou, K.; Smith, S.R.; Greenberg, A.S.; Fried, S.K. Sex Differences in Human Adipose Tissues – the Biology of Pear Shape. *Biology of Sex Differences* **2012**, *3*, 13, doi:10.1186/2042-6410-3-13.
91. Eisner, B.H.; Zargooshi, J.; Berger, A.D.; Cooperberg, M.R.; Doyle, S.M.; Sheth, S.; Stoller, M.L. Gender Differences in Subcutaneous and Perirenal Fat Distribution. *Surg Radiol Anat* **2010**, *32*, 879–882, doi:10.1007/s00276-010-0692-7.
92. Frank, A.P.; de Souza Santos, R.; Palmer, B.F.; Clegg, D.J. Determinants of Body Fat Distribution in Humans May Provide Insight about Obesity-Related Health Risks. *J Lipid Res* **2019**, *60*, 1710–1719, doi:10.1194/jlr.R086975.

93. Toth, M.J.; Tchernof, A.; Sites, C.K.; Poehlman, E.T. Effect of Menopausal Status on Body Composition and Abdominal Fat Distribution. *Int J Obes* **2000**, *24*, 226–231, doi:10.1038/sj.ijo.0801118.
94. Pouliot, M.C.; Després, J.P.; Moorjani, S.; Lupien, P.J.; Tremblay, A.; Nadeau, A.; Bouchard, C. Regional Variation in Adipose Tissue Lipoprotein Lipase Activity: Association with Plasma High Density Lipoprotein Levels. *Eur J Clin Invest* **1991**, *21*, 398–405, doi:10.1111/j.1365-2362.1991.tb01387.x.
95. Verheggen, R.J.H.M.; Maessen, M.F.H.; Green, D.J.; Hermus, A.R.M.M.; Hopman, M.T.E.; Thijssen, D.H.T. A Systematic Review and Meta-Analysis on the Effects of Exercise Training versus Hypocaloric Diet: Distinct Effects on Body Weight and Visceral Adipose Tissue. *Obes Rev* **2016**, *17*, 664–690, doi:10.1111/obr.12406.
96. Dadson, P.; Landini, L.; Helmiö, M.; Hannukainen, J.C.; Immonen, H.; Honka, M.-J.; Bucci, M.; Savisto, N.; Soinio, M.; Salminen, P.; et al. Effect of Bariatric Surgery on Adipose Tissue Glucose Metabolism in Different Depots in Patients With or Without Type 2 Diabetes. *Diabetes Care* **2016**, *39*, 292–299, doi:10.2337/dc15-1447.
97. Liao, J.; Cao, C.; Hur, J.; Cohen, J.; Chen, W.; Zong, X.; Colditz, G.; Yang, L.; Stamatakis, E.; Cao, Y. Association of Sedentary Patterns with Body Fat Distribution among US Children and Adolescents: A Population-Based Study. *Int J Obes* **2021**, *45*, 2048–2057, doi:10.1038/s41366-021-00874-7.
98. Jung, U.J.; Choi, M.-S. Obesity and Its Metabolic Complications: The Role of Adipokines and the Relationship between Obesity, Inflammation, Insulin Resistance, Dyslipidemia and Nonalcoholic Fatty Liver Disease. *International Journal of Molecular Sciences* **2014**, *15*, 6184–6223, doi:10.3390/ijms15046184.
99. Angelini, G.; Castagneto Gisse, L.; Del Corpo, G.; Giordano, C.; Cerbelli, B.; Severino, A.; Manco, M.; Basso, N.; Birkenfeld, A.L.; Bornstein, S.R.; et al. New Insight into the Mechanisms of Ectopic Fat Deposition Improvement after Bariatric Surgery. *Sci Rep* **2019**, *9*, 17315, doi:10.1038/s41598-019-53702-4.

100. Johannsen, D.L.; Tchoukalova, Y.; Tam, C.S.; Covington, J.D.; Xie, W.; Schwarz, J.-M.; Bajpeyi, S.; Ravussin, E. Effect of 8 Weeks of Overfeeding on Ectopic Fat Deposition and Insulin Sensitivity: Testing the “Adipose Tissue Expandability” Hypothesis. *Diabetes Care* **2014**, *37*, 2789–2797, doi:10.2337/dc14-0761.
101. Green, M.H. Are Fatty Acids Gluconeogenic Precursors? *J Nutr* **2020**, *150*, 2235–2238, doi:10.1093/jn/nxaa165.
102. Miyazaki, Y.; Mahankali, A.; Matsuda, M.; Glass, L.; Mahankali, S.; Ferrannini, E.; Cusi, K.; Mandarino, L.J.; DeFronzo, R.A. Improved Glycemic Control and Enhanced Insulin Sensitivity in Type 2 Diabetic Subjects Treated with Pioglitazone. *Diabetes Care* **2001**, *24*, 710–719, doi:10.2337/diacare.24.4.710.
103. Kelley, D.E. Skeletal Muscle Fat Oxidation: Timing and Flexibility Are Everything. *J Clin Invest* **2005**, *115*, 1699–1702, doi:10.1172/JCI25758.
104. Goossens, G.H.; Moors, C.C.M.; Jocken, J.W.E.; van der Zijl, N.J.; Jans, A.; Konings, E.; Diamant, M.; Blaak, E.E. Altered Skeletal Muscle Fatty Acid Handling in Subjects with Impaired Glucose Tolerance as Compared to Impaired Fasting Glucose. *Nutrients* **2016**, *8*, 164, doi:10.3390/nu8030164.
105. Hui, S.; Ghergurovich, J.M.; Morscher, R.J.; Jang, C.; Teng, X.; Lu, W.; Esparza, L.A.; Reya, T.; Zhan, L.; Guo, J.Y.; et al. Glucose Feeds the TCA Cycle via Circulating Lactate. *Nature* **2017**, *551*, 115–118, doi:10.1038/nature24057.
106. Komarnytsky, S.; Wagner, C.; Gutierrez, J.; Shaw, O.M. Berries in Microbiome-Mediated Gastrointestinal, Metabolic, and Immune Health. *Curr Nutr Rep* **2023**, *12*, 151–166, doi:10.1007/s13668-023-00449-0.
107. Vong, C.I.; Rathinasabapathy, T.; Moncada, M.; Komarnytsky, S. All Polyphenols Are Not Created Equal: Exploring the Diversity of Phenolic Metabolites. *J. Agric. Food Chem.* **2022**, *70*, 2077–2091, doi:10.1021/acs.jafc.1c07179.
108. Alghamdi, M.; Gutierrez, J.; Komarnytsky, S. Essential Minerals and Metabolic Adaptation of Immune Cells. *Nutrients* **2023**, *15*, 123, doi:10.3390/nu15010123.

109. John, G.K.; Mullin, G.E. The Gut Microbiome and Obesity. *Curr Oncol Rep* **2016**, *18*, 45, doi:10.1007/s11912-016-0528-7.
110. Kaoutari, A.E.; Armougom, F.; Gordon, J.I.; Raoult, D.; Henrissat, B. The Abundance and Variety of Carbohydrate-Active Enzymes in the Human Gut Microbiota. *Nat Rev Microbiol* **2013**, *11*, 497–504, doi:10.1038/nrmicro3050.
111. Almeida, A.; Mitchell, A.L.; Boland, M.; Forster, S.C.; Gloor, G.B.; Tarkowska, A.; Lawley, T.D.; Finn, R.D. A New Genomic Blueprint of the Human Gut Microbiota. *Nature* **2019**, *568*, 499–504, doi:10.1038/s41586-019-0965-1.
112. Devaraj, S.; Hemarajata, P.; Versalovic, J. The Human Gut Microbiome and Body Metabolism: Implications for Obesity and Diabetes. *Clinical Chemistry* **2013**, *59*, 617–628, doi:10.1373/clinchem.2012.187617.
113. Lloyd-Price, J.; Abu-Ali, G.; Huttenhower, C. The Healthy Human Microbiome. *Genome Medicine* **2016**, *8*, 51, doi:10.1186/s13073-016-0307-y.
114. Miller, T.L.; Wolin, M.J. Fermentations by Saccharolytic Intestinal Bacteria. *Am J Clin Nutr* **1979**, *32*, 164–172, doi:10.1093/ajcn/32.1.164.
115. Dudek-Wicher, R.K.; Junka, A.; Bartoszewicz, M. The Influence of Antibiotics and Dietary Components on Gut Microbiota. *Gastroenterology Rev* **2018**, *13*, 85–92, doi:10.5114/pg.2018.76005.
116. Albenberg, L.; Esipova, T.V.; Judge, C.P.; Bittinger, K.; Chen, J.; Laughlin, A.; Grunberg, S.; Baldassano, R.N.; Lewis, J.D.; Li, H.; et al. Correlation between Intraluminal Oxygen Gradient and Radial Partitioning of Intestinal Microbiota. *Gastroenterology* **2014**, *147*, 1055-1063.e8, doi:10.1053/j.gastro.2014.07.020.
117. Overall, J.; Bonney, S.A.; Wilson, M.; Beermann, A.; Grace, M.H.; Esposito, D.; Lila, M.A.; Komarnytsky, S. Metabolic Effects of Berries with Structurally Diverse Anthocyanins. *Int J Mol Sci* **2017**, *18*, 422, doi:10.3390/ijms18020422.

118. Turnbaugh, P.J.; Ley, R.E.; Mahowald, M.A.; Magrini, V.; Mardis, E.R.; Gordon, J.I. An Obesity-Associated Gut Microbiome with Increased Capacity for Energy Harvest. *Nature* **2006**, *444*, 1027–1031, doi:10.1038/nature05414.
119. Bäckhed, F.; Manchester, J.K.; Semenkovich, C.F.; Gordon, J.I. Mechanisms Underlying the Resistance to Diet-Induced Obesity in Germ-Free Mice. *Proc Natl Acad Sci U S A* **2007**, *104*, 979–984, doi:10.1073/pnas.0605374104.
120. Arora, T.; Sharma, R. Fermentation Potential of the Gut Microbiome: Implications for Energy Homeostasis and Weight Management. *Nutrition Reviews* **2011**, *69*, 99–106, doi:10.1111/j.1753-4887.2010.00365.x.
121. Coquant, G.; Grill, J.-P.; Seksik, P. Impact of N-Acyl-Homoserine Lactones, Quorum Sensing Molecules, on Gut Immunity. *Front Immunol* **2020**, *11*, 1827, doi:10.3389/fimmu.2020.01827.
122. Palatini, K.M.; Durand, P.-J.; Rathinasabapathy, T.; Esposito, D.; Komarnytsky, S. Bitter Receptors and Glucose Transporters Interact to Control Carbohydrate and Immune Responses in the Gut. *The FASEB Journal* **2016**, *30*, 682.6-682.6, doi:10.1096/fasebj.30.1_supplement.682.6.
123. Kim, J.I.; Huh, J.Y.; Sohn, J.H.; Choe, S.S.; Lee, Y.S.; Lim, C.Y.; Jo, A.; Park, S.B.; Han, W.; Kim, J.B. Lipid-Overloaded Enlarged Adipocytes Provoke Insulin Resistance Independent of Inflammation. *Mol Cell Biol* **2015**, *35*, 1686–1699, doi:10.1128/MCB.01321-14.
124. Hotamisligil, G.S. Inflammation and Metabolic Disorders. *Nature* **2006**, *444*, 860–867, doi:10.1038/nature05485.
125. Kim, J.-Y.; van de Wall, E.; Laplante, M.; Azzara, A.; Trujillo, M.E.; Hofmann, S.M.; Schraw, T.; Durand, J.L.; Li, H.; Li, G.; et al. Obesity-Associated Improvements in Metabolic Profile through Expansion of Adipose Tissue. *J Clin Invest* **2007**, *117*, 2621–2637, doi:10.1172/JCI31021.
126. Kubota, N.; Kubota, T.; Kajiwara, E.; Iwamura, T.; Kumagai, H.; Watanabe, T.; Inoue, M.; Takamoto, I.; Sasako, T.; Kumagai, K.; et al. Differential Hepatic Distribution of Insulin

Receptor Substrates Causes Selective Insulin Resistance in Diabetes and Obesity. *Nat Commun* **2016**, *7*, 12977, doi:10.1038/ncomms12977.

127. Chen, G.; Goeddel, D.V. TNF-R1 Signaling: A Beautiful Pathway. *Science* **2002**, *296*, 1634–1635, doi:10.1126/science.1071924.

128. Fink, L.N.; Oberbach, A.; Costford, S.R.; Chan, K.L.; Sams, A.; Blüher, M.; Klip, A. Expression of Anti-Inflammatory Macrophage Genes within Skeletal Muscle Correlates with Insulin Sensitivity in Human Obesity and Type 2 Diabetes. *Diabetologia* **2013**, *56*, 1623–1628, doi:10.1007/s00125-013-2897-x.

129. Lee, B.; Moon, K.M.; Kim, C.Y. Tight Junction in the Intestinal Epithelium: Its Association with Diseases and Regulation by Phytochemicals. *J Immunol Res* **2018**, *2018*, 2645465, doi:10.1155/2018/2645465.

130. Xia, L.; Oyang, L.; Lin, J.; Tan, S.; Han, Y.; Wu, N.; Yi, P.; Tang, L.; Pan, Q.; Rao, S.; et al. The Cancer Metabolic Reprogramming and Immune Response. *Molecular Cancer* **2021**, *20*, 28, doi:10.1186/s12943-021-01316-8.

131. Schéle, E.; Grahnemo, L.; Anesten, F.; Hallén, A.; Bäckhed, F.; Jansson, J.-O. Regulation of Body Fat Mass by the Gut Microbiota: Possible Mediation by the Brain. *Peptides* **2016**, *77*, 54–59, doi:10.1016/j.peptides.2015.03.027.

132. Acosta, A.; Camilleri, M.; Abu Dayyeh, B.; Calderon, G.; Gonzalez, D.; McRae, A.; Rossini, W.; Singh, S.; Burton, D.; Clark, M.M. Selection of Antiobesity Medications Based on Phenotypes Enhances Weight Loss: A Pragmatic Trial in an Obesity Clinic. *Obesity (Silver Spring)* **2021**, *29*, 662–671, doi:10.1002/oby.23120.

CHAPTER 2- Obesity-resistant mice on high fat diet display a distinct phenotype linked to enhanced lipid metabolism

Abstract

Individually, metabolic variations can significantly influence predisposition to obesity in the form of the obesity-prone (super-responders) and the obesity-resistant (non-responders) phenotypes in response to modern calorie-dense diets. In this study, C57BL/6J mice (n=76) were randomly assigned to either low-fat diet (LFD) or high-fat diet (HFD) for 6 weeks, followed by selection of the normally obese (HFD), non-responders (NR), super-responders (SR), or super-responders switched back to the low-fat diet (SR-LFD) for additional 8 weeks. SR mice showed highest gains in body weight, lean and fat body mass, total and free water, in part due to increased feed efficiency and despite having respiratory exchange ratio (RER) similar to that of NR mice. A switch to the LFD diet was sufficient to revert most of the observed physiological changes in the SR-LFD mice, however voluntary physical activity and exercise capacity have not returned to the basal level. NR mice showed highest food intake, lowest feed efficiency, increased oxygen consumption during the light (rest) cycle, increased physical activity during the dark (active) cycle, and increased heat production during both cycles. These variations were observed in the absence of changes in food intake and fecal parameters; however, NR fecal lipid content was lower, and NR fecal microbiome profile was characterized by reduced abundance of *Actinobacteria*. Taken together, our findings suggest that NR mice showed an increased ability to metabolize excessive dietary fats in skeletal muscle, at the expense of reduced exercise capacity that persisted for the duration of the study. These findings underscore the need for further comprehensive investigations into the

mechanisms of obesity resistance, as they hold potential implications for weight loss strategies in human subjects.

1. Introduction

The variety of individual responses to obesogenic environment, the onset of obesity, and its direct relationship to various health outcomes is not fully understood [1]. It has been established that obesity as defined by the body mass index (BMI) is heritable across the lifetime with an overall effect of up to 70% [2]. However, within a specific environment, significant differences in body weight and fat mass among individuals imply that adiposity is additionally shaped by intricate interplays of other metabolic, behavioral, and environmental factors. Aside from the monogenic genetic aberrations in the central appetite regulatory pathway, or the syndromic forms [3], obesity is highly polygenic in its nature, and involves millions of common genetic variants, each having a small effect on an individual's susceptibility to gaining weight [4]. Although genome-wide association studies (GWAS) were successful at identifying the *FTO* locus with a relatively large effect on BMI (1 kg of additional body weight for an average adult), the combined effects of this and other 750 minor GWAS loci known to date explain only 6% of variation [5]. Recent additional GWAS studies that focused on more refined obesity outcomes such as resistance to weight gain suggested that characterization of obesity-resistant (non-responders) phenotypes may provide an alternative understanding of the metabolic complexity of body weight regulation [6].

Dietary fats are essential nutrients and a concentrated source of energy that serves various vital functions in the human body [7]. Consuming fats contributes to feelings of fullness and satisfaction, signaling to the brain that the body has received sufficient energy [8]. Unlike carbohydrates, which are stored in limited quantities as glycogen in the liver and muscles, fats can be stored in adipose tissue in virtually unlimited amounts [1]. While daily carbohydrate balance is tightly regulated so the majority of carbohydrates are immediately and preferentially metabolized when available [9], dietary fats are primarily targeted for deposition

and storage [10]. Insulin secreted in response to the carbohydrate load of the mixed meal further facilitates fat storage and decreases fat oxidation [11]. Previous rodent studies suggested that progressive metabolic abnormalities in response to calorie-dense meals follow the sequence of hyperinsulinemia, increased adipocyte size, greater adiposity, lower energy expenditure, and eventually, increased hunger [12]. The excess energy is therefore deposited into conventional adipose depots, as well as ectopic non-target organs like liver and muscle, based on the individual, hypothetical body weight set points and patterns of fat accumulation [13].

Previously, a few animal studies aimed at understanding the differences between the obesity-prone versus obesity-resistant phenotypes, with limited success. Among the reported observations, ability of muscle fibers type I (slow) [14], type IIa (fast, oxidative) [15], and type IIb (fast, glycolytic) to alter nutrient partitioning for oxidation, upregulation of uncoupling proteins in the mitochondrial inner membrane of white and brown adipose tissue to increase dissipative heat [16], and decreased AMPK phosphorylation and PPAR γ activity [17] have been suggested as putative aberrations without further mechanistic explanations. Several attempts at investigating gene pathways associated with lipid deposition in the adipose tissues were either inconclusive [18], or suggested several gene candidates, including *Acaca*, *Acly*, *Acss2*, *Aldh1a1*, *Elvol6*, *Scd1*, and *Slc25a1* [19] for further studies. Finally, serum profiles of obesity-resistant animals showed relative decreases in intermediates of Krebs cycle (citrate, malate, α -ketoglutarate), ornithine, increase in glycine, and reduced amounts of catecholamine metabolites including homovanillic acid, vanillylmandelic acid, and p-hydroxyphenylacetic acid alongside increased citrate in urine [20]. However, the precise metabolic changes

responsible for partial resistance to obesity after consuming large amounts of dietary fats have not been determined.

In this study, we utilized C57BL/6J mice as a well-recognized model of polygenic obesity [21] to analyze a biological phenotype of resistance to obesity (non-responders) after exposure to excessive dietary fats. Obesity-prone super-responders (SR) and obesity-resistant non-responders (NR) were compared to differentiate changes in body composition and energy metabolism. SR mice switched back to a low-calorie diet served as additional control to assess reversibility of the observed changes and pinpoint tissues that failed to recover their function upon returning to normal body weight. Finally, for the first time, we assessed changes in fecal microbiome profiles associated with these perturbations.

2. Materials and Methods

2.1. Animals and diets

Male, 4-week-old C57BL/6J mice were purchased from the Jackson Laboratory (Bar Harbor, ME, USA) and housed four animals per cage under controlled temperature (24 ± 2 °C) and light (12 h light–dark cycle, lights on at 7:00 p.m.). Immediately upon arrival, animals were allowed to adapt to new conditions for 7 days and handling the animals was performed daily to reduce the stress of physical manipulation. Mice were then randomized into *ad libitum* access to Research Diets (New Brunswick, NJ, USA) low fat diet (LFD, D12450J, 10 kcal % fat, 3.85 kcal/g, n=32) or high fat diet (HFD, D12492, 60 kcal % fat, 5.24 kcal/g, n=44) for 6 weeks. Obese animals were further randomized into normally obese (HFD), non-responders (NR), super-responders (SR), or super-responders switched back to the low-fat diet (SR-LFD) for additional 8 weeks of the respective diets (Figure 1). All animal experiments were

performed according to procedures approved by the NC Research Campus Institutional Animal Care and Use Committee in the David H. Murdock Research Institute (Kannapolis, NC), the AAALAC accredited animal care facility.

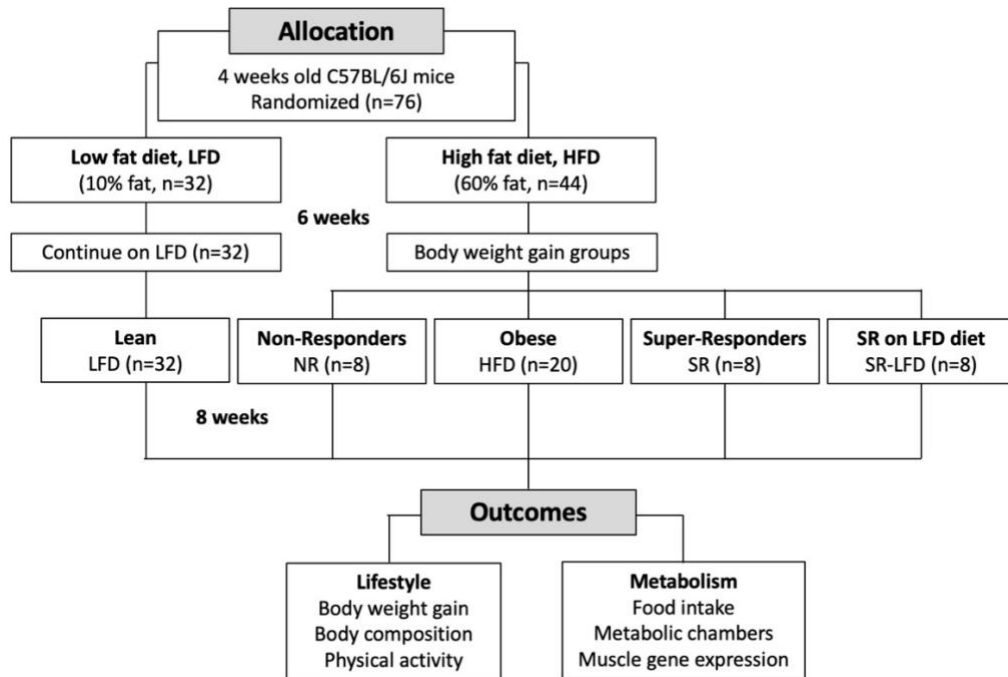


Figure 2.1. Flowchart of the study.

2.2. Body composition

Animal weight and food intake (accounting for spillage) were recorded weekly for the duration of the study. Body composition analysis was performed on unanesthetized mice using EchoMRI (Echo Medical Systems, Houston, TX, USA) during the last week of the study.

2.3. Energy expenditure

An open-circuit LabMaster Metabolism Research Platform (TSE Systems, Bad Homburg, Germany) was used to assess indirect calorimetry and activity at the Animal

Metabolism Phenotyping Core, UNC Nutrition Obesity Research Center. Rates of oxygen consumption (VO_2) and carbon dioxide production (VCO_2) were recorded in accordance with a reference cage every 12 minutes for 72 hours. VCO_2/VO_2 was defined as the respiratory exchange ratio (RER), and energy expenditure (EE) was estimated using the equation = $[3.815 + (1.232 \times \text{RER})] \times \text{VO}_2$. The nonprotein respiratory quotient table [22] was used to compute lipid and carbohydrate oxidation rates. The ActiMot system (TSE) was applied to measure activity by measuring infrared beam breaks in horizontal (x and y direction, running) and vertical (z direction, rearing) planes.

2.4. Exercise capacity

Endurance exercise capacity (run time) was determined on a rodent treadmill (Columbus Instruments, Columbus, OH), with shock grid set at <0.34 mA and 1 Hz. The treadmill intensity was set at 10 and 0 incline. After 2 min of accommodation time, treadmill speed was set at 16 cm/s and progressively increased by 2 cm/s every 2 min until a maximum speed of 24 cm/s was reached. The test was terminated when animals received 3 consecutive electrical stimuli, failed to move, or 20 min passed.

At the end of experiment, blood was collected into serum tubes by heart puncture after CO_2 inhalation. Metabolic tissues (liver, fat, muscle, brain) were collected and stored at -80°C to determine the temporal sequence and signaling events that are responsible for changes in physiology and metabolism.

2.5. Fecal parameters

Fecal pellets were collected over 1-2 consecutive days the end of the study. Fresh trays were gently removed, and pellets were collected using clean forceps into Eppendorf tubes. Pellets in contact with other surfaces were excluded. After collection, pellets were counted, weighed individually, and immediately frozen at -80 °C until analyzed.

Total fecal lipids were extracted from pre-weighed fecal pellet using the Folch method [23]. The pellets were homogenized with chloroform/methanol (2/1) to a final volume 20 times the weight of the sample, and incubated at room temperature for 2 h. Samples were then centrifuged at 3,000 g for 10 min, and the supernatant was mixed with an equal amount of 0.9% NaCl solution. Following a second centrifugation, the upper aqueous phase was discarded and the lower chloroform phase containing the fat was evaporated using Rotavapor R210 (Buchi Labortechnik, Flawil, Switzerland) under vacuum. The lipid weight was determined as the percentage of the wet fecal pellet weight.

2.6. Fecal microbiome profile

Genomic DNA was extracted from mouse fecal samples using QIAamp Fast DNA Stool Mini kits (Qiagen, Germantown, MD, USA), quantified using Take3 plate and Synergy H1 microplate spectrophotometer (BioTek, Sunnyvale, CA, USA), and adjusted to the final concentration of 1 ng/μl. Quantitative real-time PCR was performed on an ABI 7500 Fast instrument (Life Technologies, Carlsbad, CA, USA) in a total volume of 20 μl containing 10 μl 2x SYBR Green PCR Master Mix, 1 μl of each primer from the GUT Low-Density Array (GULDA) [24], 4.4 μl of nuclease-free water and 3.6 μl of template DNA. The amplification program consisted of 50 °C for 2 min; 95 °C for 10 min; 40 cycles of 95 °C for 15 s and 60 °C

for 1 min. A dissociation curve was recorded at 95 °C for 15 s, 60 °C for 15 s, then increasing temperature to 95 °C at 2% rate). The mean Ct-value was determined based on a set threshold value of 0.2 and using the automatic baseline correction. Differences in Ct-values for each bacterial target (NO-normalization) were calculated between those obtained with the universal and target-specific primers and log-transformed. Fold-changes for target amplicons were calculated as the (log 2) ratio of normalized abundances, and determined as a percent of the microbiome composition.

2.7. Statistical analysis

Data was analyzed by one-way ANOVA followed by Dunnett's multiple-range tests using Prism 8.0 (GraphPad Software, San Diego, CA). Temporal measures were analyzed by two-factor repeated-measures ANOVA, with time and treatment as independent variables. All data was presented as means \pm SEM. Significant differences were accepted when the p-value was <0.05 .

3. Results

3.1. Changes in body weight and body weight gain

At the beginning of the study, 4-week-old C57BL/6J mice (n=76) were randomly assigned to either LFD (n=32) or HFD (n=44) diet *ad libitum* for 6 weeks. During this initial period, there was no significant difference in food intake between HFD and LFD mice, however the increased caloric density of the HFD diet (5.24 versus 3.85 kcal/g, respectively) allowed for early induction of obesity in the HFD group.

C57BL/6J mice being a polygenic developmental model of diet-induced obesity [21], allowed us to select the HFD animals differing in body weight and fat accumulation despite of their inbred genetic background. Mice highly susceptible to the development of obesity that reached body weights in excess of 36 g after being fed HFD for 6 weeks were designated as obesity-prone or super-responders (SR, n=16). These animals were further divided in two equal groups, one of which was switched back to LFD treatment for the duration of the study (SR-LFD, n=8). On the other hand, mice that failed to cross the 30 g body weight threshold under similar dietary conditions were designated as obesity-resistant or non-responders (NR, n=8). Control animals fed the corresponding LFD or HFD diets, reached the average body weights of 26.2 ± 2.3 and 33.1 ± 3.1 g in the same timeline, respectively.

All mice were kept on their respective diets for additional 8 weeks. This allowed us to differentiate and further amplify the individual variations in response to the obesogenic dietary fats. Control LFD animals continued a slow gradual increase in the body weight and reached an average body weight of 30.8 ± 3.9 g at the end of the study. The HFD controls reached 45.6 ± 3.5 g body weights ($p < 0.05$). Obesity-prone SR mice rapidly gained the excessive body weight and plateaued at the average of 50.6 ± 3.0 g for the last 4 weeks of the study. Obesity-resistant NR mice failed to gain body weight in the excess of 38.6 ± 2.1 g, a -15.4% decrease from the HFD controls and -23.7% decrease from the SR mice. Obesity-prone SR-LFD mice fed the LFD diet rapidly lost weight within 3 weeks of the dietary change, and their body weight remained undistinguished from the LFD controls at the end of the study (Figure 2).

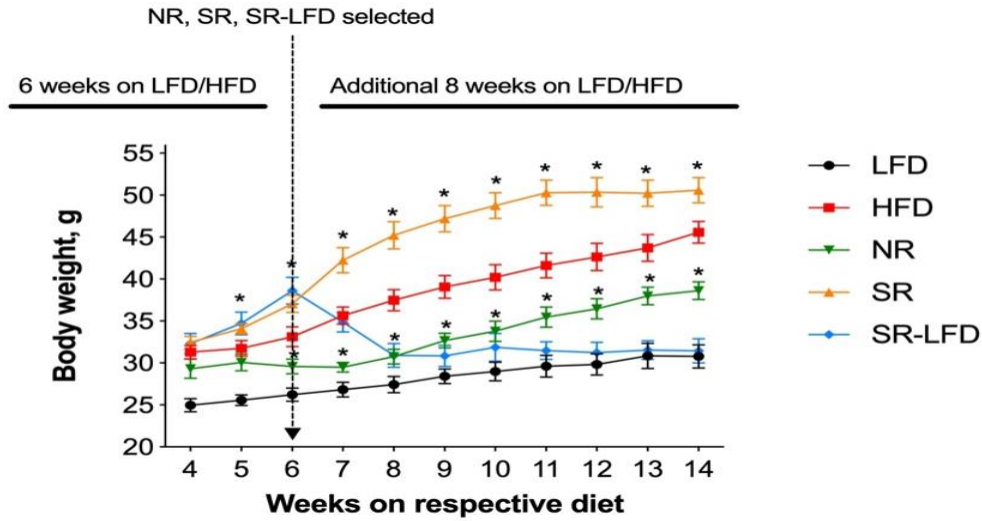


Figure 2.2. Body weight of lean controls (LFD), obese controls (HFD), obesity-resistant non-responders (NR), obesity-prone super-responders (SR), and super-responders fed LFD diet during the study weeks -14 (SR-LFD). Results are expressed as means \pm SEM (n=8). Data were analyzed using a two-factor repeated-measures ANOVA, *p< 0.05 versus the HFD controls.

When body weight gains were determined for the study weeks 4-14, SR mice gained 18.1 ± 4.5 g, an excess of 20.9% over the HFD controls (14.3 ± 4.5 g). NR mice showed reduced body weight gain of 9.3 ± 1.7 g that has not reached statistically significant difference from that of the LFD controls (5.8 ± 3.2 g). When compared directly, SR mice gained 48.6% more body weight than their NR counterparts, highlighting the individual differences despite the shared C57BL/6J background and identical HFD diet. The SR-LFD animals that returned to the LFD diet for the last 8 weeks of the study showed negative body weight gain (-0.9 ± 1.9), essentially losing additional body weight accumulated during the first part of the study (Figure 3).

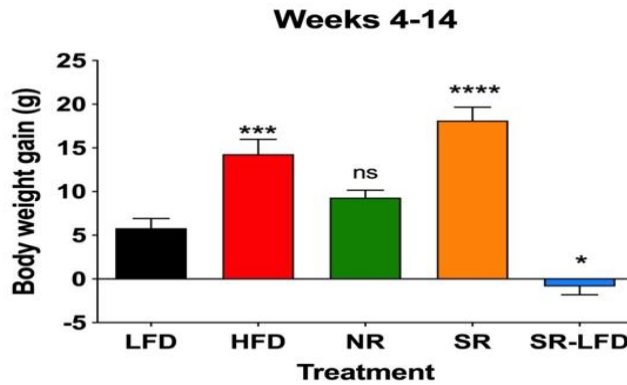


Figure 2.3. Body weight gain of lean controls (LFD), obese controls (HFD), obesity-resistant non-responders (NR), obesity-prone super-responders (SR), and super-responders fed LFD diet during the study weeks -14 (SR-LFD). Results are expressed as means \pm SEM (n=8). Data were analyzed using one-way ANOVA followed by Dunnett’s multiple comparisons, * $p < 0.05$, *** $p < 0.001$, **** $p < 0.00001$ versus the LFD controls.

3.2. Changes in body composition

Body weight gains correlated with significant changes in body composition of all groups at the end of the study. As expected, HFD mice increased their mean body weights by 59.4% over the LFD controls, and this increase consisted of 11.5% increase in lean body mass and 56.8% increase in fat body mass due to the high fat nature of the HFD diet (Figure 4a, c). Similar to HFD mice, NR animals fed HFD diet gained 13.6% more lean body weight, but only 43.2% increase in fat body mass, indicating changes in the skeletal muscle tissues and reduced development of the adipose depots under the same feeding conditions. SR mice gained 21.6% more lean body mass and 67.7% more fat body mass over the LFD controls, which is also a 25.2% increase in fat body mass over normally obese HFD mice ($p < 0.01$, Figure 4c). The SR-LFD animals that returned to the LFD diet showed both lean and fat body mass that returned to that of the LFD controls.

SR mice, however, showed a dramatic increase in free water that exceeded the HFD controls by a factor of 3.1-fold, and the LFD controls by the factor of 5.8-fold. NR mice showed free water content equal to that of the LFD controls (Figure 4b). This was observed in the background of marginally increased total body water (1.3-fold over LFD mice and 1.1-fold over HFD mice, respectively), that cannot explain the difference in free water that is generally associated with bladder content (Figure 4d).

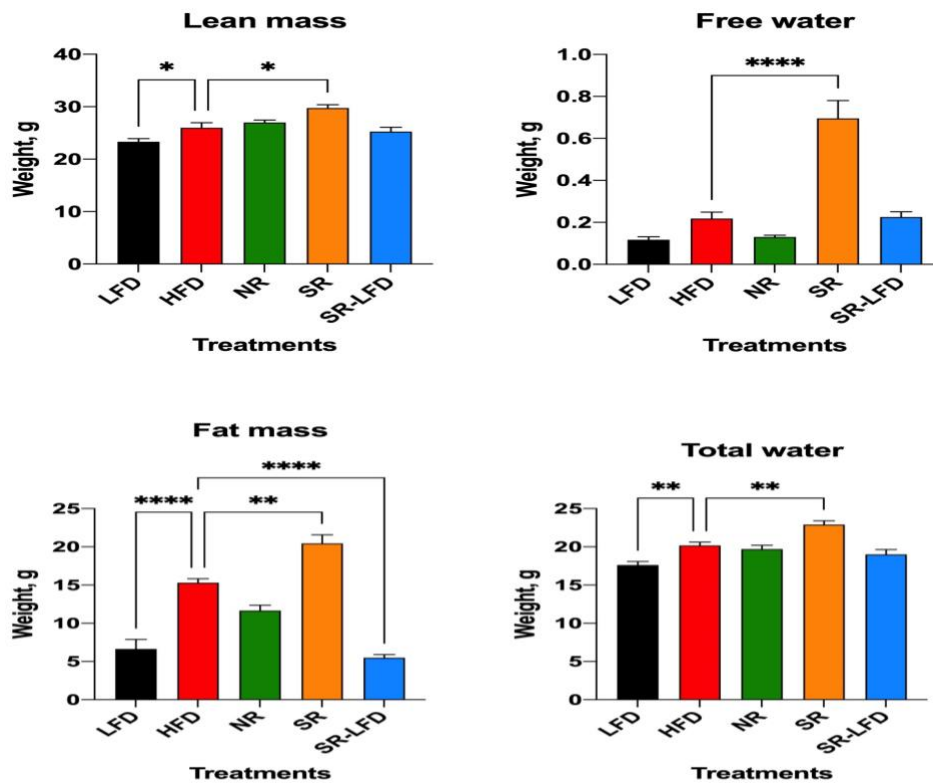
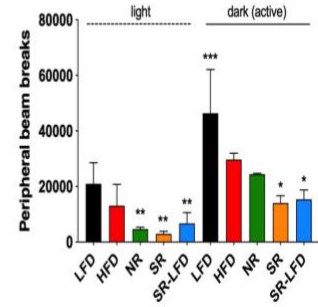
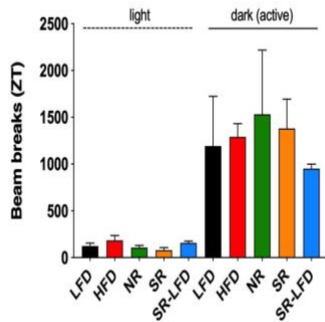
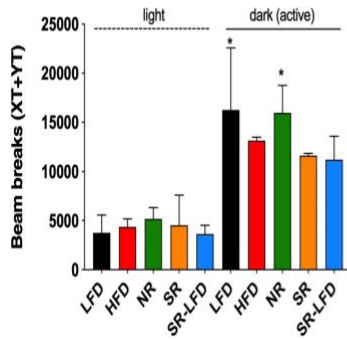
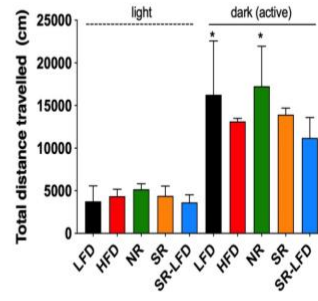
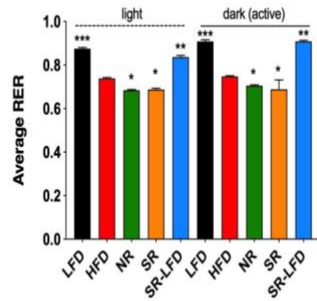
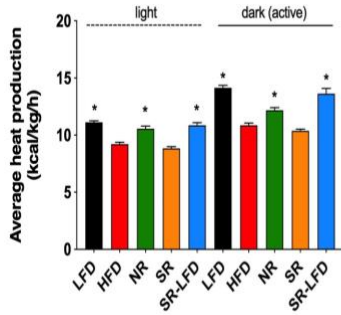
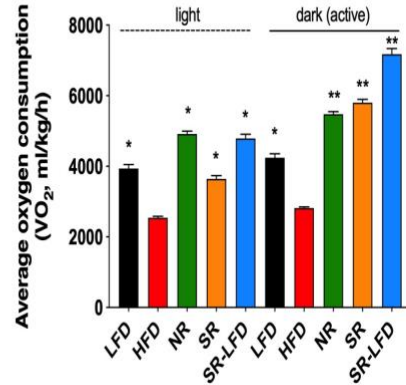
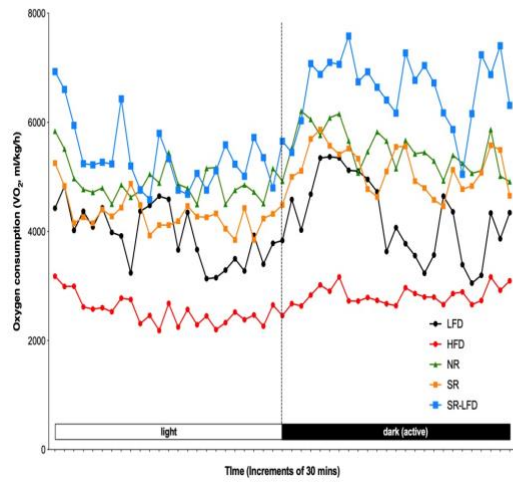


Figure 2.4. Body composition of lean controls (LFD), obese controls (HFD), obesity-resistant non-responders (NR), obesity-prone super-responders (SR), and super-responders fed LFD diet, including (a) lean body mass, (b) free water, (c) fat body mass, (d) total water. Results are expressed as means \pm SEM (n=8). Data were analyzed using one-way ANOVA followed by Dunnett’s multiple comparisons, * $p < 0.05$, ** $p < 0.01$, **** $p < 0.00001$ versus the HFD controls.

3.3. Metabolic responses to dietary fat

We next used open circuit indirect calorimetry to measure energy expenditure, including VO_2 , VCO_2 , RER, and voluntary physical activity using infrared beam breaks in the horizontal and vertical planes (Figure 5). All metabolic parameters related to energy metabolism were normalized to lean body mass to account for differences in the animal body weights, as per standard considerations [25].

Figure 2.5. Changes in whole-body energy balance in response to dietary fats as compared among lean controls (LFD), obese controls (HFD), obesity-resistant non-responders (NR), obesity-prone super-responders (SR), and super-responders fed LFD diet. Indirect calorimetry determines (a) dynamics of oxygen consumption, (b) average oxygen consumption, (c) average heat production, (d) average RER, (e) distance traveled, (f) voluntary physical activity in horizontal plane, (g) voluntary rearing, (h) fine, agitation-like movements. Results are expressed as means \pm SEM (n=8). Data were analyzed using one-way ANOVA followed by Dunnett's multiple comparisons, *p< 0.05, **p<0.01, ***p<0.001 versus the HFD controls.



The dynamics of oxygen consumption during light (inactive) and dark (active) cycle are shown in Figure 5a and averaged in Figure 5b. As expected, HFD mice showed decreased oxygen consumption relative to LFD controls in both cycles with mean VO₂ values of 2542 ± 300 and 2815 ± 269 ml/kg/h, respectively. Both SR and NR mice showed elevated oxygen consumption during the active cycle, but only NR mice kept oxygen consumption levels high during the inactive cycle (4918 ± 548 ml/kg/h, p<0.05). This subsequently translated to higher levels of heat production during both the inactive (10.6 ± 1.6 kcal/kg/h, p<0.05) and active cycle (12.2 ± 1.7 kcal/kg/h, p<0.05). SR mice failed to upregulate heat production in both cycles, which serves as indirect evidence for an inefficient energy metabolism despite increased oxygen consumption during the active cycle (Figure 5c).

All animal groups fed HFD diet showed respiratory exchange ratios (RER) in the range of 0.685-0.748, indicating that all of them relied on dietary fats the primary metabolic fuel. The lowest mean RER value was observed in NR mice during the inactive cycle (0.685 ± 0.022, p<0.05), suggesting an upregulated lipid metabolism despite relative inactivity at rest (Figure 5d).

Voluntary physical activity was increased in NR mice and reached the basal levels of the LFD controls in the active cycle both in total distance traveled (Figure 5e), horizontal plane movements (Figure 5f), but not vertical rearing (Figure 5g). Peripheral beam breaks that capture fine, agitation-like movements, were reduced (Figure 5h).

SR-LFD mice fed LFD diet showed clear signs of increased energy expenditure (Figure 5 b,c) and a fuel shift towards utilization of carbohydrates (Figure 5d) that matched the body weight loss observed after the dietary switch. Their voluntary physical activity, however, remained at the level of SR mice and has not improved with time (Figure 5 e,h).

3.5. Irreversible changes in exercise capacity

Obese HFD, SR, and SR-LFD mice showed decreased voluntary physical activity that can be partially explained by excessive body weight. Inability of SR-LFD mice to restore the voluntary physical activity to the basal levels (Figure 5 e, h), despite the switch to the LFD diet and the corresponding weight loss (Figure 2), prompted us to evaluate changes in their exercise capacity using a rodent treadmill. Similar to the metabolic chamber data, obese HFD controls showed decreased exercise capacity to maintain the running exercise on a treadmill (511 ± 204 s versus 856 ± 160 s for the LFD controls, $p < 0.05$) (Figure 6).

Notably, both NR mice, as well as SR-LFD mice that lost the excessive body weight after a dietary switch to the LFD diet, failed to alter or regain the basal exercise capacity despite significantly lower body weights (Figure 2) and comparable lean body mass (Figure 4a) at the end of the study. This data suggested of yet unknown changes in the physiology of the skeletal muscle induced by high dietary fats that failed to resolve even after the LFD diet was introduced, at least within the timeline of this study (8 weeks).

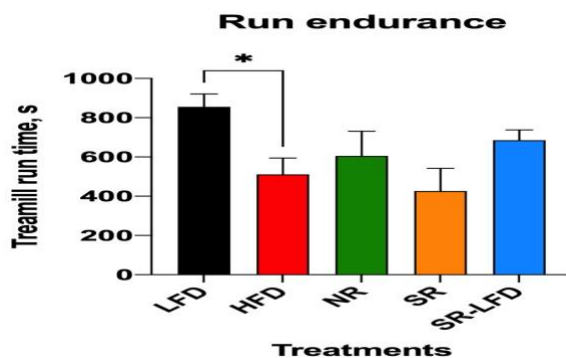


Figure 2.6. Exercise capacity of lean controls (LFD), obese controls (HFD), obesity-resistant non-responders (NR), obesity-prone super-responders (SR), and super-responders fed LFD diet at the end of the study. Results are expressed as means \pm SEM (n=8). Data were analyzed using one-way ANOVA followed by Dunnett's multiple comparisons, * $p < 0.05$ versus the HFD controls.

3.6. Food intake and feed efficiency

Control animals consumed on average 2.68 ± 0.21 g per LFD animal per day and 2.84 ± 0.29 g per HFD animal per day for the duration of the study (Figure 7a). Although daily food intakes were similar between LFD and HFD animals, caloric densities of these diets differed significantly (3.85 kcal/g versus 5.24 kcal/g). Therefore, HFD mice experienced larger energy intakes in the range of 14.88 kcal/animal/day versus 10.32 kcal/animal/day for the LFD counterparts. Nearly all additional calories came in the form of dietary fats due to the nature of the HFD diet.

Both SR mice and NR mice showed average food intakes similar to those of HFD controls, suggesting that differences in energy intakes were not responsible for the observed changes in body weight gain and body composition (Figure 7 a,b). If anything, NR mice trended to an increased food intake that nearly reached statistical significance (3.18 ± 0.28 g

per animal per day, $p=0.066$). Their feed efficiency, or the ability to convert consumed food into a body weight gain, was reduced by 39.6% (0.033 ± 0.002 g/kcal versus 0.053 ± 0.002 g/kcal for HFD controls, $p=0.043$). SR-LFD mice showed a negative feed efficiency due to a progressive body weight loss after switching from HFD to the LFD diet (Figure 7c).

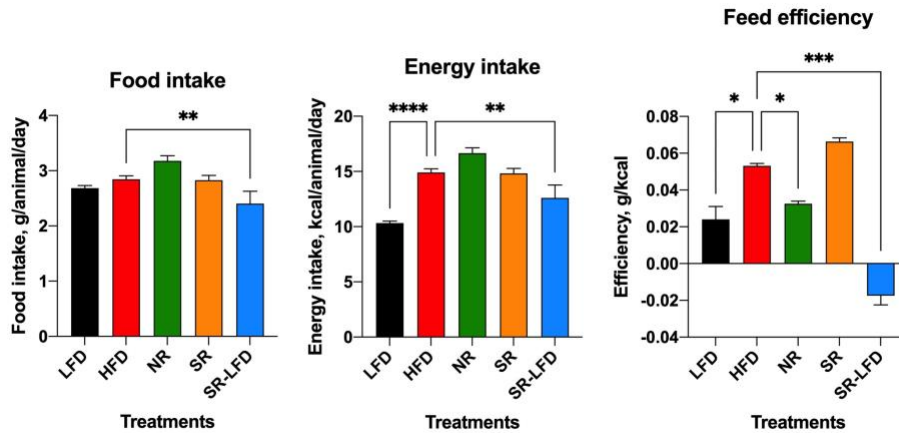


Figure 2.7. Changes in (a) food intake, (b) energy intake, and (c) feed efficiency among lean controls (LFD), obese controls (HFD), obesity-resistant non-responders (NR), obesity-prone super-responders (SR), and super-responders fed LFD diet. Results are expressed as means \pm SEM ($n=8$). Data were analyzed using one-way ANOVA followed by Dunnett's multiple comparisons, * $p<0.05$, ** $p<0.01$, *** $p<0.00001$ versus the HFD controls.

3.7. Fecal lipids and microbiome profiles

We also quantified fecal output and fecal lipid content to account for discrepancies between intake and metabolism of dietary fat in SR and NR mice. There were no changes in fecal pellet characteristics among all study groups (Figure 8a). However, the lipid content of the feces was higher for HFD controls ($8.8 \pm 2.9\%$) versus the LFD controls ($5.7 \pm 1.4\%$, $p=0.008$). Unexpectedly, both SR and NR mice showed lipid fecal content similar to the LFD controls (Figure 8b), suggesting that both groups absorbed dietary lipids more efficiently than

the HFD mice, yet they processed and/or metabolized it differently which resulted in the body weight gain and fat body mass disparities among these groups.

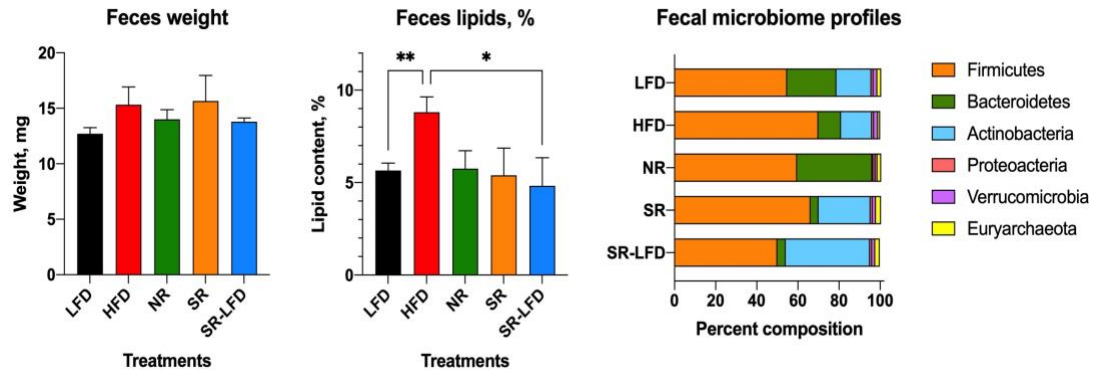


Figure 2.8. Fecal outputs and microbiome profiles determined at the end of the study among lean controls (LFD), obese controls (HFD), obesity-resistant non-responders (NR), obesity-prone super-responders (SR), and super-responders fed LFD diet, including (a) fecal pellet weight, (b) fecal fat content, (c) microbiome composition at the phylum level. Results are expressed as means \pm SEM (n=8). Data were analyzed using one-way ANOVA followed by Dunnett’s multiple comparisons, * $p < 0.05$, ** $p < 0.01$ versus the HFD controls.

Fecal microbial profiles were strongly affected by the obesity-prone or obesity-resistant phenotypes. The LFD controls showed a typical murine fecal microbiome profile consisting of 55% *Firmicutes*, 24% *Bacteroidetes*, 17% *Actinobacteria*, 1.8% *Verrucomicrobia*, 1.8% *Euryarchaeota*, and 1% *Proteobacteria*. Feeding the HFD diet resulted in subtle shifts in the fecal microbiome profile towards increased *Firmicutes* (70%) and decreased *Bacteroidetes* (11%). These changes were potentiated in the SR obesity-prone mice with a further reduction in *Bacteroidetes* (4%) and expansion of *Actinobacteria* (25%). The NR obesity-resistant mice

showed a clear opposing trend with expansion of *Bacteroidetes* (37%) and reduction of *Actinobacteria* (1%). Even after switching to the LFD diet, SR-LFD mice preserved the obesity-prone fecal microbiome profile with reduced *Bacteroidetes* (4%) and expanded *Actinobacteria* (41%) until the end of the study (Figure 8c).

4. Discussion

Individual metabolic variations can significantly influence predisposition to obesity, especially in the face of contemporary dietary habits [26]. Human bodies metabolize nutrients differently based on a multiplicity of factors, influencing how efficiently dietary fats, carbohydrates, and proteins are processed. This inherent diversity means that some individuals might have a lower metabolic efficiency and a higher propensity to store excess calories as fat, making them more susceptible to weight gain [27]. When these metabolic differences intersect with the prevalence of modern processed foods, the impact on obesity rates becomes significant. The calorie-dense, yet nutritionally poor options, can lead to weight gain, particularly when combined with larger meal sizes that have become the norm in many societies. Additional calories not only contribute to weight gain but also pose serious health risks, impacting cardiovascular health and further elevating the risk of obesity-related complications [28]. Moreover, individuals prone to fat accumulation and obesity face additional hidden malnutrition challenges through acute and chronic metabolic disorders that often are present in overweight and obese states [29]. This is particular true for sarcopenic obesity associated with skeletal muscle tissues developing insulin resistance, ectopic fat accumulation, and mitochondrial dysfunction [30].

As animals were fed HFD diet excessive in dietary fats during the first 6 weeks of the study, they gained body weight and adjusted their body composition to accommodate for additional energy intake. Due to the polygenic nature of C57BL/6J obesity, there was a significant variation in this process that allowed us to select obese-prone, super-responders in the upper quartile (SR) and obese-resistant, non-responders (NR) in the lower quartile similar to the previous studies [14,16,17,19]. Highest body weight gains observed in SR mice were accompanied by higher lean body mass, fat body mass, total, and free water. The last measure is rather peculiar because it largely determines free urine in the bladder. This seems to indicate that SR mice tried to counteract excessive dietary fat by increasing their water intake [31] (which was not measured in this study), or required more water to suppress whole-body lipolysis [32]. Otherwise, SR mice had similar food intake, fecal output, and RER quotient to those of NR mice, suggesting that differences in energy metabolism were the primary reason behind the observed individual variation.

Some of the energy expenditure data hinted at the target tissues that may be responsible for this difference. NR mice showed higher oxygen consumption during the light (rest) cycle of the day, suggesting that their resting metabolic rate (RMR) became higher. RMR is one of the major contributors to weight stability that consists predominantly from the thermic effects of skeletal muscles (including heart) and the digestive tract [33]. Average heat production was also increased in NR animals, as was the voluntary physical activity similar to what was observed in the previous studies [16,19]. There might not be a single ideal RMR given the impact of food availability in natural settings that are highly variable, however overall reproductive success in mammals was often positively correlated with resting metabolic rate [34]. As NR mice consumed on average 12% more HFD diet, excreted similar amounts of

lipids in feces, and accumulated 75.6% less fat body mass than SR animals, the net balance of the remaining lipids requires increased capacity for their metabolism normally achieved by the metabolic flexibility of the skeletal muscle [35]. Shifting towards increased reliance on fat oxidation may conserve the use of plasma glucose and postpone the depletion of muscle glycogen under the conditions of high dietary fat intake (by elevated plasma fatty acids), or after fasting when food is not available. As such, diminished metabolic flexibility of skeletal muscle to oxidize fat under conditions of low carbohydrate and high dietary fat load is strongly predictive of weight gain [36].

Although there is considerable interest in understanding the adaptive significance of variations in metabolic rates, there have been surprisingly few empirical efforts to test whether there is a correlation between metabolic rates and individual fitness, or at least components of fitness. This study evaluated the exercise capacity of both NR and SR mice in comparison with control animals, and showed a 29.2-50.2% decrease as compared to healthy lean animals, but only 15.5-16.6% variation when compared to the obese controls. These findings suggest that metabolic flexibility of the skeletal muscle to increase fat oxidation is achieved at the expense of muscle function. This is especially highlighted in SR-LFD mice that were fed low-fat diet during the last 8 weeks of the study, and showed a near complete return to healthy body weight, lean and fat body mass, and increased energy metabolism that persisted to sustain the weight loss. However, despite returning to the normal body weight, SR-LFD mice failed to regain the exercise capacity similar to that of control animals, once again suggesting an irreversible change to the skeletal muscle function that has not resolved for the duration of the study.

The contribution of microbial enterotypes to individual nutrition and obesity management remains largely unexplored [37]. It is well established that out of thousands

bacterial species found in the gut, the majority belong to two phyla *Firmicutes* and *Bacteroidetes* that encompass ~90% of the microbiota, and the minimal model microbiome additionally contains *Proteobacteria*, *Actinobacteria*, *Fusobacteria*, *Verrucomicrobia*, and *Euryarchaeota* [38]. Microbial enterotypes can be polarized based on the predominant macronutrients and energy substrates in the diet [39], as seen for *Bacteroidetes* that can be dominated by the genus *Bacteroides* on diets high in animal protein and fat, or by the genus *Prevotella* on plant fiber-rich diets [40]. Some studies have reported that major enterotypes remain largely unchanged even after 6 months of dietary adjustments [41]. The stability of the less prominent phyla is poorly understood, for example, *Actinobacteria* seem to dominate young children gastrointestinal tracts due to consumption of human milk, but plummet to a minor status shortly after weaning [42]. In this study, we observed that obese-resistant NR mice expanded the *Bacteroidetes* phylum at the expense of highly diminished *Actinobacteria* phylum. The significance of this finding remains to be elucidated, as it was previously reported that enriching gut microbiome with *Actinobacteria* (specifically, the genus *Bifidobacterium*) with oligofructose prebiotics positively correlated with improved glucose tolerance and insulin secretion [43].

5. Conclusions

Together, these findings underscore the significant role of individual metabolic variations in influencing susceptibility to obesity in the context of contemporary dietary habits and modern centralized agricultural production systems [44]. The inherent diversity in nutrient utilization contributes to differences in metabolic efficiency, impacting the storage of excess calories as fat and increasing the vulnerability to weight gain. Differences in energy

metabolism in the form of resting metabolic rate, skeletal muscle metabolic flexibility, and weight stability suggest a trade-off between supporting high rates of fat metabolism and maintaining healthy muscle function.

Furthermore, this study draws attention to the unexplored contribution of microbial enterotypes to individual nutrition and obesity management, emphasizing the need for further investigation into the stability of gut microbiome composition in response to dietary adjustments. The major divergence in obesity phenotypes, energy metabolism, fecal microbiome profiles, and functional status of skeletal muscles in subjects prone or resistant to developing obesity warrants a critical new look into biochemistry and gene expression pathways in the muscle tissues that are responsible for these effects.

REFERENCES

1. Milhem, F.; Komarnytsky, S. Progression to Obesity: Variations in Patterns of Metabolic Fluxes, Fat Accumulation, and Gastrointestinal Responses. *Metabolites* **2023**, *13*, 1016, doi:10.3390/metabo13091016.
2. Stunkard, A.J.; Harris, J.R.; Pedersen, N.L.; McClearn, G.E. The Body-Mass Index of Twins Who Have Been Reared Apart. *N Engl J Med* **1990**, *322*, 1483–1487, doi:10.1056/NEJM199005243222102.
3. Thaker, V.V. GENETIC AND EPIGENETIC CAUSES OF OBESITY. *Adolesc Med State Art Rev* **2017**, *28*, 379–405.
4. Khera, A.V.; Chaffin, M.; Wade, K.H.; Zahid, S.; Brancale, J.; Xia, R.; Distefano, M.; Senol-Cosar, O.; Haas, M.E.; Bick, A.; et al. Polygenic Prediction of Weight and Obesity Trajectories from Birth to Adulthood. *Cell* **2019**, *177*, 587-596.e9, doi:10.1016/j.cell.2019.03.028.
5. Yengo, L.; Sidorenko, J.; Kemper, K.E.; Zheng, Z.; Wood, A.R.; Weedon, M.N.; Frayling, T.M.; Hirschhorn, J.; Yang, J.; Visscher, P.M.; et al. Meta-Analysis of Genome-Wide Association Studies for Height and Body Mass Index in ~700000 Individuals of European Ancestry. *Hum Mol Genet* **2018**, *27*, 3641–3649, doi:10.1093/hmg/ddy271.
6. Riveros-McKay, F.; Mistry, V.; Bounds, R.; Hendricks, A.; Keogh, J.M.; Thomas, H.; Henning, E.; Corbin, L.J.; Understanding Society Scientific Group; O’Rahilly, S.; et al. Genetic Architecture of Human Thinness Compared to Severe Obesity. *PLoS Genet* **2019**, *15*, e1007603, doi:10.1371/journal.pgen.1007603.
7. Liu, A.G.; Ford, N.A.; Hu, F.B.; Zelman, K.M.; Mozaffarian, D.; Kris-Etherton, P.M. A Healthy Approach to Dietary Fats: Understanding the Science and Taking Action to Reduce Consumer Confusion. *Nutr J* **2017**, *16*, 53, doi:10.1186/s12937-017-0271-4.
8. Astrup, A. The Role of Dietary Fat in Obesity. *Semin Vasc Med* **2005**, *5*, 40–47, doi:10.1055/s-2005-871740.

9. Flatt, J. Use and Storage of Carbohydrate and Fat. *The American Journal of Clinical Nutrition* **1995**, *61*, 952S-959S, doi:10.1093/ajcn/61.4.952S.
10. Nagarajan, S.R.; Cross, E.; Sanna, F.; Hodson, L. Dysregulation of Hepatic Metabolism with Obesity: Factors Influencing Glucose and Lipid Metabolism. *Proc Nutr Soc* **2022**, *81*, 1–11, doi:10.1017/S0029665121003761.
11. Ludwig, D.S.; Ebbeling, C.B. The Carbohydrate-Insulin Model of Obesity: Beyond ‘Calories In, Calories Out.’ *JAMA Intern Med* **2018**, *178*, 1098–1103, doi:10.1001/jamainternmed.2018.2933.
12. Pawlak, D.B.; Kushner, J.A.; Ludwig, D.S. Effects of Dietary Glycaemic Index on Adiposity, Glucose Homeostasis, and Plasma Lipids in Animals. *Lancet* **2004**, *364*, 778–785, doi:10.1016/S0140-6736(04)16937-7.
13. Anderson, A.S.; Key, T.J.; Norat, T.; Scoccianti, C.; Cecchini, M.; Berrino, F.; Boutron-Ruault, M.-C.; Espina, C.; Leitzmann, M.; Powers, H.; et al. European Code against Cancer 4th Edition: Obesity, Body Fatness and Cancer. *Cancer Epidemiology* **2015**, *39*, S34–S45, doi:10.1016/j.canep.2015.01.017.
14. Abou Mrad, J.; Yakubu, F.; Lin, D.; Peters, J.C.; Atkinson, J.B.; Hill, J.O. Skeletal Muscle Composition in Dietary Obesity-Susceptible and Dietary Obesity-Resistant Rats. *Am J Physiol* **1992**, *262*, R684-688, doi:10.1152/ajpregu.1992.262.4.R684.
15. Pagliassotti, M.J.; Pan, D.; Prach, P.; Koppenhafer, T.; Storlien, L.; Hill, J.O. Tissue Oxidative Capacity, Fuel Stores and Skeletal Muscle Fatty Acid Composition in Obesity-Prone and Obesity-Resistant Rats. *Obes Res* **1995**, *3*, 459–464, doi:10.1002/j.1550-8528.1995.tb00175.x.
16. Surwit, R.S.; Wang, S.; Petro, A.E.; Sanchis, D.; Raimbault, S.; Ricquier, D.; Collins, S. Diet-Induced Changes in Uncoupling Proteins in Obesity-Prone and Obesity-Resistant Strains of Mice. *Proceedings of the National Academy of Sciences* **1998**, *95*, 4061–4065, doi:10.1073/pnas.95.7.4061.

17. Allerton, T.D.; Primeaux, S.D. High-Fat Diet Differentially Regulates Metabolic Parameters in Obesity-Resistant S5B/Pl Rats and Obesity-Prone Osborne-Mendel Rats. *Can J Physiol Pharmacol* **2016**, *94*, 206–215, doi:10.1139/cjpp-2015-0141.
18. Choi, J.-Y.; McGregor, R.A.; Kwon, E.-Y.; Kim, Y.J.; Han, Y.; Park, J.H.Y.; Lee, K.W.; Kim, S.-J.; Kim, J.; Yun, J.W.; et al. The Metabolic Response to a High-Fat Diet Reveals Obesity-Prone and -Resistant Phenotypes in Mice with Distinct mRNA-Seq Transcriptome Profiles. *Int J Obes* **2016**, *40*, 1452–1460, doi:10.1038/ijo.2016.70.
19. Chu, D.-T.; Malinowska, E.; Jura, M.; Kozak, L.P. C57BL/6J Mice as a Polygenic Developmental Model of Diet-Induced Obesity. *Physiol Rep* **2017**, *5*, e13093, doi:10.14814/phy2.13093.
20. Li, H.; Xie, Z.; Lin, J.; Song, H.; Wang, Q.; Wang, K.; Su, M.; Qiu, Y.; Zhao, T.; Song, K.; et al. Transcriptomic and Metabonomic Profiling of Obesity-Prone and Obesity-Resistant Rats under High Fat Diet. *J. Proteome Res.* **2008**, *7*, 4775–4783, doi:10.1021/pr800352k.
21. Reed, D.R.; Li, X.; McDaniel, A.H.; Lu, K.; Li, S.; Tordoff, M.G.; Price, R.A.; Bachmanov, A.A. Loci on Chromosomes 2, 4, 9, and 16 for Body Weight, Body Length, and Adiposity Identified in a Genome Scan of an F2 Intercross between the 129P3/J and C57BL/6ByJ Mouse Strains. *Mamm Genome* **2003**, *14*, 302–313, doi:10.1007/s00335-002-2170-y.
22. Péronnet, F.; Massicotte, D. Table of Nonprotein Respiratory Quotient: An Update. *Can J Sport Sci* **1991**, *16*, 23–29.
23. Folch, J.; Lees, M.; Sloane Stanley, G.H. A Simple Method for the Isolation and Purification of Total Lipides from Animal Tissues. *J Biol Chem* **1957**, *226*, 497–509.
24. Bergström, A.; Licht, T.R.; Wilcks, A.; Andersen, J.B.; Schmidt, L.R.; Grønlund, H.A.; Vigsnaes, L.K.; Michaelsen, K.F.; Bahl, M.I. Introducing Gut Low-Density Array (GULDA): A Validated Approach for qPCR-Based Intestinal Microbial Community Analysis. *FEMS Microbiol Lett* **2012**, *337*, 38–47, doi:10.1111/1574-6968.12004.
25. Speakman, J. Measuring Energy Metabolism in the Mouse – Theoretical, Practical, and Analytical Considerations. *Frontiers in Physiology* **2013**, *4*.

26. Piaggi, P. Metabolic Determinants of Weight Gain in Humans. *Obesity (Silver Spring)* **2019**, *27*, 691–699, doi:10.1002/oby.22456.
27. Abiri, B.; Valizadeh, M.; Nasreddine, L.; Hosseinpanah, F. Dietary Determinants of Healthy/Unhealthy Metabolic Phenotype in Individuals with Normal Weight or Overweight/Obesity: A Systematic Review. *Crit Rev Food Sci Nutr* **2023**, *63*, 5856–5873, doi:10.1080/10408398.2021.2025036.
28. Drewnowski, A. Nutrient Density: Addressing the Challenge of Obesity. *Br J Nutr* **2018**, *120*, S8–S14, doi:10.1017/S0007114517002240.
29. Barazzoni, R.; Gortan Cappellari, G. Double Burden of Malnutrition in Persons with Obesity. *Rev Endocr Metab Disord* **2020**, *21*, 307–313, doi:10.1007/s11154-020-09578-1.
30. Kalinkovich, A.; Livshits, G. Sarcopenic Obesity or Obese Sarcopenia: A Cross Talk between Age-Associated Adipose Tissue and Skeletal Muscle Inflammation as a Main Mechanism of the Pathogenesis. *Ageing Res Rev* **2017**, *35*, 200–221, doi:10.1016/j.arr.2016.09.008.
31. Dennis, E.A.; Dengo, A.L.; Comber, D.L.; Flack, K.D.; Savla, J.; Davy, K.P.; Davy, B.M. Water Consumption Increases Weight Loss during a Hypocaloric Diet Intervention in Middle-Aged and Older Adults. *Obesity (Silver Spring)* **2010**, *18*, 300–307, doi:10.1038/oby.2009.235.
32. Keller, U.; Szinnai, G.; Bilz, S.; Berneis, K. Effects of Changes in Hydration on Protein, Glucose and Lipid Metabolism in Man: Impact on Health. *Eur J Clin Nutr* **2003**, *57 Suppl 2*, S69-74, doi:10.1038/sj.ejcn.1601904.
33. Tran, L.T.; Park, S.; Kim, S.K.; Lee, J.S.; Kim, K.W.; Kwon, O. Hypothalamic Control of Energy Expenditure and Thermogenesis. *Exp Mol Med* **2022**, *54*, 358–369, doi:10.1038/s12276-022-00741-z.
34. Boratyński, Z.; Koteja, P. Sexual and Natural Selection on Body Mass and Metabolic Rates in Free-Living Bank Voles. *Functional Ecology* **2010**, *24*, 1252–1261, doi:10.1111/j.1365-2435.2010.01764.x.

35. Kelley, D.E. Skeletal Muscle Fat Oxidation: Timing and Flexibility Are Everything. *J Clin Invest* **2005**, *115*, 1699–1702, doi:10.1172/JCI25758.
36. Zurlo, F.; Lillioja, S.; Esposito-Del Puente, A.; Nyomba, B.L.; Raz, I.; Saad, M.F.; Swinburn, B.A.; Knowler, W.C.; Bogardus, C.; Ravussin, E. Low Ratio of Fat to Carbohydrate Oxidation as Predictor of Weight Gain: Study of 24-h RQ. *Am J Physiol* **1990**, *259*, E650–657, doi:10.1152/ajpendo.1990.259.5.E650.
37. Christensen, L.; Roager, H.M.; Astrup, A.; Hjorth, M.F. Microbial Enterotypes in Personalized Nutrition and Obesity Management. *Am J Clin Nutr* **2018**, *108*, 645–651, doi:10.1093/ajcn/nqy175.
38. Kaoutari, A.E.; Armougom, F.; Gordon, J.I.; Raoult, D.; Henrissat, B. The Abundance and Variety of Carbohydrate-Active Enzymes in the Human Gut Microbiota. *Nat Rev Microbiol* **2013**, *11*, 497–504, doi:10.1038/nrmicro3050.
39. Komarnytsky, S.; Wagner, C.; Gutierrez, J.; Shaw, O.M. Berries in Microbiome-Mediated Gastrointestinal, Metabolic, and Immune Health. *Curr Nutr Rep* **2023**, *12*, 151–166, doi:10.1007/s13668-023-00449-0.
40. Wu, G.D.; Chen, J.; Hoffmann, C.; Bittinger, K.; Chen, Y.-Y.; Keilbaugh, S.A.; Bewtra, M.; Knights, D.; Walters, W.A.; Knight, R.; et al. Linking Long-Term Dietary Patterns with Gut Microbial Enterotypes. *Science* **2011**, *334*, 105–108, doi:10.1126/science.1208344.
41. Roager, H.M.; Licht, T.R.; Poulsen, S.K.; Larsen, T.M.; Bahl, M.I. Microbial Enterotypes, Inferred by the Prevotella-to-Bacteroides Ratio, Remained Stable during a 6-Month Randomized Controlled Diet Intervention with the New Nordic Diet. *Appl Environ Microbiol* **2014**, *80*, 1142–1149, doi:10.1128/AEM.03549-13.
42. D’Argenio, V.; Salvatore, F. The Role of the Gut Microbiome in the Healthy Adult Status. *Clin Chim Acta* **2015**, *451*, 97–102, doi:10.1016/j.cca.2015.01.003.
43. Cani, P.D.; Neyrinck, A.M.; Fava, F.; Knauf, C.; Burcelin, R.G.; Tuohy, K.M.; Gibson, G.R.; Delzenne, N.M. Selective Increases of Bifidobacteria in Gut Microflora Improve High-

Fat-Diet-Induced Diabetes in Mice through a Mechanism Associated with Endotoxaemia. *Diabetologia* **2007**, *50*, 2374–2383, doi:10.1007/s00125-007-0791-0.

44. Komarnytsky, S.; Retchin, S.; Vong, C.I.; Lila, M.A. Gains and Losses of Agricultural Food Production: Implications for the Twenty-First Century. *Annu Rev Food Sci Technol* **2022**, *13*, 239–261, doi:10.1146/annurev-food-082421-114831.

CHAPTER 3- Molecular insights into obesity resistance in C57BL/6J mice include biomarkers of muscle fiber dynamics and mitochondrial adaptation to high dietary fats

Abstract

Obesity-resistant (non-responder, NR) phenotypes that exhibit reduced susceptibility to developing obesity despite being exposed to high dietary fat are crucial in exploring the metabolic responses that protect against obesity. Although several efforts have been made to study them in mice and humans, the individual protective mechanisms are poorly understood. In this exploratory study, we used a polygenic C57BL/6J mouse model of diet-induced obesity to show that NR mice developed healthier fat/lean body mass ratios (0.43 ± 0.05) versus the obesity-prone (super-responder, SR) phenotypes (0.69 ± 0.07 , $p < 0.0001$) by upregulating gene expression networks that promote the accumulation of type 2a, fast-twitch, oxidative muscle tissues. This was achieved in part by a metabolic adaptation in the form of blood glucose sparing, thus aggravating glucose tolerance. Resistance to obesity in NR mice was associated with 4.9-fold upregulated mitoferrin 1 (*Slc25a37*), an essential mitochondrial iron importer. SR mice also showed fecal volatile metabolite signatures of enhanced short-chain fatty acid metabolism, including increases in detrimental methyl formate and ethyl propionate, and these effects were reversed in NR mice. Continued research into obesity-resistant phenotypes can offer valuable insights into the underlying mechanisms of obesity and metabolic health, potentially leading to more personalized and effective approaches for managing weight and related health issues.

Published as: Milhem, F., Hamilton, L. M., Skates, E., Wilson, M., Johanningsmeier, S. D., & Komarnytsky, S. (2024). Biomarkers of Metabolic Adaptation to High Dietary Fats in a Mouse Model of Obesity Resistance. *Metabolites*, *14*(1), Article 1.

<https://doi.org/10.3390/metabo14010069>

1. Introduction

Modern conveniences, such as energy-dense foods and sedentary lifestyles, contribute significantly to weight gain and difficulty in weight management [1]. Genetic factors, cultural associations with certain types of foods, environmental pollutants, socioeconomic disparities, as well as stigmatization and discrimination against individuals struggling with their weight can further exacerbate obesity [2]. The abundance of conflicting information about diets, exercise regimens, and weight loss methods may add to ineffective or unsustainable approaches to for those who struggle with excessive weight. Though it is commonly thought that altering physical activity levels could balance energy intake and create a negative energy state, the extent of these compensatory mechanisms is frequently underestimated. For instance, an adult who consumes a 290-kcal meal would need to walk approximately 90 min or 5 km to reach a theoretical energy equilibrium [3]. A multifaceted approach involving education about nutrition and lifestyle choices, policy changes to promote healthier food production systems, and enhancing access to affordable, nutritious foods is a clear priority [4]. Additionally, personalized approaches that consider individual differences in genetics, metabolism, and behavioral patterns cannot be overlooked [5].

Resistance to obesity associated with overconsumption of calorie-dense foods is a very interesting phenomenon [6]. Although the body can restrain food intake below the levels of maximum consumption, the precise mechanism that modulates this process remains unclear [7]. If food intake cannot be restrained for a variety of reasons, the flow of nutrients between the metabolically active tissues and timely oxidation of the energy substrates must be controlled. Yet a small but constant margin of error of 175 kcal energy intake per day may translate to 3 kg body weight gain or loss per year, highlighting a critical need to understand individual variation in nutrient absorption and metabolism [8]. Resistance to body weight gain

despite excessive calorie intake has been observed both in rodents and humans, yet it is unclear how skeletal muscle [9] and adipose tissue [10] cooperate in this process. Free fatty acids sourced from the adipose tissue (fasted state) and circulating dietary triglycerides (fed state) are the principal lipid types used for oxidation. Because in healthy states, at least in rodents, dietary lipids are slow to absorb and the majority of them partition to the gut, liver, and skeletal muscle but not adipose tissue in the first 24 hours following food intake [11], it is logical to conclude that differences at the level of muscle tissue physiology and fat oxidation are the primary contributors to the inefficient handling of dietary fats and their subsequent partition into the adipose tissue. Indeed, resistance to obesity was observed to be associated in part with activation of mitochondrial oxidative pathways [12].

This concept challenges the traditional notion that all obese individuals are at equal risk for metabolic complications as discussed elsewhere [13], and predicts a subset of obese population that presents with a more favorable skeletal muscle metabolic profile that allows them to accumulate less visceral and ectopic fat, and build up resilience to the detrimental metabolic effects commonly associated with obesity. This, however, may come at the expense of disturbances in carbohydrate metabolism [14]. This state can occur independently of body weight and is observed in both lean and obese individuals, emphasizing the importance of metabolic health beyond weight alone.

Our previous work suggested that obesity-resistant phenotype in C57BL/6J mice was linked to increased oxygen consumption during the light (sleep) cycle, increased physical activity during the dark (active) cycle, and increased heat production during both cycles, and this was achieved at the expense of decreased exercise capacity of skeletal muscles. In this study, we further explored differences between obesity-prone and obesity-resistant phenotypes

focusing on lean body mass, specifically skeletal muscle tissue, and a set of physiological and mitochondrial adaptations that may be responsible for these effects. We also attempted to correlate these in our previous study with changes in fecal volatile metabolite profiles focusing on short-chain fatty acids and their esters.

2. Materials and Methods

2.1. Animals and diets

Male, 4-week-old C57BL/6J mice were purchased from the Jackson Laboratory (Bar Harbor, ME, USA) and housed four animals per cage under controlled temperature (24 ± 2 °C) and light (12 h light–dark cycle, lights on at 7:00 p.m.). Immediately upon arrival, animals were allowed to adapt to new conditions for 7 days and handling the animals was performed daily to reduce the stress of physical manipulation. Mice were then randomized into ad libitum access to Research Diets (New Brunswick, NJ, USA) low fat diet (LFD, D12450J, 10 kcal % fat, 3.85 kcal/g, n=32) or high fat diet (HFD, D12492, 60 kcal % fat, 5.24 kcal/g, n=44) for 6 weeks. Obese animals were further randomized into normally obese (HFD), non-responders (NR), super-responders (SR), or super-responders switched back to the low-fat diet (SR-LFD) for additional 8 weeks of the respective diets. All animal experiments were performed according to procedures approved by the NC Research Campus Institutional Animal Care and Use Committee in the David H. Murdock Research Institute (Kannapolis, NC), the AAALAC accredited animal care facility.

2.2. Body composition and fat/lean body mass ratios

Animal weight and food intake (accounting for spillage) were recorded weekly for the duration of the study. Body composition analysis was performed on unanesthetized mice using

EchoMRI (Echo Medical Systems, Houston, TX, USA) during the last week of the study. To determine the relative changes in skeletal muscle and adipose tissues, additional ratios of lean body mass/total body weight, fat body mass/total body weight, and fat body mass/lean body mass were calculated based on this data.

2.3. Fasting glucose and oral glucose tolerance (OGTT)

At the end of the study, mice were fasted overnight (12 h), and fasting blood glucose was determined from blood collected from a tail nick using a handheld True Metrix glucometer (Trividia Health, Fort Lauderdale, FL). Immediately after, animals were challenged with an oral gavage of glucose normalized to 1.5 g/kg body weight, and blood sugar spike was monitored at 30, 60, and 120 min following the challenge. Gavage volume (μ l) of 20% glucose solution was calculated for each animal as 7.5x fasted body weight (g). To identify animals with impaired glucose tolerance, area under the curve (AUC) was calculated using the linear trapezoid method and presented as arbitrary AUC units [15].

2.4. Insulin glucose tolerance (ITT)

At the end of the study, but on a separate occasion, mice were fasted for 6 h, and fasting blood glucose was determined from blood collected from a tail nick using a handheld True Metrix glucometer (Trividia Health, Fort Lauderdale, FL). Immediately after, animals were challenged with an intraperitoneal injection of insulin (Actrapid 100 UI/ml, Novo Nordisk, Bagsværd, Denmark) normalized to 0.75 IU/kg body weight, and disappearance of blood sugar was monitored from a tail nick at 20, 40, 80, and 120 min following the challenge. Injection volume (μ l) of 0.25 IU/ml insulin stock solution (1:400) was calculated for each animal as 3x

fasted body weight (g). To identify animals with insulin tolerance, area under the curve (AUC) was calculated using the linear trapezoid method and presented as arbitrary AUC units [16].

2.5. RNA extraction and cDNA synthesis

The total RNA was isolated from tissues using TRIzol reagent (Life Technologies, Carlsbad, CA) following the manufacturer's instructions. RNA was quantified using the BioTek SynergyH1/Take 3 plate (Agilent, Santa Clara, CA). The cDNAs were synthesized using 2 µg of RNA for each sample using a high-capacity cDNA Reverse Transcription kit following the manufacturer's protocol on an ABI GeneAMP 9700 (Life Technologies).

2.6. RT2 Profiler qPCR Array

The resulting cDNA was amplified by real-time quantitative PCR using SYBR green PCR master mix (Life Technologies). The amplifications were performed on an ABI 7500 Fast real-time PCR using 1 cycle at 50 °C for 2 min and 1 cycle at 95 °C for 10 min, followed by 40 cycles of 15 s at 95 °C and 1 min at 60 °C. The dissociation curve was completed with 1 cycle of 1 min at 95 °C, 30 s at 55 °C, and 30 s at 95 °C.

Pathway expression analysis was performed initially to compare obesity-resistant NR mice to the corresponding HFD controls using the PAMM-099Z RT2 Profiler qPCR Array (Qiagen, Valencia, CA) with a set of 84 genes related to a broad set of skeletal muscle functions. Following these results, a pairwise comparison among all study groups was performed using the PAMM-087Z RT2 Profiler qPCR Array (Qiagen) with a set of 84 genes to specifically focus on the mitochondria function.

Differentially expressed genes from the PCR array were quantified as the fold difference in the expression of each gene between the test and control samples. The scatter plot matrixes were constructed with the center line indicating fold change ($2^{-\Delta Ct}$) of 1, and the minimal 2-fold change in gene expression that was considered significant.

2.7. Volatile fecal metabolites

Whole fecal pellets were extracted in a sample vial with NaCl (0.4 g), deionized water (965 μ l), 5 ppm aqueous d-11 hexanoic acid (10 μ l), and 3N H₂SO₄ (15 μ l) to acidify sample solution to pH 2. Headspace solid phase microextraction (HS-SPME) sampling was automated by a CombiPal autosampler (LEAP Technologies, Carrboro, NC) by agitating the samples at 500 rpm (5s on and 2s off) and 40°C, followed by a 30 min equilibration. Volatiles were sampled with a 1 cm 50/30 μ m DVB/CAR/PDMS SPME fiber (Supelco, Bellefonte, PA) for 30 min at 40°C, before thermal desorption into the gas chromatography inlet. Nontargeted GCxGC-ToFMS was performed on LECO Pegasus III coupled with Agilent GC (Agilent Technologies, Santa Clara, CA). The detector voltage was optimized by ChromaTOF between -1418.0 to -1472.2V, and masses 25-500 were collected at a rate of 500 spectra per second as described previously. Abundance of each metabolite was expressed as the log₂-transformed average change in the metabolite peak area from that of the LFD controls.

2.8. Cell culture

The mouse macrophage cell line RAW 264.7 (ATCC TIB-71) were maintained in DMEM (Life Technologies) supplemented with 10% fetal bovine serum, 100 IU/ml penicillin, and 100 μ g/ml streptomycin (Fisher Scientific, Pittsburg, PA) at a density not exceeding 5×10^5

cells/ml. Passages were performed every 3-4 days in 57-cm² cell culture dishes (Nalge Nunc International, Rochester, NY) maintained at 37 °C in a humidified 5% CO₂ Thermo Forma Series II incubator (Fisher Scientific).

2.9. Nitric oxide production and gene expression

For nitric oxide quantification, RAW 264.7 cells were seeded in 96-well plates in triplicate at the concentration of 5x10⁴ cells/well in a 200 µl culture medium and allowed to adhere for 24 h. The cells were then pre-treated with 3-300 µM dose ranges of the target metabolites and elicited with 1 µg/ml LPS for additional 6 h. Nitric oxide released from the stimulated macrophages was quantified using the Greiss reagent system (Promega, Madison, WI) and SynergyH1 microplate reader (BioTek) at 530 nm.

For gene expression studies, RAW 264.7 cells were seeded in 24-well plates at the concentration of 5x10⁵ cells/well in a 1 ml culture medium and treated as described. RNA extraction, cDNA synthesis, and qPCR analysis was performed as described in sections 2.5-2.6, using the following set of primers: β-actin (housekeeping), forward primer: 5'-AAC CGT GAA AAG ATG ACC CAG AT-3', reverse primer: 5'-CAC AGC CTG GAT GGC TAC GT-3'; iNOS, forward primer: 5'-CCC TCC TGA TCT TGT GTT GGA-3', reverse primer: 5'-TCA ACC CGA GCT CCT GGA A-3'; COX-2, forward primer: 5'-TGG TGC CTG GTC TGA TGA TG-3', reverse primer: 5'-GTG GTA ACC GCT CAG GTG TTG-3'; TNF-α, forward primer: 5'-GTT CTA TGG CCC AGA CCC TCA CA-3', reverse primer 5'-TAC CAG GGT TTG AGC TCA GC-3'; IL-1β, forward primer: 5'-CAA CCA ACA AGT GAT ATT CTC CAT G-3', reverse primer: 5'-GAT CCA CAC TCT CCA GCT GCA-3'; IL-6, forward primer: 5'-TAG TCC TTC CTA CCC CAA TTT CC-3', reverse primer: 5'-TTG GTC CTT AGC CAC

TCC TTC-3'; IL-17, forward primer: 5'-ATC TGG TCC TAC ACG AAG CC-3', reverse primer: 5'-GTC CCG GAC TTC AAG ACC C-3'; IL-18, forward primer: 5'-AGG ACA AAG AAA GCC GCC TC-3', reverse primer: 5'-TCA TTT CCT TGA AGT TGA CGC AAG AGT-3'. Fold differences in gene expression relative to the LPS-induced controls were analyzed using the $\Delta\Delta$ CT method and normalized with respect to the expression of β -actin.

2.10. Statistical analysis

Data was analyzed by one-way ANOVA followed by Dunnett's multiple-range tests using Prism 8.0 (GraphPad Software, San Diego, CA). All data was presented as means \pm SEM. Significant differences were accepted when the p-value was <0.05 .

3. Results

3.1. Body weight gain and metabolic phenotypes

All C57BL/6J mice (n=72) at the age of 4 weeks started on the respective low-fat (3.85 kcal/g) LFD and high-fat (5.24 kcal/g) HFD diets for 6 weeks. Due to the polygenic nature of C57BL/6J obesity, there was a significant variation in body weight gain that allowed us to select obese-prone, super-responders in the upper quartile (SR) and obese-resistant, non-responders (NR) in the lower quartile among the normal obese controls (HFD). All animals were kept on the respective diets for 8 more weeks before a series of physiological and metabolic tests was completed during the week 14 of the study. A group of SR-LFD mice was further randomly selected from SR mice and fed LFD diet during the second phase of the study (weeks 7-14) to evaluate body weight loss and metabolic responses of the SR mice when switched back to the LDF diet.

NR mice fed HFD diet showed small food intake increases of +11.8% over HFD controls and +12.4% over SR mice that did not reach significance ($p=0.066$). Both NR and SR mice showed increased VO_2 oxygen consumption over the HFD controls, however NR mice consumed +50.2% more oxygen over SR mice only during the light (sleep) cycle of the day ($p<0.01$), thus indicating a higher resting metabolic rate (RMR). Heat production normalized to body weight was also higher in NR mice over SR mice during both light (resting, +19.5%) and dark (active, +17.3%) cycles of the day. Taken together, this data suggested that muscle tissue was a major point of physiological adaptation to the high dietary fats, as described by our group previously.

3.2. Relative changes in lean and fat body mass

To focus on relative contribution of muscle tissues to the observed obesity-resistant phenotype, we quantified relative lean mass (Figure 1a), relative fat mass (Figure 1b), and fat to lean mass ratio in these animals. As expected, HFD diet promoted higher adiposity and therefore lower lean/total body mass ration in HFD mice (0.58 ± 0.06) when compared to lean LFD mice (0.76 ± 0.05). Obesity-resistant NR mice showed a significant improvement in this parameter (0.69 ± 0.02 , $p=0.002$), while obesity-prone SR mice maintained lean mass similar to the HFD controls (0.59 ± 0.06). This suggests that SR mice failed to expand lean body mass in response to high dietary fats, and most of the body weight gain was directed towards expansion of the adipose tissue. When fat and lean body mass were compared directly (Figure 1c), this was even more obvious as fat to lean ration of SR mice (0.69 ± 0.07) was 60.5% higher than that of NR mice (0.43 ± 0.05 , $p<0.0001$).

It is interesting to note that the reversal of the diet from HFD to LFD during the second phase of the study (8 weeks) was sufficient for SR-LFD mice to adjust their lean and fat body masses to those of LFD controls.

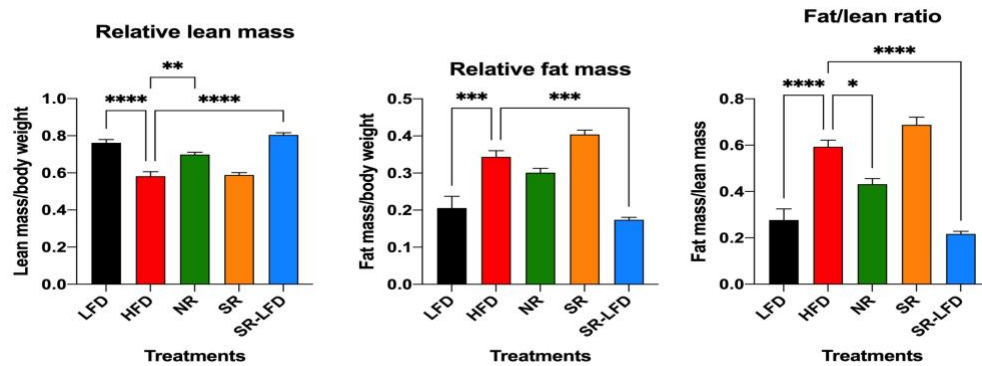


Figure 3.1. Ratios of (a) lean/total body mass, (b) fat/total body mass, and (c) fat/lean body mass as determined by EchoMRI body composition analysis after 14 weeks of high dietary fats challenge in lean controls (LFD), obese controls (HFD), obesity-resistant non-responders (NR), obesity-prone super-responders (SR), and super-responders fed LFD diet (SR-LFD). Results are expressed as means \pm SEM (n=8). Data were analyzed using one-way ANOVA followed by Dunnett's multiple comparisons, * $p < 0.05$, ** $p < 0.01$, *** $p < 0.001$, **** $p < 0.00001$ versus the LFD controls.

3.3. Nutrigenomic profiling of skeletal muscles

As a first step to understand differences between NR mice and HFD controls that allowed NR mice to remain obesity-resistant despite similar food and energy intakes, we evaluated pooled RNA samples from the gastrocnemius muscles of NR and HFD mice, as legs hold the largest muscle group that is expected to consume the most VO₂ oxygen. The RT2 Profiler Array PAMM-099Z was used to quantify changes in gene expression pathways related

to skeletal muscle contractility, energy metabolism, slow and fast twitch fibers, skeletal myogenesis, skeletal muscle hypertrophy, skeletal muscle autocrine signaling, skeletal muscle wasting, skeletal muscle dystrophy, and insulin resistance (Figure 2).

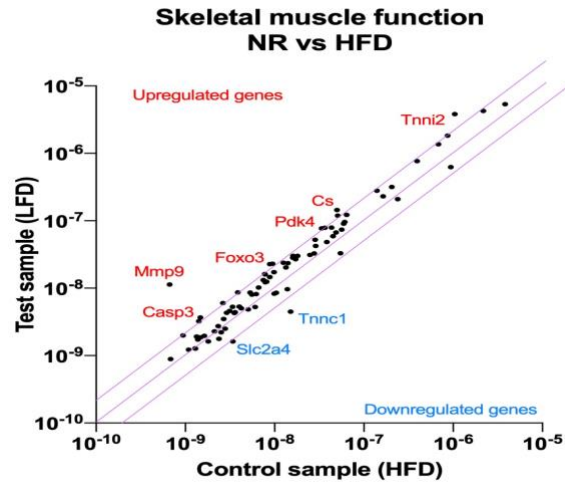


Figure 3.2. Nutrigenomic responses to high dietary fats of the obesity-resistant non-responders (NR) versus the normal obese controls (HFD). RNA was extracted from the pooled (n=4) gastrocnemius muscle samples and RT2 Profiler Arrays were used to determine relative levels of the gene expression networks that modulate skeletal muscle physiology. Central line indicates no fold change, while the top and bottom lines indicate a 2-fold significance in the gene expression threshold.

Obese-resistant phenotype of NR mice was strongly associated with skeletal muscle tissue remodeling. Among the highest upregulate genes, matrix metalloproteinase 9 (Mmp9, 17.0-fold), forkhead box O3 (Foxo3, 2.6-fold), caspase 3 (Casp3, 2.5-fold), inhibitor of kappaB kinase beta (Ikkbb, 2.3-fold) and interleukin (IL1b, 2.3-fold) indicated upregulation of the autophagy pathway in the skeletal muscle tissue.

Another group of upregulated genes provided further evidence about the direction of the skeletal muscle tissue remodeling. Alongside autophagy, a new signature of skeletal muscle myogenesis was evident from the expression of myocyte enhancer factor 2C (Mef2c,

2.3-fold), muscle receptor tyrosine kinase (Musk, 2.1-fold), lamin A (Lmna, 2.1-fold), and calpain 2 (Capn2, 2.0-fold). This form of myogenesis was driven in the direction of muscle fiber remodeling in favor of type 2a, fast-twitch, oxidative muscle fibers as indicated by higher abundance of the type 2a biomarkers: skeletal troponin I fast 2 (Tnni2, 3.7-fold) and myosin heavy polypeptide 2 (Myh2, 2.0-fold). At the same time, troponin C, the biomarker for type 1 slow-twitch fiber, was significantly reduced (Tnnc1, -3.4-fold).

Finally, changes in a smaller group of genes related to nutrient partitioning and energy metabolism indicated a physiological adjustment to higher energy intakes by upregulation of citrate synthase (Cs, 2.9-fold), pyruvate dehydrogenase kinase 4 (Pdk4, 2.3-fold), and a concurrent downregulation of the GLUT4 glucose transporter (Slc2a4, -2.1-fold) (Supplementary Table S1).

3.4. Changes in glucose metabolism and insulin resistance

Upregulation of citrate synthase with a simultaneous decrease in GLUT4 glucose transporter abundance is highly suggestive of a metabolic adaptation in the form of blood glucose sparing to favor increased fat oxidation in the muscle tissues. To test this hypothesis, we evaluated glucose and insulin sensitivity in all study animals. Baseline blood glucose levels were measured on week 14 of the study after an overnight fast (Figure 3). As expected for diet-induced C57BL/6J obesity, HFD controls developed high fasting blood glucose (189.3 ± 6.1 mg/dl) versus the lean LFD controls (88.0 ± 9.8 mg/dl, $p < 0.0001$). Resistance to obesity in NR mice was not associated with changes in fasting blood glucose (175.0 ± 12.8 mg/dl). SR mice also maintained high blood glucose (244.7 ± 4.0 mg/dl), which trended to decline in the direction of basal levels after SR-LFD mice were returned to the LFD diet (144.1 ± 16.1 mg/dl).

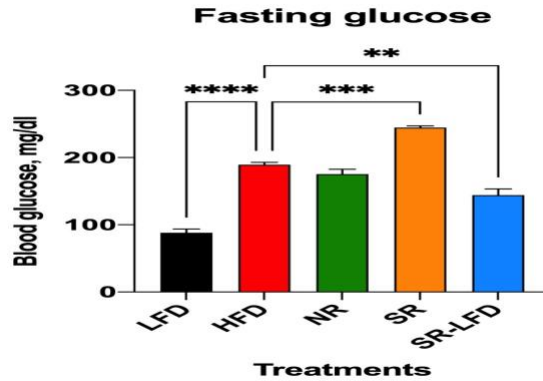


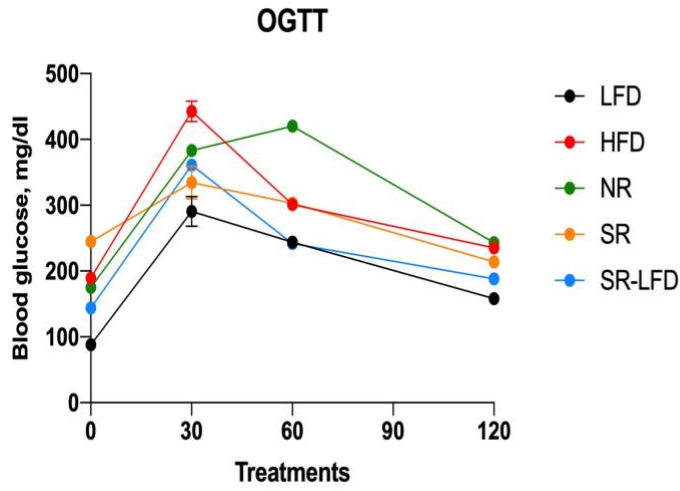
Figure 3.3. Changes in fasting blood glucose as observed after 14 weeks of high dietary fats challenge in lean controls (LFD), obese controls (HFD), obesity-resistant non-responders (NR), obesity-prone super-responders (SR), and super-responders fed LFD diet (SR-LFD). Results are expressed as means \pm SEM (n=8). Data were analyzed using one-way ANOVA followed by Dunnett's multiple comparisons, **p< 0.01, ***p<0.001, ****p<0.00001 versus the HFD controls.

In line with these findings, both oral glucose tolerance (Figure 4 a,b) and insulin tolerance (Figure 4 c,d) were highly affected by excessive dietary fats. The OGTT data that indicated whether animals could use and store glucose normally, was rather peculiar. Reduced tissue ability to remove glucose from bloodstream was evident for all animals challenged with high dietary fats such as HFD, NR, and SR mice (Figure 4 a,b). However, while glucose intolerance was established for these groups, it was even more pronounced in NR mice that showed peak glucose values not only at 30 min, but also at 60 min OGTT (Figure 4a). The resulting AUC for NR mice was significantly higher than that of HFD controls (p=0.004), while SR mice showed a small but significant decrease in AUC as compared to that of HFD controls (p=0.016). This data suggested that NR mice gained a yet unknown metabolic

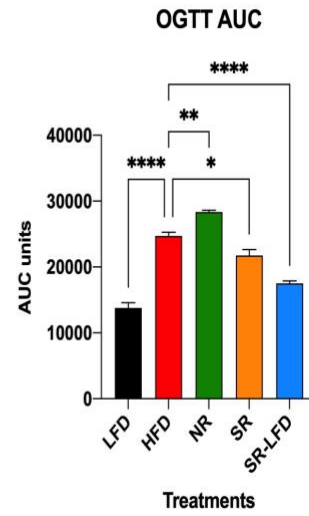
advantage by counterintuitively increasing the glucose sparing effect in their metabolically active tissues.

The insulin tolerance determined via ITT (Figure 4 c, d) showed a matching reversal of the observed effects. SR mice trended to show increased insulin tolerance over the HFD controls, while NR mice showed a decreased tolerance, even though both trends have not reached significance (Figure 4d). It is also notable that SR-LFD mice nearly fully restored their glucose and insulin tolerance after 8 weeks on the LFD diet.

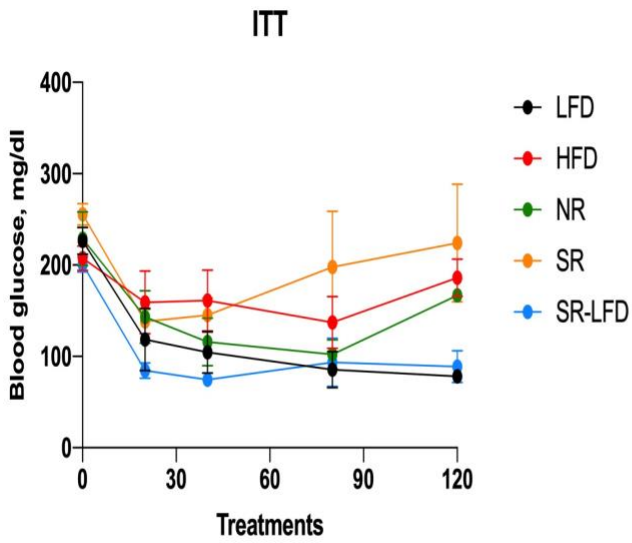
Figure 3.4. Parameters of carbohydrate metabolism affected by high dietary fats in lean controls (LFD), obese controls (HFD), obesity-resistant non-responders (NR), obesity-prone super-responders (SR), and super-responders fed LFD diet at the end of the study. These include (a) oral glucose tolerance (OGTT) and the calculated (b) area under the curve (AUC), as well as (c) insulin tolerance test (ITT) with the corresponding (d) AUC data. Results are expressed as means \pm SEM (n=8). Data were analyzed using one-way ANOVA followed by Dunnett's multiple comparisons, *p< 0.05, **p<0.01, ****p<0.00001 versus the HFD controls.



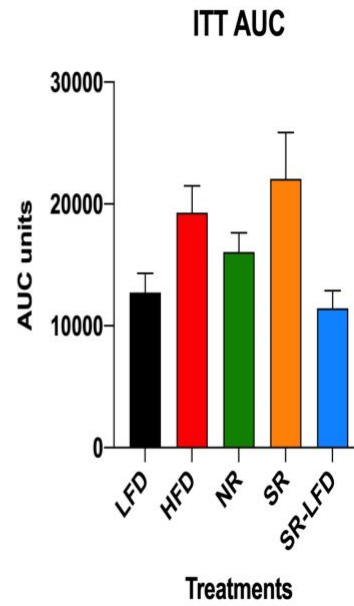
(a)



(b)



(c)

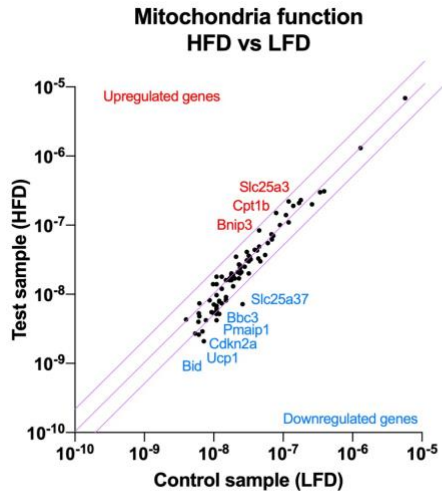


(d)

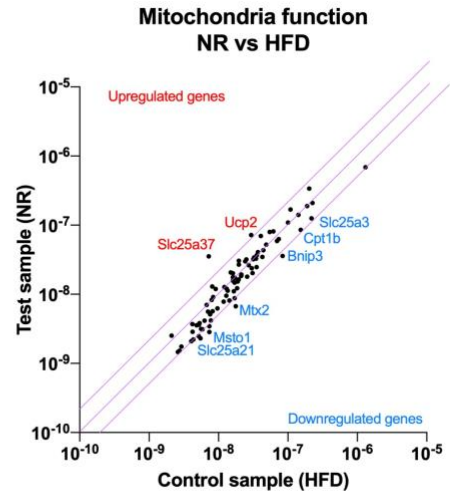
3.5. Nutrigenomic profiling of skeletal muscle mitochondria

To further understand the metabolic adaptation of muscle tissues to high dietary fats, and nutrigenomic responses associated with obesity-resistant and obesity-prone phenotypes, we evaluated pooled RNA samples from the gastrocnemius muscles of all treatment groups using the RT2 Profiler Array PAMM-087Z to target gene expression pathways related to mitochondria. The array included the networks related to mitochondrial membrane polarization, mitochondrial transport, small molecule transport, protein targeting and import to mitochondria, inner and outer membrane translocation, mitochondrial fission and fusion, mitochondrial localization and apoptosis (Figure 3.5).

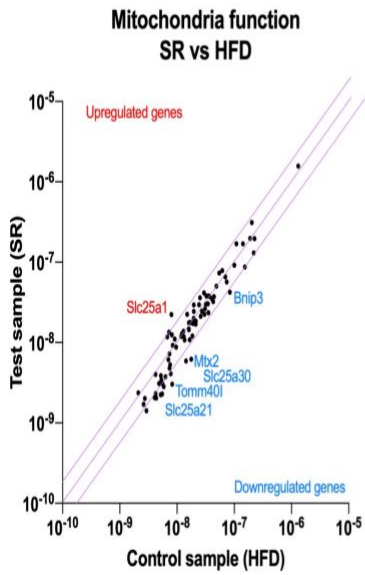
Figure 3.5. Nutrigenomic responses to high dietary fats of (a) lean controls (LFD), (b) obesity-resistant non-responders (NR), (c) obesity-prone super-responders (SR), (d) super-responders fed LFD diet during the second phase of the study (SR-LFD) as compared to the obese controls (HFD), and (e) obesity-resistant non-responders (NR) as compared to the obesity-prone super-responders (SR). RNA was extracted from the pooled (n=4) gastrocnemius muscle samples and RT2 Profiler Array PAMM-087Z was used to determine relative levels of the gene expression networks that modulate muscle tissue mitochondria. Central line indicates no fold change, while the top and bottom lines indicate a 2-fold significance in the gene expression threshold.



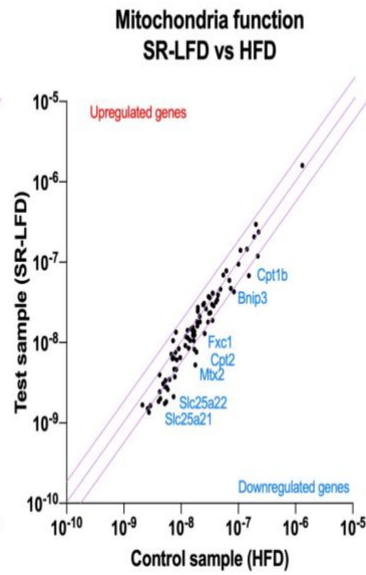
(a)



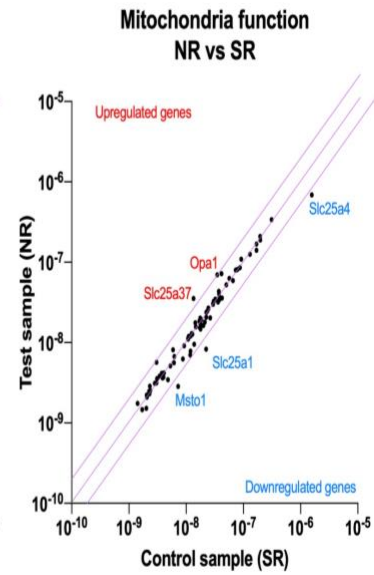
(b)



(c)



(d)



(e)

High dietary fats as a part of the HFD diet upregulated genes that support fatty acid oxidation such as carnitine palmitoyltransferase 1b (Cpt1b) and phosphate carrier Slc25a3 (import of phosphate into mitochondria matrix), as well as mitochondrial dysfunction via BCL2/adenovirus E1B interacting protein 3 (Bnip3) in the near-significant 1.84 to 1.92-fold range (Figure 5a). A series of genes was downregulated including mitoferrin 1 (Slc25a37) solute carrier localized in the mitochondrial inner membrane (-3.59-fold), the apoptosis regulatory network (Bid, Pmaip1, Cdkn2a, Bbc3, Sfn), and a series of solute carriers in the near-significant 1.69 to 1.98-fold range. These included Slc25a10 (import of malate and succinate), Slc25a13 (import of glutamate in exchange for aspartate), Slc25a24 (import of ATP-Mg in exchange for phosphate), Slc25a27 (fatty acid-activated uncoupling protein 4), and Slc25a21 (import of the 2-oxoadipate intermediate from the catabolism of lysine, tryptophan, and hydroxylysine). Finally, a set of 3 genes (Msto1, Nefl, Uxt) responsible for the regulation of mitochondrial distribution and morphology were also downregulated in the sub-significant -1.63 to -1.83-fold range (Supplementary Table S2).

When compared to HFD controls, obesity resistant NR mice showed the capacity to powerfully upregulate mitoferrin 1 (Slc25a37, 4.9-fold) and the uncoupling protein 2 (Ucp2, 2.4-fold) (Figure 5b). This unique phenotype was also associated with further downregulations of the same gene expression networks as observed in the HFD controls, including solute carriers (Slc25a10, Slc25a13, Slc25a21, but also Slc25a22, Slc25a31, Slc25a4, Slc25a2), apoptosis (Bnip3, Bbc3), and mitochondrial distribution (Mtx2, Msto1, Nefl) (Supplementary Table S3).

Obesity-prone SR mice, when contrasted against the HFD controls, showed a unique upregulation of citrate transport protein (Slc25a1, 2.8-fold) responsible for export of citrate in

exchange for malate from cytosol (Figure 5c). The remaining gene expression profile was unremarkable, with similar downregulation of networks responsible for the solute carriers (Slc25a30, Slc25a13, Slc25a21, Slc25a31, Slc25a2), apoptosis (Bbc3, Bnip3, Cdkn2a, Pmaip1), and mitochondrial distribution (Mtx2, Nefl) (Supplementary Table S4).

SR-LFD mice fed LFD diet showed a similar pattern in gene expression networks modulated by the HFD feeding (Figure 5d), including solute carriers (Slc25a10, Slc25a13, Slc25a21, Slc25a22, Slc25a31, Slc25a2, Slc25a20), apoptosis (Bbc3, Bnip3), mitochondrial distribution (Mtx2, Nefl) pathways (Supplementary Table S5).

When contrasted directly to SR animals (Figure 5e), NR mice showed only a few significant differences in gene expression networks. These included a consistent upregulation of mitoferrin 1 (Slc25a37, 2.6-fold), optic atrophy 1 homolog protein (Opa1, 2.0-fold), translocase of outer mitochondrial membrane 40 homolog protein (Tomm40l, 1.9-fold), and the uncoupling protein 2 (Ucp2, 1.7-fold). Only three genes were significantly downregulated, including solute carriers (Slc25a4, but also Slc25a1), and mitochondrial distribution (Msto1) (Supplementary Table S6).

3.6. Fecal microbiome metabolites

Phylum-level diversity of microbiomes showed a moderate change associated with different experimental diets. Consuming HFD diet produced a typical shift in Firmicutes (+15.2%) and Bacteroidetes (-12.9%) groups expected in the presence of high dietary fats. Obesity-prone SR mice showed a further reduction in Bacteroidetes (-7.1%) group at the expense of Actinobacteria (+10.3%), an enterotype that persisted in SR-LFD animals as well.

Obesity-resistant NR mice, on the other hand, showed an expansion of Bacteroidetes (+25.6%) at the expense of Actinobacteria (-14.5%) (Figure 6).

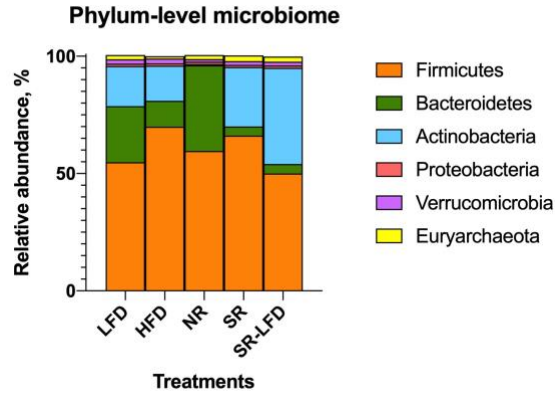


Figure 3.6. Shifts in the phylum-level microbiome profiles determined at the end of the study among lean controls (LFD), obese controls (HFD), obesity-resistant non-responders (NR), obesity-prone super-responders (SR), and super-responders fed LFD diet.

Microbiome shifts also resulted in changes in fecal metabolite signatures, including several metabolites related to the short-chain fatty acids, their esters, and trans-2-dodecenol, a saturated fatty alcohol (Table 1). Consumption of the HFD diet resulted in significant increases in methyl formate, ethyl ester of propanoic acid, 2-methyl-butanoic acid, and Z-2-dodecenol. NR and SR mice showed an opposing effect in handling volatile short-chain acid metabolites and their esters in the gastrointestinal tracts: they were reduced in NR and increased in SR animals. Return of SR-LFD mice to the LFD diet showed a general trend to reduce these differences in the direction of the LFD metabolic signature.

Table 3.1. Fecal volatile metabolites signatures exhibiting significant differences (*p<0.0023).

Abundances for each treatment group were calculated as the log2-transformed metabolite peak averages, and expressed as fold changes from those of HFD mice.

Metabolite	LFD	HFD	NR	SR	SR-LFD
Methyl formate*	0.18	1	0.02	5.67	1.99
Formic acid, heptyl ester	0.85	1	2.09	1.24	11.56
Acetic acid*	0.80	1	0.12	1.14	0.88
Ammonium acetate*	0.92	1	0.01	3.19	0.05
Propanoic acid, ethyl ester *	0.06	1	0.18	13.56	10.25
Propanoic acid (propionic acid)	1.21	1	0.96	1.45	0.71
Propanoic acid (isobutyric acid), 2-methyl	0.94	1	0.84	1.10	0.58
Propanoic acid, 2,2-dimethyl	0.99	1	1.02	1.06	0.84
Butanoic acid (butyric acid)*	0.23	1	0.23	0.32	0.23
Butanoic acid, 2-methyl-*	0.01	1	0.17	0.01	0.01
Z-2-Dodecenol*	0.01	1	0.78	0.37	0.55

3.7. Inflammatory responses

As many of these metabolites are known to reach the systemic circulation in micromolar concentrations [17], we next explored their putative effects on skeletal muscle tissues, and specifically on the inflammatory status of tissue macrophages that regulate muscle remodeling and repair. This was done in the model LPS-stimulated mouse RAW 264.7 macrophage cell culture. In the range of physiological concentrations tested (3-300 μ M), short-chain fatty acids showed no dose-dependent effects on nitric oxide production (Figure 7, a-d). On the contrary, trans-2-dodecenol showed a dose-dependent suppression of nitric oxide production, thus indicating that this metabolite has a moderate anti-inflammatory effect (Figure 7e). Citrate was also tested in this model system due to upregulation of citrate synthase (Cs) and citrate transport protein (Slc25a1) observed in the gene expression datasets (Figure 5), but was shown to be inactive (Figure 7f).

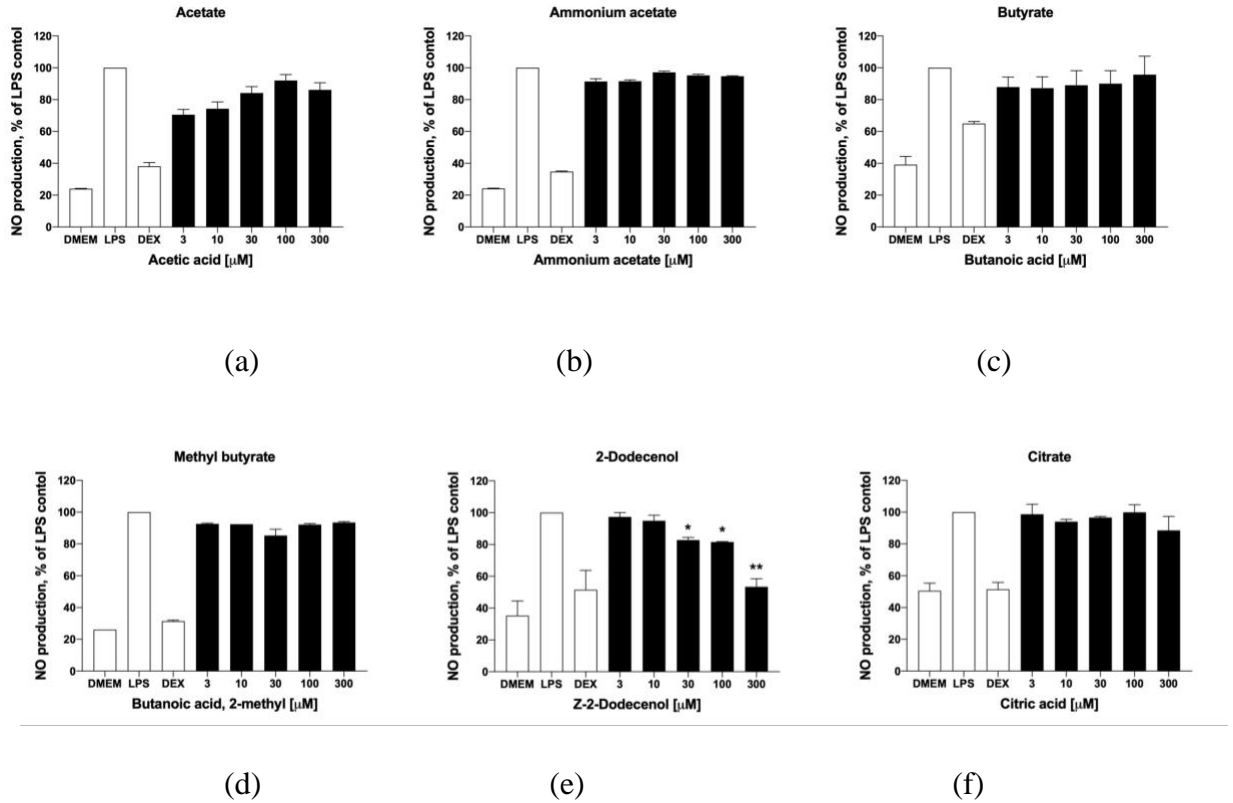


Figure 3.7. Effects of selected metabolites on nitric oxide production in activated macrophages, including (a) acetic acid, (b) ammonium acetate, (c) butanoic acid, (d) 2-methylbutanoic acid, (e) trans-2-dodecenol, and (f) citric acid. Cells were pre-treated with the target metabolites and inflammatory response was induced with 1 μg/ml LPS for 6 h. Changes in nitrite concentration as an indirect measure of nitric oxide production were reported as mean ± SEM relative to the LPS controls (* p < 0.05, ** p < 0.01).

To correlate results of the NO production assay, we next evaluated trans-2-dodecenol for its ability to modulate expression of the pro-inflammatory gene expression network that is associated with acute and chronic inflammation. The metabolite was tested in the same dose range (3-300 μM) that was effective at reducing nitric oxide production (Figure 7e). As expected, the strongest anti-inflammatory effect associated with trans-2-dodecenol was observed in the expression levels of the inducible nitric oxide synthase (iNOS), with the

expression levels returning to the basal levels similar to that of non-induced controls at 100-300 μM (Figure 8). Even in a lower dose range (3-30 μM), iNOS expression was reduced by 22-34%. A similar, albeit a weaker response was also observed for COX-2 expression, with 58-62% suppression of the LPS-induced levels at the higher concentration ranges of 100-300 μM . Gene expression levels for TNF- α , IL-1 β , IL-6, and IL-18 have not been affected, and IL-17 showed a weak response that has not reached significance.

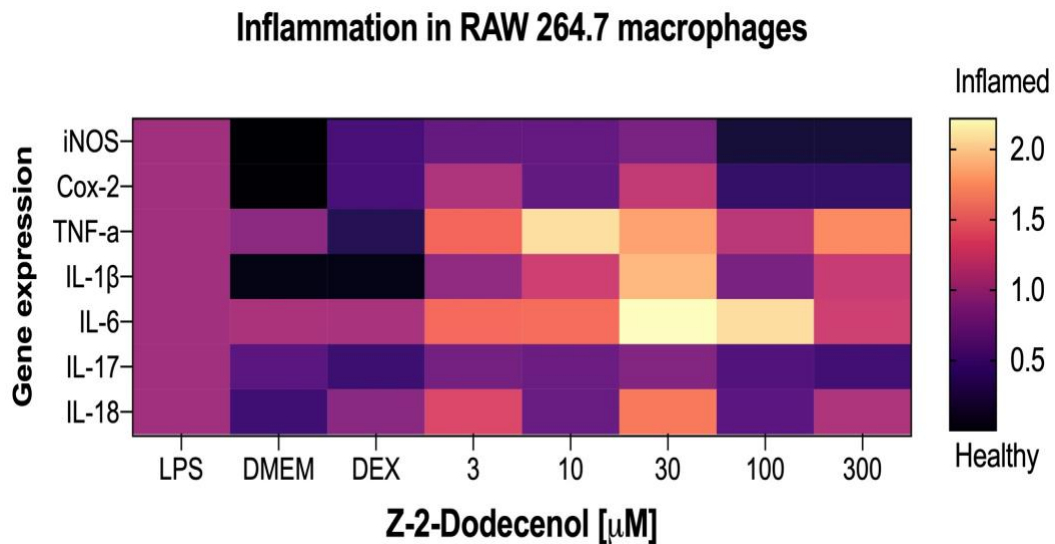


Figure 3.8. Heatmap of anti-inflammatory effects of trans-2-dodecenol based on the qPCR gene expression profiles of key biomarkers of acute and chronic inflammation, including inducible nitric oxide synthase (iNOS), cyclooxygenase-2 (Cox-2), tumor necrosis factor alpha (TNF- α), interleukins IL-1 β , IL-6, IL-17 and IL-18. Macrophages were pre-treated with trans-2-dodecenol as the specified, and inflammatory response was induced with 1 $\mu\text{g}/\text{ml}$ LPS for 6h. DMEM (baseline) and dexamethasone 10 μM (DEX) were used as negative and positive controls. Total RNAs were isolated from triplicate treatments and pooled for qPCR analysis. Fold changes in gene expression are reported as means relative to the LPS controls.

4. Discussion

Resistance to obesity is a natural phenotype that has been observed both in rodents and humans. It is described by lower body weight gain and adiposity despite 10-25% increase in calorie intake over control obese animals fed HFD [18]. In our previous study we confirmed these findings by showing that obesity-resistant NR mice gained 48.6% less body weight while consuming 11.9% calories than their obesity-prone SR counterparts, which resulted in dramatically reduced feed efficiency as shown in our previous study. This data presents a strong argument that obesity-resistant NR mice partition and metabolize dietary fats differently. Upon absorption, dietary fats are delivered to gut, liver, and muscle rather than the adipose tissue within the initial 24 hours after eating [11]. Primary variations in skeletal muscle tissue physiology and fat oxidation capacity may be therefore responsible for the initial inefficient processing of lipids that results in their excessive accumulation in the adipose tissue or the off-target ectopic deposition [19].

Increased ability to oxidize dietary fats in the skeletal muscle requires a set of physiological adaptations to support the excessive energy fluxes. Higher proportion of lean-to-fat body mass observed in the obesity-resistant NR mice supports this conclusion, and the activity of several gene expression networks further suggests the direction in which skeletal muscle tissue adaptation takes place. In this study, we observed a simultaneous upregulation of autophagy and skeletal muscle myogenesis pathways in the NR mice, indicative of ongoing muscle remodeling. Healthy muscles contain a mixture of four muscle fiber types in a relative proportion according to species and anatomical site [20]. These include type 1 (red, slow-twitch, oxidative fibers that express myosin heavy chain Myh7), type 2a (pink, fast-twitch, oxidative fibers that express Myh2), type 2x (purple, fast-twitch, glycolytic fibers that express

Myh1), and type 2b (blue, fast-twitch, glycolytic fibers that express Myh4), although the latter appears to be absent in humans [21]. Existence of a continuous spectrum of hybrid fiber types including 1/2a, 2a/2x, and 2x/2b, especially during the muscle type transition and regeneration, was also observed [22]. Muscle fiber types are also tightly coupled to troponin isoforms both in rodents [23] and humans [24]. NR mice showed a very prominent gene expression signature characterized by up regulation of Myh2 and troponin I2 (Tnni2) biomarkers indicative of increased presence of type 2a oxidative fibers, with a concurrent downregulation of the troponin C1 (Tnnc1) biomarker of type 1 fibers. Upregulation of the Myh1 biomarker associated with type 2x fibers is also expected to increase muscle oxidative capacity, as in rodents (but not humans) type 2x fibers have moderate to strong succinate dehydrogenase activity, reflecting increased oxidative metabolism [25]. Together, these findings predict that resistance to obesity in NR mice is mediated in part by expansion and higher oxidative function of the skeletal muscle type 2a fibers, which also explains the decreased exercise capacity observed in these animals earlier.

Increased ability to oxidize dietary lipids was likely followed with the concurrent changes in carbohydrate metabolism. NR mice showed a very diminished oral glucose tolerance (OGTT), even though insulin tolerance (ITT) was slightly improved over the HFD controls, and especially over the obesity-prone SR animals. This possibly suggests that NR animals employed a different protective mechanism to allow for additional glucose sparing. In the adipose and muscle tissues, insulin increases GLUT4 translocation to the cell membrane which allows enhanced glucose uptake but these tissues [26]. Our data suggests that NR mice express GLUT4 in the muscle tissue at the level of half that of the HFD controls. This adaptation may be helpful in allowing skeletal muscle to preferentially uptake and oxidize lipid

substrates, although this hypothesis needs to be verified at the protein level in the future studies. Another indirect support for this conclusion comes from the observed simultaneous upregulation of pyruvate dehydrogenase kinase 4 (Pdk4) and citrate synthase (Cs) transcripts. Pdk4 is an inhibitor of pyruvate dehydrogenase that increases the influx of acetyl-CoA from β -oxidation into the TCA cycle, thereby leading to enhanced fatty acid oxidation and slowing of glycolysis [27]. Citrate synthase, in its turn, has a key role in the TCA cycle by performing an irreversible commitment of acetyl-CoA with oxaloacetate to form citrate [28].

The data from the mitochondrial gene expression networks revealed two most prominent targets associated with the obesity-resistant NR phenotype. The first target was mitoferrin 1 (Slc25a37), an essential iron importer for the synthesis of mitochondrial heme and iron-sulfur clusters [29]. Expression of mitoferrin 1 was suppressed by dietary fats in HFD controls as well as obese-prone SR mice, but upregulated above the basal levels in the NR phenotype. Previously, anemia has been associated with increased fat accumulation [30], and mild iron deficiency has adversely affected lipid metabolism in rats [31]. Iron inadequacy is one of the four most common deficiencies around the world due to a variety of dietary, agricultural, and gastrointestinal factors [32]. As mitochondria are major hubs of iron utilization and accumulation [33], it is very plausible that iron inadequacy directly (low iron) or indirectly (inability to effectively transport iron into mitochondria) contribute to the development of obese phenotypes.

The second prominent characteristic of obesity-resistant NR phenotype in our study was upregulation of the uncoupling protein 2 (Ucp2). Ucp2 dissipates the mitochondrial membrane potential as heat, thus protecting mitochondria from reactive oxygen species overload and taking part in many metabolic adaptive processes [34], and its functionality to

transport protons similar to the archetypal protein Ucp1, which is activated by fatty acids and inhibited by purine nucleotides, was described previously [35]. In the latter role, Ucp2 acts as a metabolic switch that suppresses glucose utilization in the skeletal muscle in favor of utilizing lipids as major energy substrates [36]. It also catalyzes the exchange of oxaloacetate, malate, aspartate for phosphate, and therefore regulates pyruvate oxidation in the mitochondrial matrix [37]. Another transcript revealed by direct comparison obesity-resistant NR to obesity-prone SR phenotypes was optic atrophy 1 (Opa1), a protein essential for mitochondrial fusion, lipid, metabolism, and for supporting cellular energetics [38]. Opa1 deficiency reduced mitochondrial respiratory capacity in white adipocytes, impaired lipolytic signaling, and promoted adipose tissue senescence [39]. In skeletal muscles, Opa1 fuses the inner membranes of adjacent mitochondria, allowing for an increase in oxidative phosphorylation [40], in line with the findings reported in this study.

We also observed several transcriptional changes associated with expression of other members of the SLC25 mitochondrial carrier family [41]. HFD diet was associated with downregulation of Slc25a10 (import of malate and succinate), Slc25a13 (import of glutamate in exchange for aspartate), Slc25a21 (import of the 2-oxoadipate), Slc25a24 (import of ATP-Mg in exchange for phosphate), and Slc25a27 (fatty acid-activated uncoupling protein 4). Obesity-prone SR mice showed further downregulation of Slc25a13, Slc25a21, as well as Slc25a2 (transport of the positively charged amino acids ornithine, lysine and arginine), Slc25a4 and Slc25a31 (enable ATP:ADP antiporter uncoupling activity), Slc25a22 (import of glutamate), and a unique upregulation of Slc25a1 (citrate export in exchange for malate). None of these changes were counteracted in the obesity-prone NR mice, suggesting that import of

various energy substrates into mitochondria is not a primary mode of resistance to obesity in these animals.

Finally, we attempted to evaluate changes in microbiome profiles and associated alterations in short-chain acid metabolism in volatile fecal metabolome (Table 1). Obesity-resistant NR phenotype showed a remarkable expansion of Bacteroidetes at the expense of a near-loss of Actinobacteria. As a result, Firmicutes to Bacteroidetes ratio has increased with HFD diet (6.4:1), and returned to the control LFD baseline (2.29:1) in NR mice (1.63:1). This also translated to differences in fecal volatile short-chain fatty acids (SCFA) profiles that included metabolites with formate (C1), acetate (C2), propionate (C3), butyrate (C4), and isobutyrate (C5) carbon chain, as seen previously [42]. Although the majority of SCFAs are produced by fermentation of complex carbohydrates by Bifidobacteria (early stages of life) and Firmicutes (later on), they also can be produced from metabolism of proteins and amino acids [43].

Across all classes, the obesity-resistant NR phenotype was associated with reduced SCFAs production, at least at the level of fecal SCFAs, as circulating SCFAs have not been evaluated in this study. HFD diet was particularly associated with increased accumulation of methyl formate and propanoic acid ethyl ester (ethyl propionate) that have potential to exacerbate gastrointestinal and metabolic health outcomes [44–46], and both metabolites were further increased in the feces of the obesity-prone SR mice. Both metabolites were present in the near-basal levels in the obesity-resistant NR mice, suggesting that they can be used as volatile biomarkers in studies targeting lipid metabolism and obesity.

SCFAs are generally regarded as protective [47], but different SCFAs can have contrasting effects on the lipid metabolism depending on the metabolic health of the individual

[48], and often enough, increased fecal SCFAs correlate with obesity [49,50], and obesity-related dysbiosis [51]. When we tested some of these SCFAs metabolites in the cell culture model of LPS-induced inflammation, they showed no defined anti-inflammatory effects, similar to what we observed in a previous study [52]. Another volatile fecal metabolite (Z)-2-dodecenol, on the other hand, dose dependently inhibited nitric oxide production from the LPS-induced macrophages, and its anti-inflammatory potential was supported by a dose-dependent suppression of the iNOS and Cox-2 expression from the panel of the genes associated with acute and chronic inflammation. (Z)-2-dodecenol was likely of dietary origin, as this metabolite can be found in soybean oil [53], a standard component of the HFD diets used in this study.

5. Conclusions

The findings from this study on individual obesity resistance in C57BL/6J mice reveal a complex interplay of physiological adaptations that contribute to their phenotype. The distinct metabolic traits observed in the skeletal muscle, in particular the upregulation of biomarkers for the oxidative muscle type 2a fibers, enhanced expression of mitochondrial iron importer mitoferrin 1, and proton transport carrier Ucp2 hint at possible adaptive mechanisms that promote an effective lipid utilization and mitigate the associated oxidative stress. Concurrently, the shift in gut microbiota composition and fecal volatile metabolite profiles suggest methyl formate and ethyl propionate as potential volatile biomarkers to monitor the pathophysiology and progression of obese states.

Understanding the intricate mechanisms governing resistance to obesity in the obesity-resistant NR mice not only provides valuable insights into metabolic adaptations but

also unveils potential molecular targets aimed at modulating energy metabolism and mitigating obesity-related complications. Further exploration, especially at the protein level to validate hypotheses, and clinical studies investigating the translatability of these findings to human contexts, will be crucial for harnessing the full therapeutic potential of these observations.

REFERENCES

1. De Lorenzo, A.; Gratteri, S.; Gualtieri, P.; Cammarano, A.; Bertucci, P.; Di Renzo, L. Why Primary Obesity Is a Disease? *J Transl Med* **2019**, *17*, 169, doi:10.1186/s12967-019-1919-y.
2. Durrer Schutz, D.; Busetto, L.; Dicker, D.; Farpour-Lambert, N.; Pryke, R.; Toplak, H.; Widmer, D.; Yumuk, V.; Schutz, Y. European Practical and Patient-Centred Guidelines for Adult Obesity Management in Primary Care. *Obes Facts* **2019**, *12*, 40–66, doi:10.1159/000496183.
3. Swartz, J.J.; Dowray, S.; Braxton, D.; Mihas, P.; Viera, A.J. Simplifying Healthful Choices: A Qualitative Study of a Physical Activity Based Nutrition Label Format. *Nutr J* **2013**, *12*, 72, doi:10.1186/1475-2891-12-72.
4. Komarnytsky, S.; Retchin, S.; Vong, C.I.; Lila, M.A. Gains and Losses of Agricultural Food Production: Implications for the Twenty-First Century. *Annu Rev Food Sci Technol* **2022**, *13*, 239–261, doi:10.1146/annurev-food-082421-114831.
5. Milhem, F.; Komarnytsky, S. Progression to Obesity: Variations in Patterns of Metabolic Fluxes, Fat Accumulation, and Gastrointestinal Responses. *Metabolites* **2023**, *13*, 1016, doi:10.3390/metabo13091016.
6. Bessesen, D.H.; Bull, S.; Cornier, M.A. Trafficking of Dietary Fat and Resistance to Obesity. *Physiology & Behavior* **2008**, *94*, 681–688, doi:10.1016/j.physbeh.2008.04.019.
7. Flatt, J. p. What Do We Most Need to Learn about Food Intake Regulation? *Obesity Research* **1998**, *6*, 307–310, doi:10.1002/j.1550-8528.1998.tb00354.x.
8. Hall, K.D.; Sacks, G.; Chandramohan, D.; Chow, C.C.; Wang, Y.C.; Gortmaker, S.L.; Swinburn, B.A. Quantification of the Effect of Energy Imbalance on Bodyweight. *Lancet* **2011**, *378*, 826–837, doi:10.1016/S0140-6736(11)60812-X.

9. Abou Mrad, J.; Yakubu, F.; Lin, D.; Peters, J.C.; Atkinson, J.B.; Hill, J.O. Skeletal Muscle Composition in Dietary Obesity-Susceptible and Dietary Obesity-Resistant Rats. *Am J Physiol* **1992**, *262*, R684-688, doi:10.1152/ajpregu.1992.262.4.R684.
10. Chu, D.-T.; Malinowska, E.; Jura, M.; Kozak, L.P. C57BL/6J Mice as a Polygenic Developmental Model of Diet-Induced Obesity. *Physiol Rep* **2017**, *5*, e13093, doi:10.14814/phy2.13093.
11. Bessesen, D.H.; Rupp, C.L.; Eckel, R.H. Trafficking of Dietary Fat in Lean Rats. *Obesity Research* **1995**, *3*, 191–203, doi:10.1002/j.1550-8528.1995.tb00135.x.
12. Boulangé, C.L.; Claus, S.P.; Chou, C.J.; Collino, S.; Montoliu, I.; Kochhar, S.; Holmes, E.; Rezzi, S.; Nicholson, J.K.; Dumas, M.E.; et al. Early Metabolic Adaptation in C57BL/6 Mice Resistant to High Fat Diet Induced Weight Gain Involves an Activation of Mitochondrial Oxidative Pathways. *J Proteome Res* **2013**, *12*, 1956–1968, doi:10.1021/pr400051s.
13. Preda, A.; Carbone, F.; Tirandi, A.; Montecucco, F.; Liberale, L. Obesity Phenotypes and Cardiovascular Risk: From Pathophysiology to Clinical Management. *Rev Endocr Metab Disord* **2023**, *24*, 901–919, doi:10.1007/s11154-023-09813-5.
14. Xu, R.; Gao, X.; Wan, Y.; Fan, Z. Association of Metabolically Healthy Overweight Phenotype With Abnormalities of Glucose Levels and Blood Pressure Among Chinese Adults. *JAMA Network Open* **2019**, *2*, e1914025, doi:10.1001/jamanetworkopen.2019.14025.
15. Williams, L.M.; Campbell, F.M.; Drew, J.E.; Koch, C.; Hoggard, N.; Rees, W.D.; Kamolrat, T.; Thi Ngo, H.; Steffensen, I.-L.; Gray, S.R.; et al. The Development of Diet-Induced Obesity and Glucose Intolerance in C57Bl/6 Mice on a High-Fat Diet Consists of Distinct Phases. *PLoS One* **2014**, *9*, e106159, doi:10.1371/journal.pone.0106159.

16. Benedé-Ubieto, R.; Estévez-Vázquez, O.; Ramadori, P.; Cubero, F.J.; Nevzorova, Y.A. Guidelines and Considerations for Metabolic Tolerance Tests in Mice. *Diabetes Metab Syndr Obes* **2020**, *13*, 439–450, doi:10.2147/DMSO.S234665.
17. Heimann, E.; Nyman, M.; Pålbrink, A.-K.; Lindkvist-Petersson, K.; Degerman, E. Branched Short-Chain Fatty Acids Modulate Glucose and Lipid Metabolism in Primary Adipocytes. *Adipocyte* **2016**, *5*, 359–368, doi:10.1080/21623945.2016.1252011.
18. Leibowitz, S.F.; Alexander, J.; Dourmashkin, J.T.; Hill, J.O.; Gayles, E.C.; Chang, G.-Q. Phenotypic Profile of SWR/J and A/J Mice Compared to Control Strains: Possible Mechanisms Underlying Resistance to Obesity on a High-Fat Diet. *Brain Res* **2005**, *1047*, 137–147, doi:10.1016/j.brainres.2005.03.047.
19. Trouwborst, I.; Bowser, S.M.; Goossens, G.H.; Blaak, E.E. Ectopic Fat Accumulation in Distinct Insulin Resistant Phenotypes; Targets for Personalized Nutritional Interventions. *Front Nutr* **2018**, *5*, 77, doi:10.3389/fnut.2018.00077.
20. Schiaffino, S.; Reggiani, C. Fiber Types in Mammalian Skeletal Muscles. *Physiological Reviews* **2011**, *91*, 1447–1531, doi:10.1152/physrev.00031.2010.
21. Talbot, J.; Maves, L. Skeletal Muscle Fiber Type: Using Insights from Muscle Developmental Biology to Dissect Targets for Susceptibility and Resistance to Muscle Disease. *Wiley Interdiscip Rev Dev Biol* **2016**, *5*, 518–534, doi:10.1002/wdev.230.
22. Pette, D.; Staron, R.S. Myosin Isoforms, Muscle Fiber Types, and Transitions. *Microsc Res Tech* **2000**, *50*, 500–509, doi:10.1002/1097-0029(20000915)50:6<500::AID-JEMT7>3.0.CO;2-7.
23. Brotto, M.A.; Biesiadecki, B.J.; Brotto, L.S.; Nosek, T.M.; Jin, J.-P. Coupled Expression of Troponin T and Troponin I Isoforms in Single Skeletal Muscle Fibers Correlates with Contractility. *American Journal of Physiology-Cell Physiology* **2006**, *290*, C567–C576, doi:10.1152/ajpcell.00422.2005.

24. Salviati, G.; Betto, R.; Danieli Betto, D.; Zeviani, M. Myofibrillar-Protein Isoforms and Sarcoplasmic-Reticulum Ca²⁺-Transport Activity of Single Human Muscle Fibres. *Biochem J* **1984**, *224*, 215–225, doi:10.1042/bj2240215.
25. Larsson, L.; Edstrom, L.; Lindgren, B.; Gorza, L.; Schiaffino, S. MHC Composition and Enzyme-Histochemical and Physiological Properties of a Novel Fast-Twitch Motor Unit Type. *American Journal of Physiology-Cell Physiology* **1991**, *261*, C93–C101, doi:10.1152/ajpcell.1991.261.1.C93.
26. Olson, A.L. Regulation of GLUT4 and Insulin-Dependent Glucose Flux. *ISRN Mol Biol* **2012**, *2012*, 856987, doi:10.5402/2012/856987.
27. Lee, S.J.; Jeong, J.Y.; Oh, C.J.; Park, S.; Kim, J.-Y.; Kim, H.-J.; Doo Kim, N.; Choi, Y.-K.; Do, J.-Y.; Go, Y.; et al. Pyruvate Dehydrogenase Kinase 4 Promotes Vascular Calcification via SMAD1/5/8 Phosphorylation. *Sci Rep* **2015**, *5*, 16577, doi:10.1038/srep16577.
28. Kang, W.; Suzuki, M.; Saito, T.; Miyado, K. Emerging Role of TCA Cycle-Related Enzymes in Human Diseases. *Int J Mol Sci* **2021**, *22*, 13057, doi:10.3390/ijms222313057.
29. Chen, W.; Paradkar, P.N.; Li, L.; Pierce, E.L.; Langer, N.B.; Takahashi-Makise, N.; Hyde, B.B.; Shirihai, O.S.; Ward, D.M.; Kaplan, J.; et al. Abcb10 Physically Interacts with Mitoferrin-1 (Slc25a37) to Enhance Its Stability and Function in the Erythroid Mitochondria. *Proc Natl Acad Sci U S A* **2009**, *106*, 16263–16268, doi:10.1073/pnas.0904519106.
30. Meli, R.; Raso, G.M.; Irace, C.; Simeoli, R.; Pascale, A.D.; Paciello, O.; Pagano, T.B.; Calignano, A.; Colonna, A.; Santamaria, R. High Fat Diet Induces Liver Steatosis and Early Dysregulation of Iron Metabolism in Rats. *PLOS ONE* **2013**, *8*, e66570, doi:10.1371/journal.pone.0066570.

31. Stangl, G.I.; Kirchgessner, M. Different Degrees of Moderate Iron Deficiency Modulate Lipid Metabolism of Rats. *Lipids* **1998**, *33*, 889–895, doi:10.1007/s11745-998-0285-8.
32. Alghamdi, M.; Gutierrez, J.; Komarnytsky, S. Essential Minerals and Metabolic Adaptation of Immune Cells. *Nutrients* **2023**, *15*, 123, doi:10.3390/nu15010123.
33. Paul, B.T.; Manz, D.H.; Torti, F.M.; Torti, S.V. Mitochondria and Iron: Current Questions. *Expert Rev Hematol* **2017**, *10*, 65–79, doi:10.1080/17474086.2016.1268047.
34. Heinitz, S.; Piaggi, P.; Yang, S.; Bonfiglio, S.; Steel, J.; Krakoff, J.; Votruba, S.B. Response of Skeletal Muscle UCP2-Expression during Metabolic Adaptation to Caloric Restriction. *Int J Obes* **2018**, *42*, 974–984, doi:10.1038/s41366-018-0085-2.
35. Hoang, T.; Smith, M.D.; Jelokhani-Niaraki, M. Toward Understanding the Mechanism of Ion Transport Activity of Neuronal Uncoupling Proteins UCP2, UCP4, and UCP5. *Biochemistry* **2012**, *51*, 4004–4014, doi:10.1021/bi3003378.
36. Diano, S.; Horvath, T.L. Mitochondrial Uncoupling Protein 2 (UCP2) in Glucose and Lipid Metabolism. *Trends Mol Med* **2012**, *18*, 52–58, doi:10.1016/j.molmed.2011.08.003.
37. Vozza, A.; Parisi, G.; De Leonardis, F.; Lasorsa, F.M.; Castegna, A.; Amorese, D.; Marmo, R.; Calcagnile, V.M.; Palmieri, L.; Ricquier, D.; et al. UCP2 Transports C4 Metabolites out of Mitochondria, Regulating Glucose and Glutamine Oxidation. *Proc Natl Acad Sci U S A* **2014**, *111*, 960–965, doi:10.1073/pnas.1317400111.
38. Lee, H.; Smith, S.B.; Sheu, S.-S.; Yoon, Y. The Short Variant of Optic Atrophy 1 (OPA1) Improves Cell Survival under Oxidative Stress. *J Biol Chem* **2020**, *295*, 6543–6560, doi:10.1074/jbc.RA119.010983.
39. Pereira, R.O.; Olvera, A.C.; Marti, A.; Fang, S.; White, J.R.; Westphal, M.; Hewezi, R.; AshShareef, S.T.; García-Peña, L.M.; Koneru, J.; et al. OPA1 Regulates Lipid Metabolism and

Cold-Induced Browning of White Adipose Tissue in Mice. *Diabetes* **2022**, *71*, 2572–2583, doi:10.2337/db22-0450.

40. Noone, J.; O’Gorman, D.J.; Kenny, H.C. OPA1 Regulation of Mitochondrial Dynamics in Skeletal and Cardiac Muscle. *Trends in Endocrinology & Metabolism* **2022**, *33*, 710–721, doi:10.1016/j.tem.2022.07.003.

41. Ruprecht, J.J.; Kunji, E.R.S. The SLC25 Mitochondrial Carrier Family: Structure and Mechanism. *Trends Biochem Sci* **2020**, *45*, 244–258, doi:10.1016/j.tibs.2019.11.001.

42. Odamaki, T.; Kato, K.; Sugahara, H.; Hashikura, N.; Takahashi, S.; Xiao, J.-Z.; Abe, F.; Osawa, R. Age-Related Changes in Gut Microbiota Composition from Newborn to Centenarian: A Cross-Sectional Study. *BMC Microbiol* **2016**, *16*, 90, doi:10.1186/s12866-016-0708-5.

43. Macfarlane, G.T.; Gibson, G.R.; Beatty, E.; Cummings, J.H. Estimation of Short-Chain Fatty Acid Production from Protein by Human Intestinal Bacteria Based on Branched-Chain Fatty Acid Measurements. *FEMS Microbiology Ecology* **1992**, *10*, 81–88, doi:10.1111/j.1574-6941.1992.tb00002.x.

44. Ternes, D.; Tsenkova, M.; Pozdeev, V.I.; Meyers, M.; Koncina, E.; Atatri, S.; Schmitz, M.; Karta, J.; Schmoetten, M.; Heinken, A.; et al. The Gut Microbial Metabolite Formate Exacerbates Colorectal Cancer Progression. *Nat Metab* **2022**, *4*, 458–475, doi:10.1038/s42255-022-00558-0.

45. Raman, M.; Ahmed, I.; Gillevet, P.M.; Probert, C.S.; Ratcliffe, N.M.; Smith, S.; Greenwood, R.; Sikaroodi, M.; Lam, V.; Crotty, P.; et al. Fecal Microbiome and Volatile Organic Compound Metabolome in Obese Humans with Nonalcoholic Fatty Liver Disease. *Clin Gastroenterol Hepatol* **2013**, *11*, 868-875.e1-3, doi:10.1016/j.cgh.2013.02.015.

46. Walton, C.; Fowler, D.P.; Turner, C.; Jia, W.; Whitehead, R.N.; Griffiths, L.; Dawson, C.; Waring, R.H.; Ramsden, D.B.; Cole, J.A.; et al. Analysis of Volatile Organic Compounds of Bacterial Origin in Chronic Gastrointestinal Diseases. *Inflamm Bowel Dis* **2013**, *19*, 2069–2078, doi:10.1097/MIB.0b013e31829a91f6.
47. Chambers, E.S.; Viardot, A.; Psichas, A.; Morrison, D.J.; Murphy, K.G.; Zac-Varghese, S.E.K.; MacDougall, K.; Preston, T.; Tedford, C.; Finlayson, G.S.; et al. Effects of Targeted Delivery of Propionate to the Human Colon on Appetite Regulation, Body Weight Maintenance and Adiposity in Overweight Adults. *Gut* **2015**, *64*, 1744–1754, doi:10.1136/gutjnl-2014-307913.
48. Chambers, E.S. Gut-Derived Short-Chain Fatty Acids: A Friend or Foe for Hepatic Lipid Metabolism? *Nutrition Bulletin* **2019**, *44*, 154–159, doi:10.1111/nbu.12377.
49. Kim, K.N.; Yao, Y.; Ju, S.Y. Short Chain Fatty Acids and Fecal Microbiota Abundance in Humans with Obesity: A Systematic Review and Meta-Analysis. *Nutrients* **2019**, *11*, 2512, doi:10.3390/nu11102512.
50. Martínez-Cuesta, M.C.; Del Campo, R.; Garriga-García, M.; Peláez, C.; Requena, T. Taxonomic Characterization and Short-Chain Fatty Acids Production of the Obese Microbiota. *Front Cell Infect Microbiol* **2021**, *11*, 598093, doi:10.3389/fcimb.2021.598093.
51. de la Cuesta-Zuluaga, J.; Mueller, N.T.; Álvarez-Quintero, R.; Velásquez-Mejía, E.P.; Sierra, J.A.; Corrales-Agudelo, V.; Carmona, J.A.; Abad, J.M.; Escobar, J.S. Higher Fecal Short-Chain Fatty Acid Levels Are Associated with Gut Microbiome Dysbiosis, Obesity, Hypertension and Cardiometabolic Disease Risk Factors. *Nutrients* **2018**, *11*, 51, doi:10.3390/nu11010051.
52. Rathinasabapathy, T.; Lomax, J.; Srikanth, K.; Esposito, D.; Kay, C.D.; Komarnytsky, S. Effect of Wild Blueberry Metabolites on Biomarkers of Gastrointestinal and Immune Health In Vitro. *Immuno* **2022**, *2*, 293–306, doi:10.3390/immuno2020019.

53. Liu, Y.; Li, J.; Cheng, Y.; Liu, Y. Volatile Components of Deep-Fried Soybean Oil as Indicator Indices of Lipid Oxidation and Quality Degradation. *Eur Food Res Technol* **2020**, *246*, 1183–1192, doi:10.1007/s00217-020-03475-2.

CHAPTER 4- Conclusions and Future Directions

“The doctor of the future will no longer treat the human frame with drugs, but rather will cure and prevent disease with nutrition.” – Thomas Edison

The health and quality of life of individuals can be influenced by a range of circumstances, including but not limited to physical activity level, food habits, economic status, and living conditions. Healthy eating habits are one of the most important factors in maintaining both our physical and emotional well-being, as well as in the prevention and management of non-communicable illnesses, including obesity and other metabolic diseases.

Results primarily from cross-sectional research suggest that a higher degree of adherence to less nutritious dietary patterns, characterized by the consumption of refined and processed foods, is associated with a reduced chance of having a healthy metabolic profile. On the other hand, there is a correlation between better eating habits and a greater chance of preserving metabolic health. These discoveries help shape dietary plans intended to improve metabolic health in the general population (Abiri et al., 2023).

Chapter 1 of this dissertation facilitates an understanding of how individuals respond to an environment conducive to obesity, the intricacies of obesity development, and the challenging aspects of its impact on well-being. Key contributions to this understanding include heightened inflammatory responses, the presence of ectopic fat in the liver, and metabolic changes in visceral fat. Notably, a gap in knowledge pertains to altered cellular metabolism, attributed to mitochondrial dysfunction, influencing energy balance, inflammation, and metabolically active tissues, as indicated by Milhem and Komarnytsky (2023).

In chapter 2 and 3, aspects related to etiology of obesity were examined, encompassing elements related to metabolism, microbiota, genetics, and lifestyle that define several pathophysiological states. Gaining insight into the molecular processes behind this categorization is essential to attaining significant weight reduction. Important metabolic targets include high rates of lactate turnover, extracellular buildup of Krebs cycle metabolites such as citrate, variations in fatty acid oxidation, and metabolic fluxes, with a particular focus on the pyruvate-phosphoenolpyruvate-oxaloacetate node. These targets also offer promising avenues for individualized treatment of obesity and merit more research. Our research showed that the *Bacteroidetes* phylum expanded in obesity-resistant NR mice, but the *Actinobacteria* phylum was drastically decreased. It is still unclear what this finding means in its entirety.

The causes of obesity are a public health concern as they provide an alarming risk to global wellness. Although there is a connection between obesity and a high-fat diet (HFD), people have different inclinations to gain weight or remain fit (Wang et al., 2022). The outcome of our studies raises questions with respect to whether the findings of animal research can be applied to human therapeutic conditions. Further investigation is required to fully understand these metabolic pathways and use the results in practical settings. Also, to address specific obesity phenotypes, future research must examine the manipulation of gut microbiota and the brain axis by dietary interventions, pharmaceutical therapies, and surgery.

Promising approaches include phenotype-guided therapy. Future research must focus on comprehending and overcoming the many metabolic fluxes and processes that sustain obesity, considering the continual maintenance of current body weight. Furthermore, individuals prone to obesity may possess an unfavorable gut microbiome that worsens adiposity during high-fat (HF) feeding. This could serve as a potential marker for obesity

susceptibility in humans. Identifying specific bacterial groups or species that significantly contribute to obesity paves the way for potential therapeutic interventions targeting these organisms to alleviate host metabolic dysregulation.

Finally, examining the adaptive relevance of metabolic rate changes is an interesting path for additional research. Although there is much interest in the subject, there aren't sufficient studies that systematically look at whether the rate of metabolism and individual fitness, or at least certain components of fitness, are associated. Our perception of this important field would be greatly advanced by including such experimental studies in the investigation focus.

REFERENCES

- Abiri, B., Valizadeh, M., Nasreddine, L., & Hosseinpanah, F. (2023). Dietary determinants of healthy/unhealthy metabolic phenotype in individuals with normal weight or overweight/obesity: A systematic review. *Critical Reviews in Food Science and Nutrition*, 63(22), 5856–5873. <https://doi.org/10.1080/10408398.2021.2025036>
- Milhem, F., & Komarnytsky, S. (2023). Progression to Obesity: Variations in Patterns of Metabolic Fluxes, Fat Accumulation, and Gastrointestinal Responses. *Metabolites*, 13(9), Article 9. <https://doi.org/10.3390/metabo13091016>
- Wang, C., Duan, M., Lin, J., Wang, G., Gao, H., Yan, M., Chen, L., He, J., Liu, W., Yang, F., & Zhu, S. (2022). LncRNA and mRNA expression profiles in brown adipose tissue of obesity-prone and obesity-resistant mice. *iScience*, 25(8), 104809. <https://doi.org/10.1016/j.isci.2022.104809>

APPENDICES

Appendix 1- Supplementary Data

“Obesity-prone and obesity-resistant C57BL/6J phenotypes show major differences in skeletal muscle, gastrointestinal metabolic signatures, and immune functions”

Supplementary Table S1. Fold-changes in skeletal muscle function gene expression (NR versus HFD controls).

Fold	Gene	Gene description
17.0	<i>Mmp9</i>	Matrix metalloproteinase 9
3.7	<i>Tnni2</i>	Troponin I, skeletal, fast 2
2.9	<i>Cs</i>	Citrate synthase
2.6	<i>Foxo3</i>	Forkhead box O3
2.5	<i>Casp3</i>	Caspase 3
2.4	<i>Dmd</i>	Dystrophin, muscular dystrophy
2.3	<i>Mef2c</i>	Myocyte enhancer factor 2C
2.3	<i>Pdk4</i>	Pyruvate dehydrogenase kinase, isoenzyme 4
2.3	<i>Ikkkb</i>	Inhibitor of kappaB kinase beta
2.3	<i>Il1b</i>	Interleukin 1 beta
2.2	<i>Tgfb1</i>	Transforming growth factor, beta 1
2.2	<i>Ppp3ca</i>	Protein phosphatase 3, catalytic subunit, alpha isoform
2.1	<i>Musk</i>	Muscle, skeletal, receptor tyrosine kinase
2.1	<i>Actn3</i>	Actinin alpha 3
2.1	<i>Lmna</i>	Lamin A
2.0	<i>Capn2</i>	Calpain 2
2.0	<i>Myh2</i>	Myosin, heavy polypeptide 2, skeletal muscle, adult
2.0	<i>Myh1</i>	Myosin, heavy polypeptide 1, skeletal muscle, adult
-2.1	<i>Slc2a4</i>	Solute carrier family 2 (facilitated glucose transporter), member 4
-3.4	<i>Tnnc1</i>	Troponin C, cardiac/slow skeletal

Supplementary Table S2. Fold-changes in mitochondria function gene expression (HFD versus LFD controls).

Fold	Gene	Gene description
1.92	<i>Cpt1b</i>	Carnitine palmitoyltransferase 1b, muscle
1.85	<i>Bnip3</i>	BCL2/adenovirus E1B interacting protein 3
1.84	<i>Slc25a3</i>	Solute carrier family 25 (phosphate carrier), member 3 Solute carrier family 25 (oxodicarboxylate carrier), member
-1.69	<i>Slc25a21</i>	21 IMP2 inner mitochondrial membrane peptidase-like (S.
-1.73	<i>Immp2l</i>	cerevisiae) Translocase of inner mitochondrial membrane 22 homolog
-1.80	<i>Timm22</i>	(yeast)
-1.83	<i>Msto1</i>	Misato homolog 1 (Drosophila)
-1.84	<i>Slc25a27</i>	Solute carrier family 25, member 27
-1.84	<i>Slc25a24</i>	Solute carrier family 25 (phosphate carrier), member 24 Solute carrier family 25 (adenine nucleotide translocator),
-1.88	<i>Slc25a13</i>	member 13
-1.94	<i>Nefl</i>	Neurofilament, light polypeptide Solute carrier family 25 (dicarboxylate transporter), member
-1.98	<i>Slc25a10</i>	10
-2.09	<i>Sfn</i>	Stratifin
-2.31	<i>Bbc3</i>	BCL2 binding component 3
-2.32	<i>Ucp1</i>	Uncoupling protein 1 (mitochondrial, proton carrier)
-2.35	<i>Cdkn2a</i>	Cyclin-dependent kinase inhibitor 2A
-2.58	<i>Pmaip1</i>	Phorbol-12-myristate-13-acetate-induced protein 1
-3.42	<i>Bid</i>	BH3 interacting domain death agonist
-3.59	<i>Slc25a37</i>	Solute carrier family 25, member 37

Supplementary Table S3. Fold-changes in mitochondria function gene expression (NR versus HFD controls).

Fold	Gene	Gene description
4.9	Slc25a37	Solute carrier family 25, member 37
2.4	Ucp2	Uncoupling protein 2 (mitochondrial, proton carrier)
-1.8	Ucp1	Uncoupling protein 1 (mitochondrial, proton carrier)
-1.8	Slc25a13	Solute carrier family 25 (adenine nucleotide translocator), member 13
-1.8	Cpt1b	Carnitine palmitoyltransferase 1b, muscle
-1.8	Slc25a10	Solute carrier family 25 (dicarboxylate transporter), member 10
-1.9	Slc25a2	Solute carrier family 25 (ornithine transporter) member 2
-1.9	Nefl	Neurofilament, light polypeptide
-1.9	Slc25a4	Solute carrier family 25 (adenine nucleotide translocator), member 4
-1.9	Slc25a31	Solute carrier family 25 (adenine nucleotide translocator), member 31
-1.9	Fxc1	Fractured callus expressed transcript 1
-2.0	Timm9	Translocase of inner mitochondrial membrane 9 homolog (yeast)
-2.1	Bbc3	BCL2 binding component 3
-2.2	Slc25a22	Solute carrier family 25 (mitochondrial carrier, glutamate), member 22
-2.4	Bnip3	BCL2/adenovirus E1B interacting protein 3
-2.4	Slc25a21	Solute carrier family 25 (mitochondrial oxodicarboxylate carrier), member 21
-2.6	Msto1	Misato homolog 1 (Drosophila)
-2.6	Mtx2	Metaxin 2

Supplementary table S4. Fold-changes in mitochondria function gene expression (SR versus HFD controls).

Fold	Gene	Gene description
2.8	Slc25a1	Solute carrier family 25 (citrate transporter), member 1
1.9	Slc25a37	Solute carrier family 25, member 37
-1.8	Cpt1b	Carnitine palmitoyltransferase 1b, muscle
-1.8	Pmaip1	Phorbol-12-myristate-13-acetate-induced protein 1
-1.8	Slc25a13	Solute carrier family 25 (adenine nucleotide translocator), member 13
-1.9	Slc25a2	Solute carrier family 25 (ornithine transporter) member 2
-2.0	Slc25a31	Solute carrier family 25 (adenine nucleotide translocator), member 31
-2.0	Bnip3	BCL2/adenovirus E1B interacting protein 3
-2.1	Cdkn2a	Cyclin-dependent kinase inhibitor 2A
-2.1	Nefl	Neurofilament, light polypeptide
-2.1	Timm9	Translocase of inner mitochondrial membrane 9 homolog (yeast)
-2.3	Bbc3	BCL2 binding component 3
-2.4	Slc25a21	Solute carrier family 25 (mitochondrial oxodicarboxylate carrier), member 21
-2.4	Slc25a30	Solute carrier family 25, member 30
-2.7	Tomm40l	Translocase of outer mitochondrial membrane 40 homolog-like (yeast)
-2.8	Mtx2	Metaxin 2

Supplementary table S5. Fold-changes in mitochondria function gene expression (SR-LFD versus HFD controls).

Fold	Gene	Gene description
1.7	Timm22	Translocase of inner mitochondrial membrane 22 homolog (yeast)
-2.0	Bnip3	BCL2/adenovirus E1B interacting protein 3
-2.0	Slc25a20	Solute carrier family 25 (carnitine/acylcarnitine translocase), member 20
-2.0	Slc25a10	Solute carrier family 25 (dicarboxylate transporter), member 10
-2.0	Slc25a13	Solute carrier family 25 (adenine nucleotide translocator), member 13
-2.1	Fxc1	Fractured callus expressed transcript 1
-2.1	Slc25a2	Solute carrier family 25 (ornithine transporter) member 2
-2.2	Timm9	Translocase of inner mitochondrial membrane 9 homolog (yeast)
-2.2	Slc25a31	Solute carrier family 25 (adenine nucleotide translocator), member 31
-2.3	Cpt1b	Carnitine palmitoyltransferase 1b, muscle
-2.3	Nefl	Neurofilament, light polypeptide
-2.4	Cpt2	Carnitine palmitoyltransferase 2
-3.0	Bbc3	BCL2 binding component 3
-3.0	Slc25a21	Solute carrier family 25 (mitochondrial oxodicarboxylate carrier), member 21
-3.4	Mtx2	Metaxin 2
-3.5	Slc25a22	Solute carrier family 25 (mitochondrial carrier, glutamate), member 22

Supplementary table S6. Fold-changes in mitochondria function gene expression (NR versus SR mice).

Fold	Gene	Gene description
2.6	Slc25a37	Solute carrier family 25, member 37
2.0	Opa1	Optic atrophy 1 homolog (human) Translocase of outer mitochondrial membrane 40 homolog- like (yeast)
1.9	Tomm40l	
1.7	Ucp2	Uncoupling protein 2 (mitochondrial, proton carrier) Solute carrier family 25 (adenine nucleotide translocator), member 4
-2.3	Slc25a4	
-2.5	Msto1	Misato homolog 1 (Drosophila)
-2.7	Slc25a1	Solute carrier family 25 (citrate transporter), member 1